2009

Intracellular Trafficking of the Hantaviral Nucleocapsid Protein and its Function in Modulation of Immune Signaling

Steven Joe Ontiveros
University of Alabama at Birmingham

INTRACELLULAR TRAFFICKING OF THE HANTAVIRAL NUCLEOCAPSID PROTEIN AND ITS FUNCTION IN MODULATION OF IMMUNE SIGNALING

by

STEVEN J. ONTIVEROS

COLLEEN B. JONSSON, COMMITTEE CHAIR
CASEY D. MORROW
PETER E. PREVELIGE
ELIZABETH S. SZTUL
TIM M. TOWNES

A DISSERTATION

Submitted to the faculty of The University of Alabama at Birmingham,
in partial fulfillment of the requirements for the degree of
Doctor of Philosophy

BIRMINGHAM, ALABAMA

2009

INTRACELLULAR TRAFFICKING OF THE HANTAVIRAL NUCLEOCAPSID PROTEIN AND ITS FUNCTION IN MODULATION OF IMMUNE SIGNALING

STEVEN J. ONTIVEROS, B.S.

BIOCHEMISTRY AND MOLECULAR GENETICS

ABSTRACT

Old World and New World hantaviruses, family *Bunyaviridae*, mature intracellularly within cellular compartments. Although it is generally accepted they assemble and bud in the Golgi apparatus the site remains controversial for New World hantaviruses, because some studies have raised the possibility of their maturation at the plasma membrane. Furthermore, the site of assembly hantaviruses still remains undetermined. The nucleocapsid (N) protein has been proposed to play a key role in facilitating assembly. To gain insight into the assembly pathways of Old World hantaviruses, we examine the intracellular trafficking of the Hantaan (HTN) virus N protein. We show progressive redistribution of the HTN virus N protein in Vero E6 cells from the cell periphery to the perinuclear region during infection. Using confocal microscopy, we show that the HTN virus N protein specifically targets the endoplasmic reticulum-Golgi intermediate compartment (ERGIC). We did not observe colocalization of N protein with actin microfilaments, suggesting that targeting is actin independent and may use other cytoskeletal structures. Interestingly, expression of HTN virus N protein also targeted to the perinuclear region independent of other viral components, which suggests the N protein may contain an intrinsic signal sufficient for subcellular targeting. Herein, we show that the region of amino acids 270-300 may function to influence perinuclear targeting. Hantaviruses cause two human diseases, hantavirus pulmonary syndrome and hemorrhagic fever with renal syndrome. Although pathogenesis is

believed to be immunologically mediated, the underlying mechanism is unknown. Numerous reports have shown elevated levels of proinflammatory and inflammatory cytokines in human sera from patients infected with hantaviruses. We show a direct relationship between the HTN virus N protein and modulation of apoptosis. Interestingly, we observed elevated caspase-7, and -8, but not -9 activity in cells expressing N protein mutants lacking amino acids 270-330. We also observed that the HTN virus N protein is capable of circumventing the immune signaling pathway of the tumor necrosis factor receptor (TNF-R) by interfering with the nuclear import of nuclear factor kappa B (NF-κB).

DEDICATIONS

I would like to formally dedicate my Ph.D. dissertation to my wonderful children for their endless love and complete understanding in the time I have spent away from their lives', especially Nathaniel J. Ontiveros, since he is still back home in New Mexico. I have ever so cherished our phone conversations and visits I have made over the years. I would like to thank my older son, Steven J. Ontiveros, Jr. for the inspiration he gave me to pursue an academic dream, and for being such a wonderful, mature, young individual with a big heart. I love you both with all of my heart. I would also like to dedicate my dissertation to my brother and sister, Ernest Jr and Connie, for their continued support and love, and their encouragement to complete my degree. To my mom, Ernestine R. Ontiveros, I would like to thank her for taking wonderful care of my siblings and me and for influencing me to the sciences when I was just 4 or 5 years old during our "bug" hunts around our yard. To my dad, Ernest J. Ontiveros, for always making sure we were taken care of and for keeping a roof over our heads while I was growing up. I am forever in dept to the both of you for coming over to Alabama to help Steven Jr. and me during my graduate career. I would also like to dedicate my dissertation to my fiancée, Belen Moreno, for her endless love, support, patience, and complete understanding. I would also like to give her a big thank you for being my means of mental support and emotional health (personal therapist). I thank you all for the strength, patience, and support to help me fulfill and finish one of my aspirations in life. I love you all so much.

ACKNOWLEDGMENTS

I take this opportunity to express much appreciation and gratitude to my advisor, Dr. Colleen B. Jonsson for providing me guidance, support, and inspiration, and for helping me throughout my graduate career. She provided a preferable, working environment where she allowed me to investigate my own interests, while providing rich feedback to help focus my efforts. I would also like to thank my committee members: Drs. Casey D. Morrow, Peter E. Prevelige, Elizabeth S. Sztul, and Tim M. Townes for their suggestions that helped to advance my academic and scientific career. I would also like to thank Qianjun Li for his helpful discussions and for reviewing the "Modulation of apoptosis and immune signaling pathways by the hantaan virus nucleocapsid protein" manuscript. I also thank Xiaolin Xu for the cloning that she did to help complete a few studies within the above named manuscript. I thank the Graduate School and the Department of Biochemistry and Molecular Genetics for providing an outstanding curriculum, which helped to define and enhance my scientific understanding. I would also like to thank Dianne Vickers for being the most heart-warming person within the department.

I have greatly appreciated my colleagues at Southern Research Institute: Drs. Carl Bruder, and Alexis McBrayer, for very interesting conversations, Dr. Harish Ramanathan, Ron Tapp, Blake Moore, Xiaolin Xu, Fuli Jia, and in particular Drs. Yong-Kyu Chu, Doon Hoon Chung, and Sinu P. John for providing technical and optimistic discussions during my graduate career. I would also like to thank all other people at

Southern Research institute and the department of Biochemistry and Molecular Genetics that have helped in any shape or form.

I would like to personally thank Dr. Joseph “Rudy” Montoya for being a wonderful friend and for providing me the most encouraging guidance and support to complete my degree. Your continuous inspiration and encouragement to complete my degree made it very possible. I would also like to thank anyone else that provided any means of encouragement.

TABLE OF CONTENTS

Page

LIST OF TABLES

LIST OF FIGURES

LIST OF FIGURES (continued)

SPATIO-TEMPORAL DISTRIBUTION OF THE HANTAAN VIRUS NUCLEOCAPSID PROTEIN AND TRANSPORT TO THE ENDOPLASMIC RETICULUM-GOLGI INTERMEDIATE COMPARTMENT

HANTAAN VIRUS N PROTEIN FUNCITONS TO MODULATE IMMUNE SIGNALING

LIST OF FIGURES (continued)

CONCLUDING REMARKS AND FUTURE PROSPECTS

LIST OF ABBREVIATIONS

AND	Andes
ANDV	Andes virus
Apaf-1	apoptotic protease activating factor 1
BCC	Black Creek Canal
BCCV	Black Creek Canal virus
BFA	Brefeldin A
BUN	Bunyamwera
BUNV	Bunyamwera virus
CARD	Caspase-activation recruitment domain
CNX	Calnexin
CPE	Cytopathic effects
cRNA	Copy RNA
CytD	Cytochalasin D
DD	Death domain
DED	Death effector domain
DISC	Death-inducing signaling complex
DMZ	De-militarized zone
DUG	Dugbe
EE	Early endosome
EEA1	Early endosomal antigen 1

ELISA	Enzyme-linked immunosorbent assay
ER	Endoplasmic reticulum
ERGIC	Endoplasmic reticulum-Golgi intermediate complex
F-actin	Filamentous actin
FADD	Fas-associated protein with death domain
Fas-R	Fas receptor
FBS	Fetal bovine serum
FITC	Fluoroisothycyanate
GP	Glycoprotein
GPC	Glycoprotein precursor complex
HCPS	Hantavirus cardiopulmonary syndrome
HEK293	Human embryonic kidney 293 cells
HFRS	Hemorrhagic fever with renal syndrome
HPS	Hantavirus pulmonary syndrome
HTN	Hantaan
HTNV	Hantaan virus
IAPs	Inhibitors of apoptosis
IFA	Immunofluorescence
IHC	Immunohistochemistry
kDa	Kilo dalton
KHV	Korean hemorrhagic fever
L	Large
LAC	La Crosse

M	Medium
Mabs	Monoclonal antibodies
MP	Matrix protein
N	Nucleocapsid protein
NF-κB	Nuclear factor kappa B
NOC	Nocodazole
NSm	M-segment non-structural proteins
NSs	S-segment non-structural proteins
ORF	Open-reading frame
PARP	Poly-ADP-ribose polymerase
PCR	Polymerase chain reaction
PCR-EIA	Polymerase chain reaction enzyme immunoassay
PDI	Protein disulfide isomerase
PH	Prospect Hill
PNS	Postnuclear supernatant
PRNT	Plaque reduction neutralization test
PT	Punta toro
PUU	Puumala
RBV	Ribavirin
RdRp	RNA-Dependent RNA polymerase
RIP	Receptor interacting protein
RNA	Ribonucleic acid
RNP	Ribonucleocapsids

RS	Respiratory Syncytial
RSV	Respiratory Syncytial virus
RT-PCR	Real-time polymerase chain reaction
RVF	Rift Valley Fever
S	Small
SEO	Seoul
SEOV	Seoul virus
SIA	Strip immuno-assay
SN	Sin Nombre
SNV	Sin Nombre virus
SSH	Snowshoe Hare
SUMO-1	Small ubiquitin-like modivier 1
TNFR	Tumor necrosis factor receptor
TNFR-1	Tumor necrosis factor receptor type 1
TNFR-2	Tumor necrosis factor receptor type 2
TRADD	TNFR-associated via death domain
TRAF	TNFR-associated factor
TRITC	Tetramethylrhodamine
TSW	Tomato Spotted Wilt
TUL	Tula
TULV	Tula virus
Ubc9	Ubiquitin conjugating enzyme 9
UTR	Untranslated region

UUK	Uukuniemi
UUKV	Uukuniemi virus
vRNA	Viral RNA
WB	Western blot
WGA	Wheat germ agglutinin

CHAPTER 1

BUNYAVIRIDAE

The family *Bunyaviridae*, which is comprised of a large group of over 300 viruses each sharing morphogenic and antigenic properties, was established in 1975 (48). Characterization of this family began during the early 1940's when a virus, Bunyamwera (BUN) virus, was isolated from *Aedes* species mosquitoes in Uganda during yellow fever studies (195). New virus discoveries, along with many studies, and serological characterization led to the formation of a class of viruses that were closely related by their antigenic properties (134). Historically, these viruses were classified by their antigenic properties and the results of serological tests, but new genetic methods helped the characterization of these viruses, which mandated the efforts to reclassify them (166). These closely related viruses facilitated the establishment of the family *Bunyaviridae*, named after BUN virus, which now contains many human, livestock, and plant pathogens.

There are currently four genera of viruses within the *Bunyaviridae* that use animal reservoirs (*Orthobunyavirus, Hantavirus, Nairovirus* and *Phlebovirus*) and one genus that use a plant reservoir (*Tospovirus*) to maintain their lifestyles (183). The *Bunyaviridae* infect animals, plants, humans and insects. Most viruses within the *Bunyaviridae* are transmitted by arthropods, mosquitoes, ticks, sand flies, or thrips, with the exception of the *Hantavirus* genus, which are rodent-borne and found in aerosolized rodents excreta and saliva (Table 1).

Hantavirus Genus and Historical Overview

During the Korean War in the early 1950's United Nations troops were deployed to help alleviate the border conflicts between North and South Korea. Thousands of troops (approximately 3,000 cases) developed a mysterious disease, which was accompanied by fever, headache, hemorrhagic manifestations, and acute kidney failure (100, 107, 194). This disease resulted in the death of hundreds of troops, with a mortality rate of 5 to 10% (100, 107, 194). A high percentage of all cases that resulted in death were specifically due to renal failure. The disease was initially termed *Korean hemorrhagic fever* (KHV), but is now known as hemorrhagic fever with renal syndrome (HFRS). A similar disease, originally termed epidemic hemorrhagic fever, had been previously characterized in northeastern China (101) and eastern Russia (the former Soviet Union) (21). Illnesses similar to KHV have been described in Chinese medical records that date back to 960 A.D.

Approximately 26 years of field studies, a significant breakthrough took place when *Apodemus agrarius* was discovered to be the rodent reservoir for the virus agent responsible for KHV. Isolation and characterization of the virus showed that it shared similar characteristics with viruses that belonged to the family *Bunyaviridae*. Interestingly, during this time all viruses within the

Table 1: Representative viruses of the family *Bunyaviridae* (183)

Genus	Notable virus Members	Geographic Distribution	Vector	Disease
Orthobunyavirus	Bunyamwera	Africa	Mosquitoes	Human
	Cache Valley	North America	Mosquitoes	Sheep, cattle, humans
	Germiston	Africa	Mosquitoes	Human
	Bwamba	Africa	Mosquitoes	Human
	Apeu	South America	Mosquitoes	Human
	La Crosse	North America	Mosquitoes	Human
	Jamestown Canyon	North America	Mosquitoes	Human
Phlebovirus	Punta Toro	North and South America	Phlebotomine flies	Human
	Rift Valley fever	Africa	Mosquitoes	Human, cattle
	Sandlfly fever	Europe, Africa, Asia	Phlebotomine flies	Human
	Toscana	Europe	Phlebotomine flies	Human
	Uukuniemi	Europe	Ticks	Seabirds
Nairovirus	Crimean-Congo HF	Africa, Asia, Europe	Ticks	Human
	Hughes	North and South America	Ticks	Seabirds
Tospovirus	Tomato spotted wilt	World wide	Thrips	Plants

Table 1: Continued

Genus	Notable virus Members	Geographic Distribution	Vector	Disease
Hantavirus				
Old World	Hantaan	Asia	Rattus	Human
	Dobrava	Europe	Apodemus flavicollis	Human
	Seoul	Asia	Rattus	Human
	Puumala	Europe, Asia and Americas	Clethrionomys	Human
New World	Sin Nombre	North America	Peromyscus maniculatus	Human
	Bayou	North America	Otyzomys palustris	Human
	Black Creek Canal	North America	Sigmodon hispidus	Human
	Andes	South America	Oligoryzomys palustris	Human
	Laguna Negra	South America	Calomys laucha	Human
	Araraquara	South America	Bolomys lasiurus	Human

family *Bunyaviridae* were known to contain arthropod hosts (Table 1), but this virus disputed that general dogma. Since the majority of all cases took place near the Hantaan River, which is located along the de-militarized zone or DMZ between North and South Korea, the virus was named Hantaan (HTN) virus. The HTN virus eventually became the prototype of the *Hantavirus* genus (125). The isolation of the HTN virus eventually led to the discovery of other viruses that contained similar characteristics. The discovery of Puumala (PUU) virus took place when the HTN virus reacted with sera from patients that were suffering from nephropathia epidemica (a mild form of HFRS) (140). As more viruses were discovered it was observed that each of these viruses contained their own rodent reservoir (Table 1). A wide array of distinct hantaviruses have been detected in numerous rodent species throughout the world (27, 106, 111, 221). These viruses were eventually categorized within the *Hantavirus* genus.

In 1993 a new disease was recognized in the southwestern United States specifically in the Four Corners area, named for the area where Arizona, New Mexico, Colorado, and Utah meet. At the time, this new disease was termed "The Four Corners" disease, but was later described as hantavirus pulmonary syndrome (HPS) (138). A cluster of cases within this region were developing a disease with characteristics of influenza symptoms (i.e., fever, headache, muscle aches chills, etc.). Weeks after the initial outbreak, the virus was isolated and was termed the Sin Nombre (SN), which is Spanish for "No Name" virus. HPS cases developed the influenza symptoms noted above, but rapidly worsened to a respiratory disease that eventually led to shock and respiratory failure. Fluid and white blood cells accumulated in the lungs, causing hypoxia (low blood-oxygen levels), shock, and death, from a type of lung failure called

acute respiratory distress syndrome. HPS is also referred to as hantavirus cardiopulmonary syndrome (HCPS). Death occurred in approximately 50% of the cases presented (87). Within a short time, cases were found in other states throughout the United States. By the end of 1995, there were a total of 123 cases with a fatality rate of 51 percent, in over two dozen states. A similar disease was also identified in Canada, Brazil, Venezuela, and Argentina.

Hantavirus Classification

Although all hantaviruses share similarities in nucleic acid identities, genomic organization, and exhibit similar aspects of their life cycle, the differences in pathogenesis necessitated a classification system. Hantaviruses are now currently classified into two major groups: Old World and New World, which is predominantly based on the geographic distribution of their rodent hosts (181) (Fig. 1). Hantaviruses are rodent-borne, cause no known disease in their rodent reservoirs, and are transmitted by inhalation of aerosolized rodent excreta (Fig 2) (183). Old World hantaviruses, such as the HTN, PUU, and Seoul (SEO) viruses are known to cause HFRS, while New World hantaviruses, such as SN, Andes (AND) and Black Creek Canal (BCC) viruses cause HCPS (Table 1).

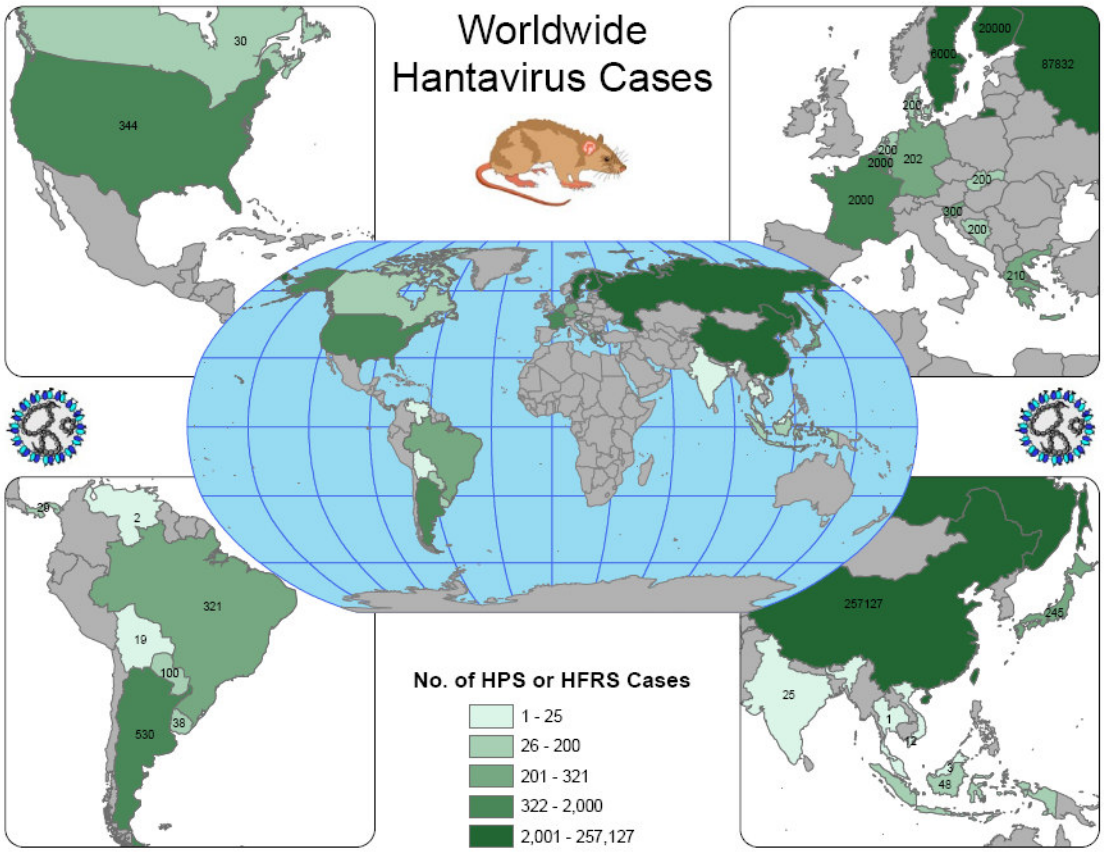

Figure 1: Map of viruses throughout the world (courtesy of Colleen B. Jonsson, Southern Research Institute, Birmingham, AL, Doug Goodin and Shawn Hutchinson, Geographic Information Systems Spatial Analysis Laboratory (GISSAL), Department of Geography, Kansas State University.

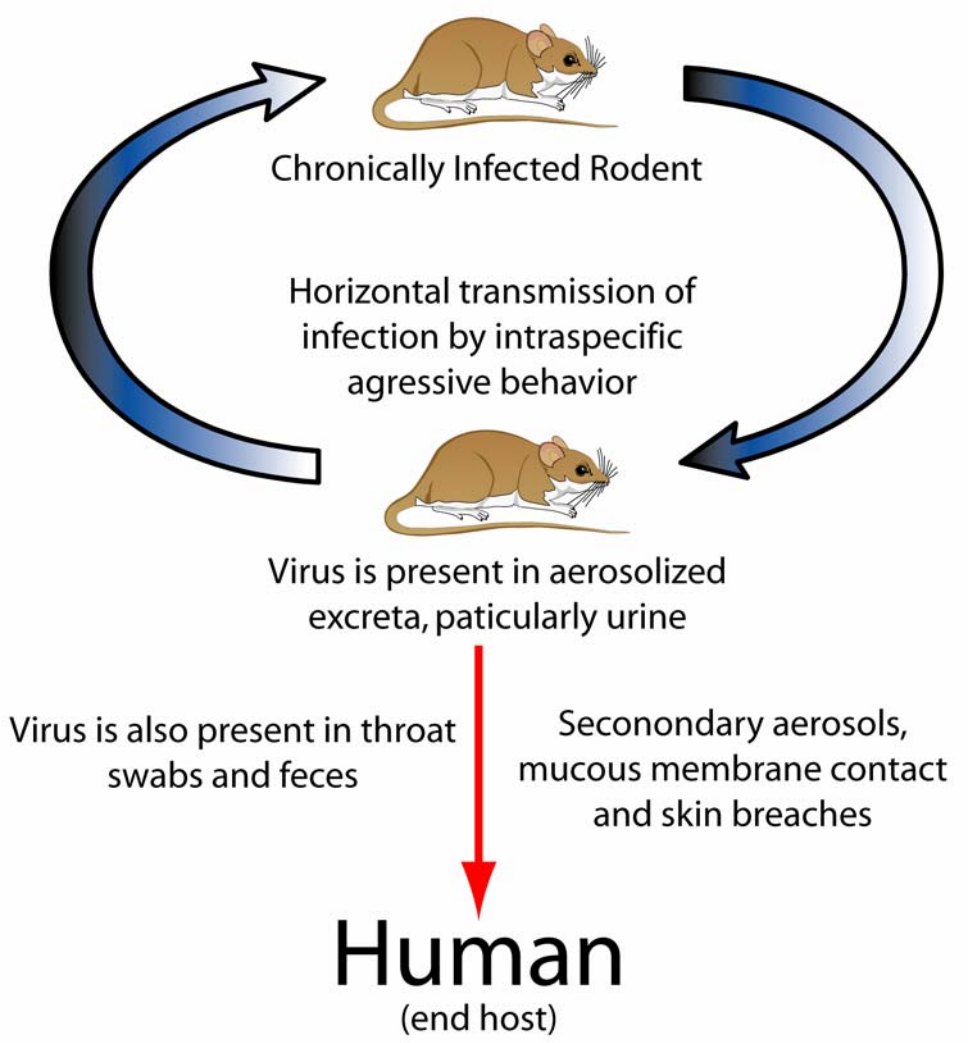

Figure 2: Transmission cycle of hantaviruses. Rodent hosts are asymptomatic to hantaviral infection. Hantaviruses are transmitted horizontally by aggressive behavior or through mating rituals. Infection in humans results through the inhalation of aerosolized excreta. Humans are incidental, dead-end hosts, which result in development of disease. Illustration was adapted from CDC.

Epidemiology and Ecology

Old World Hantaviruses

Immediately following the initial discovery of the HTN virus in 1976 (104, 105), epidemiological studies of HFRS significantly progressed. It was initially believed that HFRS only occurred in rural areas of Eurasia, specifically China, Korea, Eastern Russia, and Northern Europe (101), but later findings demonstrated that HFRS was present in urban cities and in many parts of the world (106). Initially, studies showed that farmers, soldiers and inhabitants of endemic regions had the greatest risk for exposure to rodents and HFRS, but the urban house rat, *Rattus norvegicus*, also harbors the virus. To facilitate the understanding of viral epidemiology, three epidemiological patterns of HFRS have been developed: rural, urban and animal room, which is based on the location of the outbreak, and the reservoir hosts of the disease.

Apodemus agrarius, the striped field mouse, is naturally found in rural areas, is the rodent reservoir for HFRS causing HTN virus (106). This mouse is most common in agricultural fields (26), but will invade houses during the winter months in search of food and shelter. Rural cases seem to occur bi-annually, with two seasonal peaks of cases occurring during the late spring and in the fall seasons. There are several factors could possibly play roles in the increased incidences of HFRS during the fall months, such as increased human activity in the fields during harvesting of crops, and the indoor relocation of rodents in preparation for the winter (97). The incidence of hantavirus in *Apodemus agrarius* is high in Asia during the late spring and early fall seasons. Most cases of HFRS occur in adult men ranging from 20 to 50 years of age (23, 101). There is a higher prevalence of HFRS in men than in women, which correlates with the usual

duties of men working outside in the fields while most women work at in home. HFRS cases in China are caused by the HTN virus, where about 100,000 cases are reported each year (23). Approximately 300 to 900 annual HFRS cases are estimated to occur each year in Korea and in Eastern Russia. HTN-related HFRS has been demonstrated to have a mortality rate of 10 to 15%.

Rattus norvegicus and *R. rattus*, commonly known as the house rat or domestic rat, are the main reservoirs responsible for the number of HFRS cases that occur in urbanized areas (102, 204). The common domestic rat is occurs throughout the world. Previously known as the rat virus, SEO virus is the only hantavirus known to cause HFRS in humans in urban areas. Other hantaviruses contain reservoir rodent hosts that are known to live and predominate in rural areas, while rodent reservoirs of SEO virus are found in urbanized areas. SEO virus related HFRS is rare outside of China and Korea. Over 100 cases of HFRS have been reported in large metropolitan areas of Seoul and other larger cities of Korea where patients had direct contact with the domestic rat (100). Some SEO related cases of HFRS have been observed in rural areas of China, but the majority of all cases are found in urban areas. The seasonality of SEO virus outbreaks are somewhat different from the HTN virus, with most outbreaks occurring in the spring and early summer (24).

PUU virus, the causative agent of nephropathia epidemica, is a milder form of HFRS and is found throughout Europe. The bank vole, *Clethrionomys glareolus*, plays host to the PUU virus. This virus has been found to affect both urban and rural communities of Sweden and Finland. The number of cases in rural areas usually peak in November and January, while most urban cases occur during August. A correlation has

been observed between the numbers of victims with the increased population of bank voles that cycle once every 3 to 4 years. In 1993 an outbreak PUU virus associated-HFRS was recorded in southern Belgium, which directly correlated with high number of bank vole populations (28). Similar outbreaks of HFRS have been observed in northeastern France and Germany that also correlate with the increase in the population of bank voles (154).

New World Hantaviruses

In 1993, a mysterious respiratory illness, similar to HFRS, was reported in the Four Corners region of the United States as having a high mortality rate. Tissue from infected patients and rodents caught near the patients' residences confirmed the disease was caused by a new hantavirus (138). This new finding helped spawn and advert much attention to virus associated-HCPS and New World Hantaviruses. These new viruses contained rodent hosts of the *Sigmodontinae* subfamily (Table 1). The virus was later termed the SN virus, originally Muerto Canyon virus, and has been found to be hosted by the rodent *Peromyscus* maniculatius, deer mouse. The SN virus has also been found in parts of Canada, where most HCPS-associated cases in both the United States and Canada occur through SN virus (131). As of 2001, approximately 280 cases of HCPS have been reported in the United States, spanning 30 states, with most cases occurring in the southwest, while approximately 35 cases have been reported in western Canada. Deer mice infected with the virus have been detected from Yukon to Mexico and from California to the Appalachian Mountains in the Eastern United States and Canada (128, 131). Similar to Old World Hantaviruses, HCPS disease caused by New World

Hantaviruses correlates with increased population of rodent hosts within the vicinity. The peak of HCPS cases occur in late spring or early summer, affecting both human male and females equally (87).

Another New World Hantavirus, BCC virus, was associated with a single event of HCPS in Florida (165). A serosurvey of rodents collected in the Florida region demonstrated that the cotton rat, *Sigmodon hispidus*, harbored BCC virus (165). The viral RNA was detected in the rodents by reverse transcriptase-polymerase chain reaction (RT-PCR). Nucleic acid sequences were determined for the complete S- and M- and partial L-segments. Although similar to the SN virus-associated HCPS, BCC virus-associated HCPS seemed to be predominantly pulmonary with less renal involvement (63, 86).

Numerous strains of New World Hantaviruses have been identified in Central and South America from 300 HCPS cases (219). Similar to other hantaviruses, transmission seems to stem from infected rodents with the exception of an outbreak that occurred in Patagonia (115). The outbreak in Patagonia was caused by the AND virus, which is harbored by *Olygoryzomys longicaudatus* (115). Investigations of the outbreak in Patagonia demonstrated a human-to-human transfer between a doctor and an infected patient (146, 219). The AND virus has a high mortality rate of approximately 50%.

Hantavirus Pathogenesis

World-wide, approximately 150,000 to 200,000 cases of HFRS are reported each year, with more than half occurring in China (42). Depending on which virus strain that is causing disease, variations of mortality may occur. Death occurs in less than 0.1% in

patients infected with the PUU virus. Fatalities as high as 15% have been observed for HFRS caused by the HTN virus. More than 250 cases of HCPS have been reported throughout North and South America. Fatality rates also vary for HCPS related deaths, ranging from 30 to 50% for disease caused by SN and AND viruses, respectively. Other hantaviruses from South America, such as Laguna Negra, have death rates ranging from 5 to 15%.

Rodent Infections

Although both Old World and New World Hantaviruses have distinct pathogenesis in humans, no disease occurs in their rodent hosts in which they establish a persistent infection, lasting months to several years (103). Hantaviruses are transmitted horizontally from rodent-to-rodent, with a higher prevalence in males. Higher prevalence in males is possibly due to the use of aggressive behaviors, such as scratching and biting, through aggressive territorial encounters or during mating seasons when males compete for females (53). Infectious aerosolized excreta may be another mode that can play roles in horizontal transmission.

Since hantaviruses cause asymptomatic, persistent infections in rodents, it is easily conceivable that the dynamics of a hantavirus infection is different in humans. Typically in rodents, virus infection leads to replication with a peak in viremia within 2 weeks post-infection. After these initial 2 weeks the virus can be found in most parts of the body, with the highest virus antigen titers in the lungs and kidneys, with a more preference for endothelial cells (137). The virus is reduced and eventually cleared from the rodent without ever developing any signs or symptoms of disease, then shed from the

feces and urine (139). Shedding of virus usually peaks at approximately 2 to 10 weeks post-infection (67, 103). The rodent host produces antibodies against the viral antigen, which are usually detectable at 14 days post-infection (139). The antibody titer usually peaks at 50 days post-infection and remain in the rodent for the remainder of its life (139). Although these rodents produce neutralizing antibodies, hantaviruses are capable of persisting in these animals for weeks or months with continuous shedding of virus.

Human Infections

The progression of a diseased state in HFRS or HCPS cases depends on the type of hantaviral infection. As previously stated above, transmission to humans is usually the result of inhalation of infectious aerosols produced from the rodents' excreta. Following exposure, an incubation period of approximately 7 to 21 days takes place before the development of illness. Clinical progression and manifestations of disease caused by HFRS and HCPS is outlined by five overlapping stages: febrile, hypotensive (HFRS) or cardiopulmonary (HCPS), oliguric, diuretic, and convalescent (100, 157, 190).

Disease begins with influenza-like symptoms, headache, backache, fever and chills. Once the infection has entered the febrile phase, lasting approximately 3 to 6 days for both HFRS and HCPS, slight hemorrhage manifestations are evident in the conjunctiva. This stage is characterized by headache, fever, vertigo, nausea, and myalgia. The clinical symptoms of the febrile stage eventually advance to the hypotensive (HFRS) or cardiopulmonary (HCPS) stage. Both stages are characterized by thirst, restlessness, nausea and vomiting, each lasting hours or days. Approximately one third of all patients suffering during the hypotensive stage (HFRS) develop shock and mental confusion (99).

Symptoms of vascular leakage, abdominal pain and tachycardia are observed within this stage. Shock, pulmonary edema and hypotension are observed in patients suffering from HCPS during the cardiopulmonary stage. The oliguric phase lasts from 1-16 days for HFRS or 4 to 24 hours for HCPS. Conjuctival, cerebral and gastrointestinal hemorrhage occurs in about one third of all patients (99). The oliguric stage accounts for approximately one-half of all hantavirus related deaths (116). Although a patient may completely recover from HFRS or HCPS, which may take from several weeks to months, renal or pulmonary dysfunction may persist for the life of the patient. Although there is currently no effective treatment for disease caused by hantaviruses, ribavirin could serve as a possible candidate (187).

Virion Structure, Morphology and Physical Characteristics

Virions within the *Bunyaviridae* are spherical in nature with an average diameter of approximately 80-120 nm (65, 121, 124, 183, 220)(Fig. 4). Due to the large number of viruses within this family, structures can range between 78-210 nm in diameter (65, 121, 124, 183, 220). Although generally spherical, some elongated or elliptical forms may exist, specifically within the hantavirus genus.

The virion particles contain a host-derived lipid bilayer that is approximately 5 to 7 nm thick. The lipid bilayer is derived from either of two sources, the cellular plasma membrane or the Golgi apparatus. The outer surface of the lipid bilayer contains glycoprotein (GP) projections that are approximately 5 to 10 nm in length. These GP projections are comprised of heterodimers of the two GPs, G_n (formerly designated G1) and G_c (formerly designated G2). Studies on the La Crosse (LAC) virus, family

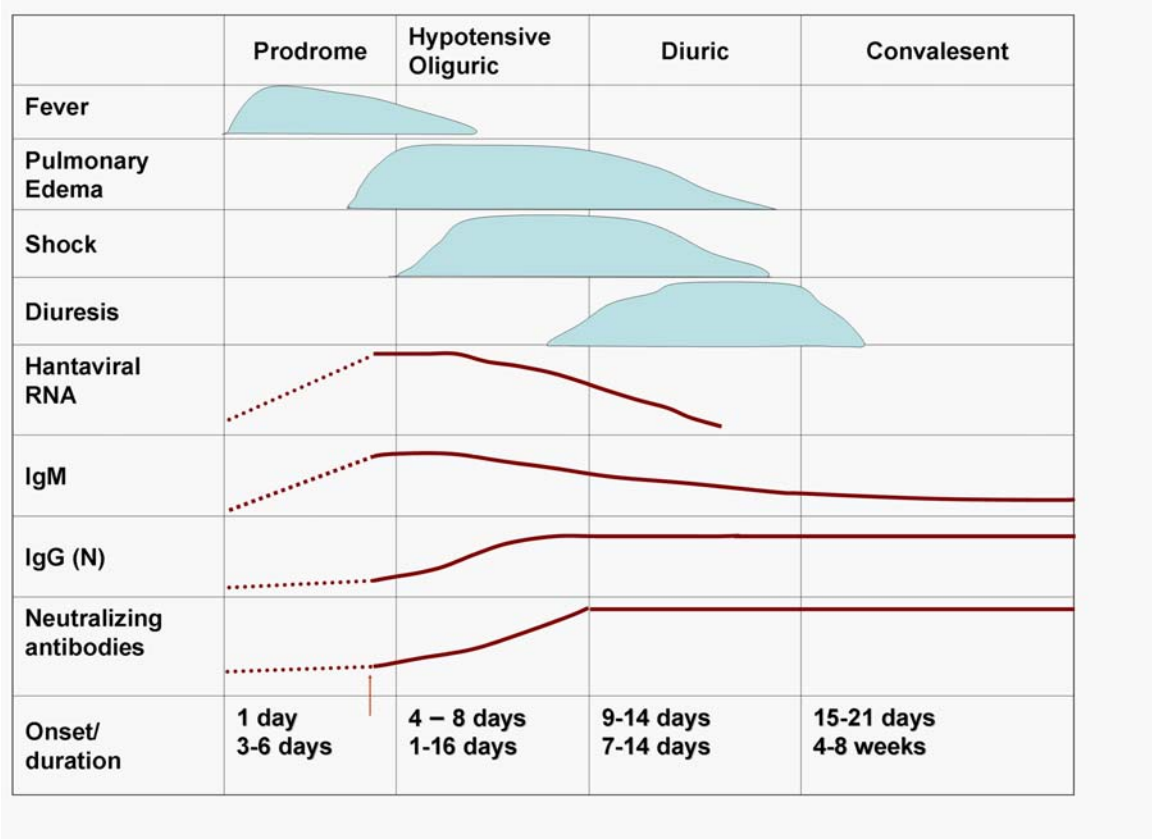

Figure 3: Clinical progression of HCPS (73). Note: From "Treatment of hantavirus pulmonary syndrome" by C.B. Jonsson, J. Hooper, and G. Mertz, 2008, *Antiviral Research*, 78, p. 162. Copyright 2007 by Elsevier B.V. Reprinted with permission.

Table 2: Clinical manifestations of disease caused by HFRS and HCPS (100, 157, 190)

Infection Phase	HFRS	HCPS
Febrile	Duration: 3-6 days Headaches, fever, dizziness, myalgia, nausea, anorexia	Duration: 3-2 days (range 1-12 days) Fever, myalgia, dizziness, nausea, anorexia
Hypotensive (HFRS) or Cardiopulmonary (HCPS)	Duration: 24h – 5 days Hypotension, shock (1/3 of patients) lumbar, backache, abdominal pain, visceral hemorrhage, tachycardia and mental confusion	Duration: 4-24 h Shock and pulmonary edema, hypotension and oliguria, dysnea, hypoxemia, drop in myocardial index to less than 2.21/min/m2
Oliguric	Duration: 1-16 days Hiccups, vomiting, rare CNS bleeding	Duration: 4-24 h Rapid clearance of pulmonary edema and resolution of fever and shock, spontaneous diuresis
Polyuric	Duration 9-14 days	
Convalescent	Duration: 3-12 weeks Patients regain weight, myalgia, polyuria and hypothenuria	Duration: Up to 2 months Patients recover fully but may have pulmonary dysfunctions

Orthobunyaviridae, show that approximately 270 to 1400 GP projections per virion exist (141). The structure of the virion surface can vary among viruses within the *Bunyaviridae*. Viruses within the *Hantavirus* genus have a square grid-like pattern (220).

The interior makeup of the virion particle consists of tightly packed ribonucleocapsids (RNPs). The three RNA genome segments, Small (S), Medium (M), and Large (L), are individually complexed with the N protein to form the three RNP structures (31, 142). These RNP complexes are the source of the virus' internal filamentous or coiled bead appearance (41). Studies have shown that the chemical composition of the Uukuniemi (UUK) virus, family *Phlebovirus*, comprise 2% RNA, 58% protein, 33% lipid, and 7% carbohydrate (143). It is presumed that since these viruses lack a matrix protein, the N protein from the three RNPs physically interact with the GP projections on the inner leaf of the lipid membrane.

Hantaviruses share similar physical properties to those of other viruses in the family *Bunyaviridae (133)*. The density of the HTN virus can range from 1.16 to 1.18 g/cm^3 in sucrose, and 1.20 to 1.21 g/cm^3 in CsCl. Treatment of the HTN virus with non-ionic detergents releases the three RNPs that sediment to densities of 1.18 and 1.25 g/cm^3 in sucrose and CsCl, respectively, using rate-zonal centrifugation methods (178, 179). Treatment of virus particles with lipid solvents or non-ionic detergents results of loss of infectivity in arthropods and mammals (143).

As previously indicated, transmission of hantaviruses is usually through the inhalation of rodent excreta. For the virus to be considered infective, the virus must remain viable in rodent urine, feces, and saliva or in dust aerosols for several days post-excretion. Studies show that the HTN virus can remain viable for 30 min in buffers from

pH 6.6 to 8.8 and in the presence of 10% fetal bovine serum (FBS), from pH 5.8 to 9.0 (176). HTN virus is infectious at temperatures ranging from 4 to 42 °C in the presence or absence of serum, and can remain infectious for 1 to 3 days when at least 10% serum is present in dried samples. These physiological limits fall within the range of their respective hosts, because the urine pH of rodents can vary from 5.5 to 8.0 and may contain as much as 30 mg of protein (77).

Genome Structure

The genomic structure of the *Hantavirus* genus is quite universal from member to member. They are negative-sensed, single stranded RNA viruses with a tripartite genome consisting of the L, M and S-segments encoding the RNA-dependent RNA polymerase (RdRp) or L-protein, the two GPs (G_n and G_c), and the N protein respectively (181, 183) (Fig. 4). The HTN virus gene sizes of S, M and L-segments are 1696, 3616, and 6533 nucleotides respectively (183). The terminal nucleotide sequences at the 5' and 3' are highly conserved between each segment. The terminal sequences are complimentary to each other and are believed to form a panhandle-like structure due to the base pairing of the terminal sequences (61) (Table 3). In support of this, electron microscopy studies of RNA extracted from the UUK virus revealed three different sizes of circular RNA (61). The terminal sequences are highly conserved between viruses within a respective genus, but are different from viruses from other genera (Table 3). The finding that viruses within the *Hantavirus* genus contained conserved and complementary sequences served as a basis to include these viruses within the *Bunyaviridae* family (178, 179).

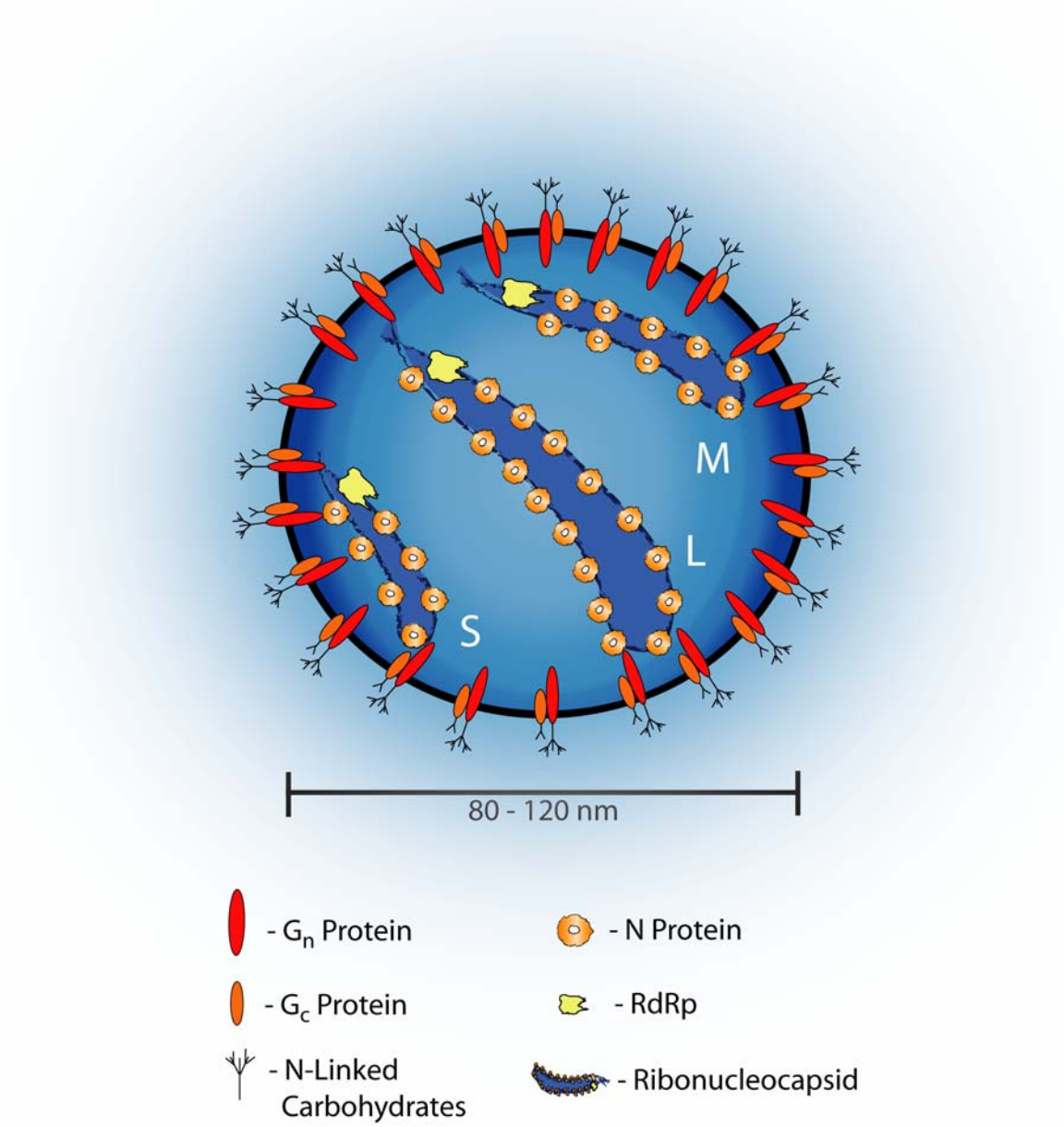

Figure 4: Schematic illustration of a virion particle. Glycoprotein projections are shown at the surface and the internal tripartite genomic structure of the ribonucleocapsids.

Although the terminal nucleotide sequences may differ from genus-to-genus, these regions could play similar and significant roles in the virus life cycle, such as RNP formation, and possibly replication and transcription (158). It is understood that the N protein encapsidates or complexes with the three RNAs to form individual L, M, and S nucleocapsids. Encapsidation was evident when helical structures, consisting of viral RNA and N protein, were observed in the LAC virus (158). LAC virions treated with nonionic detergents resulted in release of RNP structures that were observed to be in circular form, and were comprised of 4% RNA and 96% protein (158). This fully demonstrates that the 3' and 5' complementary ends can base-pair while complexed with the protein. Furthermore, using psoralen cross-linking studies, it was validated that LAC virus circular RNA was a combinations of RNA and protein (158). Within the *Tospoviridae* genus, using atomic force microscopy, the tomato spotted wilt (TSW) virus showed to contain three different lengths of ring-like structures, hence the three different RNPs (61). These ring-like structures are very reminiscent of the RNPs from other viruses from other genera within the *Bunyaviridae* family.

A mature virion particle must contain at least one each of the L, M, and S RNPs for infectivity, however equimolar amounts of each RNP may not always be packaged, as suggested by various reports of equimolar and nonequimolar rations of L, M, and S RNAs in virion particles (16, 66). Unequal packaging of the three RNPs is one possibility for the difference in virion particle size that has been observed by electron microscopy (207). It is also possible that in addition to viral RNA (vRNA), complementary sense RNA (cRNA) may get packaged into mature virion particles (91,

193), which can further substantiate the pleomorphic structures. It has been suggested that the packaging of cRNA gene(s) may play a role in early replication processes (68).

Coding Strategies of Viral Genes

Viruses within the family *Bunyaviridae* have similarities and differences in coding of their viral genes. Some viruses use negative-sense coding strategies, such as the orthobunyaviruses, hantaviruses, and nairoviruses, while phleboviruses and tospoviruses use ambisense coding strategies. All viruses within the *Bunyaviridae* encode the main structural proteins (N, G_n, G_c, and RdRp), while certain viruses encode nonstructural proteins from their cRNA or vRNA. Phleboviruses encode nonstructural proteins from the M-segment cRNA and from their S-segment vRNA, while orthobunyaviruses encode only from the S-segment cRNA. Tospoviruses have been known to encode nonstructural proteins from both M- and S-segment vRNAs. Of all the coding strategies within the *Bunyaviridae*, the *Hantavirus* genus is the simplest, because they do not code for non-structural proteins, only structural proteins.

S-segment Coding Strategies

All viruses within the family *Bunyaviridae* encode the N protein from the S-segment. The S-segment is the smallest segment, which ranges from approximately 900 nucleotides and up to 3,000 nucleotides in size (Table 3). Orthobunyaviruses, such as the Bunyamwera (BUN) virus, generally have the smallest S-segments as compared to other genera (Table 3). The S-segment of the orthobunyaviruses encodes two polypeptides, the N protein and an S-segment nonstructural protein (NSs) utilizing overlapping open

Table 3: Terminal nucleotide sequences and genome sizes of the S-, M-, and L-segments of representative members of the family *Bunyaviridae* (183)

Genus – Virus	Consensus S, M, L Terminal Nucleotides	S-segment Size	M-segment Size	L-segment Size
Orthobunyavirus	3'UCAUCACAUG-	961	4458	6875
BUN virus	5'AGUAGUGUGC-			
Hantavirus	3'AUCAUCAUCUG-	1696	3616	6533
HTN virus	5'UAGUAGUAUGC-			
Nairovirus	3'AGAGUUUCU-	1712	4888	12255
DUG virus	5'UCUCAAAGA-			
Phlebovirus	3'UGUGUUUC-	1690	3885	6404
RVF virus	5'ACACAAAG-			
Tosporivurs	3'UCUCGUUA-	2916	4821	8890
TSW virus	5'AGAGCAAU			

*Bunyamwera (BUN), Hantaan (HTN), Dugbe (DUG) Rift Valley fever (RVF), and Tomato spotted wilt (TSW) viruses

reading frames (ORF) in the cRNA (Fig. 5) (16). Several other members within this genus have also demonstrated to encode NSPs (44).

Members of the *Hantavirus* and *Nairovirus* genera encode the largest N proteins within the *Bunyaviridae*, ranging from 48-54 kDA in size (120, 182). These viruses contain a single ORF that do not encode NSPs (120, 182). Differences have been observed in the 3' noncoding regions of some hantaviruses. The SN virus contains more than 700 nucleotides with numerous repeated sequences. It is believed that polymerase slippage is the cause of these long repeats (197).

Phleboviruses and tospoviruses are the only members that utilize ambisence coding strategies within their S-segment. Evidence that they utilize such a strategy comes from time-course studies. The UUK virus, *Phleboviridae* genus, N protein was detected from 4 to 6 hours post-infection, while the NSPs were not present until 8 hours post-infection (193, 212). Similar, the mRNA for NSPs of the TSW virus was only detected 15 hours after the N protein was detected (199).

M-segment Coding Strategies

The M-segment contains a single ORF that encodes the glycoprotein precursor complex (GPC), which is then processed and proteolytically cleaved in the endoplasmic reticulum (ER) into the two envelope GPs (G_n and G_c). The M-segment ranges in size from approximately 3,600 nucleotides for hantaviruses up to 4,800 nucleotides for tospoviruses. Most viruses within the *Bunyaviridae* do not encode M-segment nonstructural proteins (NSm) with the exception of a few viruses within the *Orthobunyaviridae*, *Tospoviridae*, and *Phleboviridae*. Orthobunyaviruses contain a

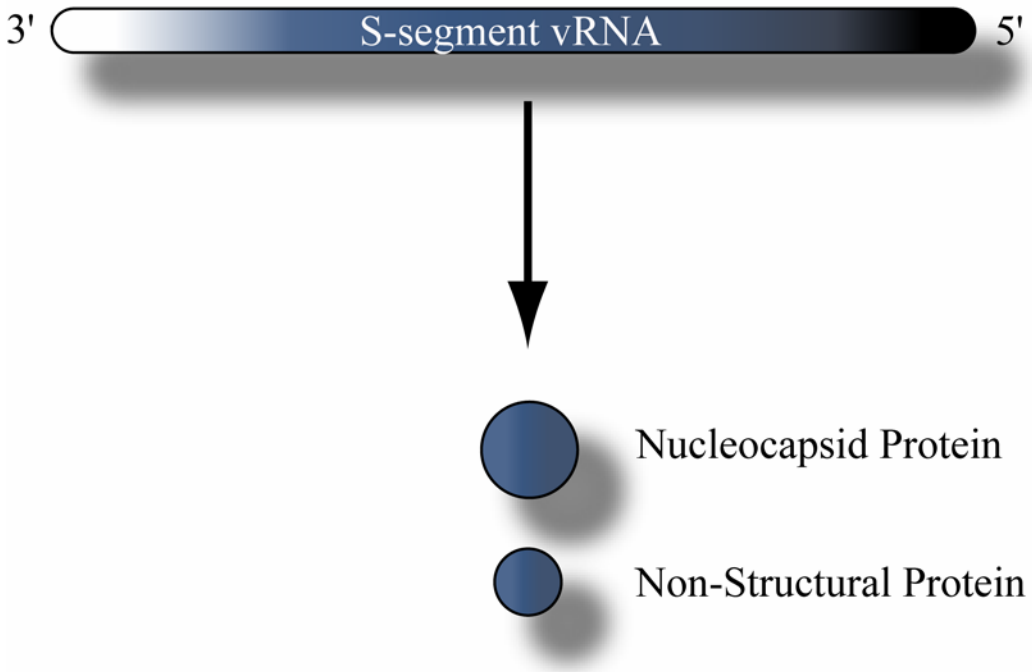

Genus	Protein (size)
Orthobunyavirus	N (19-25 kDa) NSs (10-13 kDa)
Hantavirus	N (50-54 kDa)
Nairovirus	N (48-54 kDa)
Phlebovirus	N (24-30 kDa) NSs (29-31 kDa)
Tospovirus	N (29 kDa) NSs (52 kDa)

Fig. 5: Representative nucleocapsid protein sizes from each genus.

unique region between the G_n and G_c of the M-segment that encodes the NSm (46). Tospoviruses utilize ambisense strategies, similar to the coding strategies of the S-segment, to generate NSm. The NSm of tospoviruses is readily detected in infected plants, and seems to play roles in bridging infected cells with non-infected cells by the use of plasmodesmata (91, 202).

L-segment Coding Strategies

The L-segment contains a single ORF that directly encodes the viral RdRp. All viruses within this family use negative sense coding strategies. As with the other segments, the L-segment can vary in size. Hantaviruses, orthobunyaviruses, and phleboviruses contain the smallest L-segments (approximately 6,000 nucleotides), while tospoviruses and nairoviruses contain largest L-segments of 8,000 and 12,000 nucleotides, respectively.

Hantaviral Proteins

Nucleocapsid Protein

The N protein is the most abundant viral protein synthesized in cells infected with viruses within the family *Bunyaviridae*. Early in infection, the N protein is expressed abundantly and plays major roles in important steps in the virus life cycle (181). The N protein mRNA has been detected and measured as early as 6 hours post-infection before any other mRNA, suggesting that the N protein mRNA is the first viral RNA that accumulates in significant quantities (66). Accumulation of N protein has also been observed to coordinate with the increased levels of N protein mRNA (183). Using

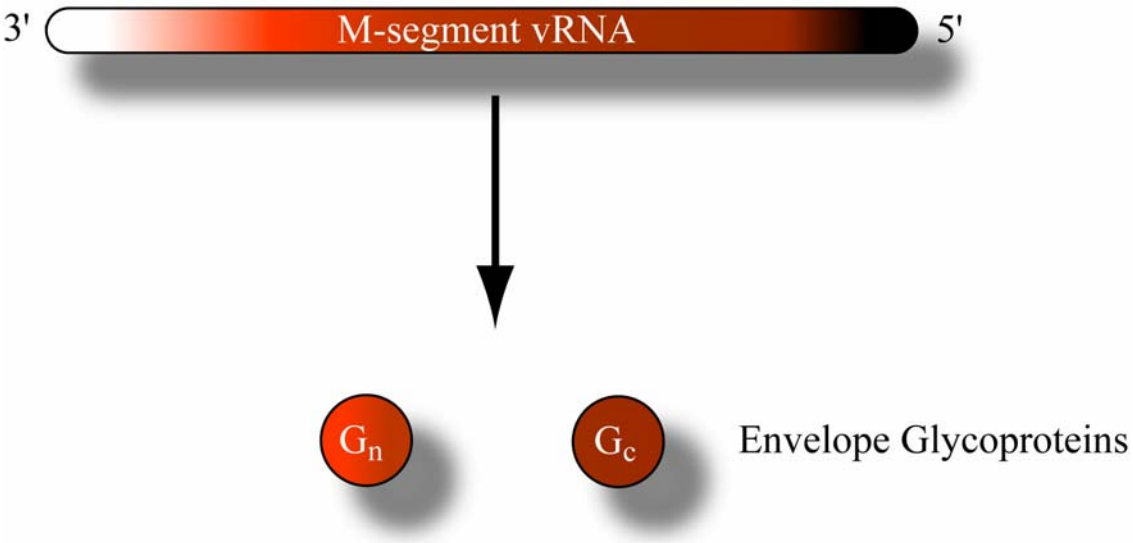

Genus	Protein (size)
Orthobunyavirus	NSm (15-18 kDa) G_n (29-41 kDa) G_c (108-120 kDa)
Hantavirus	G_n (68-76 kDa) G_c (52-58 kDa)
Nairovirus	G_n (37 kDa) G_c (75 kDa)
Phlebovirus	NSm (none-30 kDa) G_n (50-75 kDa) G_c (50-75 kDa)
Tospovirus	NSm (34 kDa) G_n (52-58 kDa) G_c (78 kDa)

Fig. 6: Representative glycoprotein sizes from each genus.

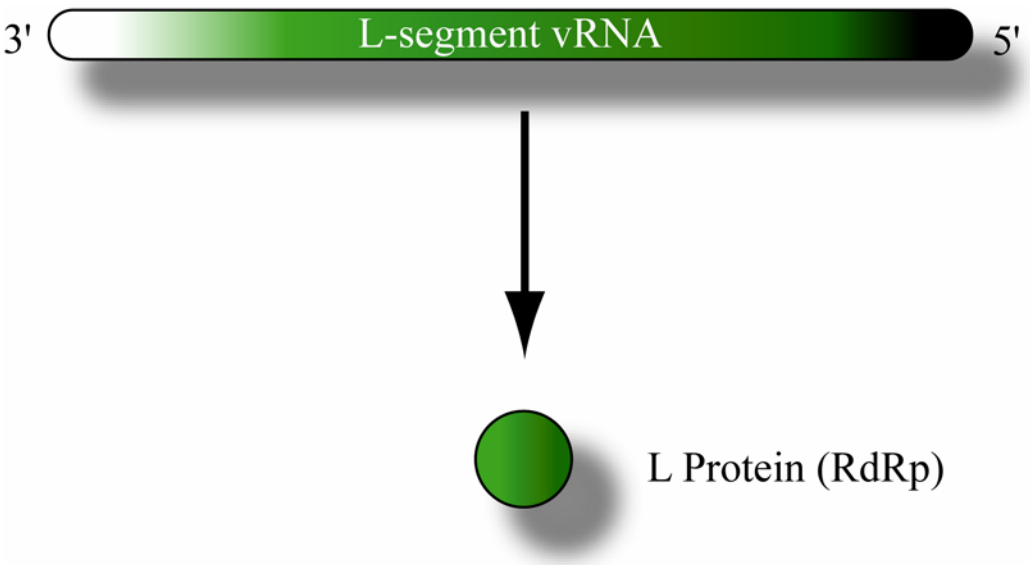

Genus	Protein (size)
Orthobunyavirus	L (259 kDa)
Hantavirus	L (246 kDa)
Nairovirus	L (459 kDa)
Phlebovirus	L (237 kDa)
Tospovirus	L (331 kDa)

Fig. 7: Representative RdRp sizes from each genus.

immunogold labeling techniques, the N protein appears to manifest granular or filamentous formations within the cell. These formations are known as inclusion bodies, and are very specific to hantavirus infections.

Hantaviruses encode a larger N protein than other viruses within the *Bunyaviridae* (Fig. 7) (181). The N protein of the *Hantavirus* genus vary in size, ranging from 48-kDa to 54-kDa. Members of the *Orthobunyaviridae* have the smallest forms of N protein, ranging from 19- to 25-kDa (Fig. 7). The N proteins of HTN, SEO, PUU, PH, and SN viruses are 50% or greater in identity. Some regions of these N proteins are highly homologous, while other regions containing less homology. For example, the carboxy terminus (amino acids 340-433) of the hantavirus' N proteins is highly homologous (85%); while a central region (amino acids 240-310) are only 11% homologous. These closely conserved sequences are sufficient enough to generate an immune response that is cross-reactive from virus-to-virus. Studies have demonstrated that antibodies raised against the N protein of one virus can cross-react with other N proteins from other hantaviruses (34, 117, 171, 204).

As mentioned, the N protein is multi-functional and should also play significant roles in virus assembly and budding (Fig. 8). Generally, the N protein protects the viral genomic RNA from nuclease degradation and facilitate the formation of RNP complexes (183). The N protein may interact with the cytoplasmic tail of the G_n for virus assembly to occur (153) and the L protein (72).

A key question in trafficking is how the viral proteins navigate within the cell. The N protein is known to traffic to the perinuclear region, specifically targeting

perinuclear components. The N protein of the BCC virus accumulates in the Golgi apparatus during perinuclear targeting (162). The association of the N protein with the Golgi apparatus has also been demonstrated in cells infected with the UUK virus (69, 153). Our studies showed that the HTN virus N protein specifically targets the ER-Golgi-intermediate compartment (ERGIC) and not the Golgi apparatus (159, 160). Expression of the N protein alone leads to the formation of N protein-like structures without the forming virus-like particles (15).

The N protein of the BCC virus, a New World hantavirus, has been shown to associate with actin microfilaments during virus infections (164). The treatment of infected cells with actin depolymerizing agents such as cytochalasin D (CytD) showed to reduce the yields of virus progeny produced (164). We also showed that the HTN virus N protein associates with cytoskeletal elements. Vero E6 cells were treated with nocodazole (NOC) or CytD, which depolymerize microtubules or actin, respectively. Our laboratory demonstrated that NOC affected the normal distribution of the HTN virus N protein, and reduced the levels of intracellular viral RNA (159). This association with microtubules was also found to be dynein-dependent, where we expressed a dominant negative form of dynamitin, which reduced the accumulation of N protein at the perinuclear region (159)

It was also demonstrated that the BCC virus N is a peripheral membrane-associated protein (162). Although posttranslational modifications of the N protein have not been described, the N protein has been demonstrated to interact with cellular components. HTN and SEO (98, 118), and Tula (TUL) (81) viruses interact with intracellular proteins, such as the small ubiquitin-like modifier (SUMO-1) and ubiquitin

conjugating enzyme 9 (Ubc9). Other SUMO-1 related molecules were also involved (98). Conjugation of viral proteins with SUMO-1 related molecules has been implicated in subcellular localization. The PUU virus N protein has been observed to interact with the apoptotic enhancer Daxx (110). Daxx binding suggests that the N protein could possible play roles in regulating apoptosis. The antivirally active MxA proteins have also been demonstrated to associate with the N protein of other family members (1, 58, 84, 167). Recently, the HTN virus N protein has been observed to inhibit the nuclear import of NF-κB, possibly through the interactions with importin molecules (209).

Although the full crystal structure of the hantavirus N protein has not been solved, using X-ray crystallography and NMR spectroscopy, the structure of the amino-terminal region of the SN and AND viruses has been defined (18, 218). The site of protein-protein interaction was determined to reside within the amino terminal 71 residues of the phlebovirus N protein (96). Amino acids 1-74 of the AND virus N protein contain a coiled-coil domain that is comprised of positively and negatively charged surfaces involving conserved polar residues that facilitate the functionality of N protein (18, 218). Although the presence of amino-terminal, coiled-coil motifs within the SN virus have been demonstrated to facilitate N protein trimerization (4), the crystal data suggest trimerization is not initiated by this region, due to the formation of intramolecular antiparallel coiled-coils (18). The SNV N protein has been observed to naturally trimerize *in vitro* and *in vivo* conditions (3); the trimeric form being the most stable form (8). Oligomerization has also been observed in TUL virus as well (80). The carboxy-terminal amino acids 393 to 398 were shown to be crucial for trimerization, while amino-terminal amino acids 1 to 43 facilitate interactions by providing a secondary, stabilizing

interaction site (79). Similar homotypic interactions were also observed in other viruses, such as SN and HTN viruses, showing both amino- and carboxy-terminal regions to be involved (3, 223). It has been postulated that N-N interactions assemble on the viral RNA, followed by further protein-protein interactions that facilitate the formation of trimers, eventually encapsidating the entire RNA (79), but other mechanisms could play roles. It is quite possible that the interaction between N and viral RNA could be the bridge to help facilitate N-N interactions. Chemical cross-linking experiments demonstrated that the N protein of the Bunyamwera (BUN) virus was able to form various ranges of dimers and trimers, using a head-to-head and tail-to-tail configuration (108). Deletion of the N- or C-terminal regions of the N protein resulted in a loss of function and abrogated multimerization (108). Similar findings were observed in the TSW virus (74, 211).

The N protein interacts directly with the vRNA (8, 55, 130, 185, 188, 222) in the formation of the RNP complex and is speculated to play roles in facilitating the transcription/replication switch. The vRNA binding domain of the HTN virus N protein has been characterized to reside within a centrally conserved region spanning amino acids 195-217 (222). In contrast, the amino- and carboxy-terminal regions of the TSW virus were observed to play roles in RNA binding (168). RNA binding studies with bacterially expressed hantavirus N protein showed that N preferentially interacts with the 5' end of the vRNA (145, 188). *Cis*-acting signals in the 5' end of the vRNA play roles in promoting its encapsidation (188). Specific and nonspecific interactions during encapsidation have been observed (188). These studies showed that during encapsidation, the N protein initially complexes with vRNA at the 5' end, single-stranded

regions of the stem-loop secondary structure. The N protein is more strongly associated with the 5' end of the vRNA and N-vRNA complexes are susceptible to digestion with RNase V1, a double-stranded nuclease, but not with RNase T1, a single-stranded nuclease (188). This data suggests that during encapsidation, mono- or dimeric N proteins bind specifically to single-stranded 5' vRNA, which promote cooperative association of additional N protein molecules, resulting in the formation of the trimeric form and a fully encapsidated vRNA.

Other reports demonstrate that the N protein binds with high affinity to the vRNA panhandle (double-stranded vRNA), and its conformation is altered upon binding (8, 130). It was also demonstrated that binding was specifically through preformed N protein trimers (130). N protein trimers were able to discriminate between vRNA and non-vRNA, while monomeric or dimeric forms bound nonspecifically to RNA (8, 130). This data suggests that multimerization of N protein, specifically the trimeric form, is required for vRNA binding and encapsidation. The panhandle structure may play a role as a trigger for encapsidation or at another step in the viral life cycle.

Envelope Glycoproteins

The M-segment is the second largest virus gene (Fig. 6). The two GPs, G_n and G_c, are translated from a single polyprotein termed glycoprotein precursor complex (GPC) (Fig. 9). Various sizes of G_n and G_c have been observed within this family, ranging from 68 to 76 kDa for G_n and 52 to 58 kDa for G_c within the *Hantavirus* genus. Other members, such as orthobunyaviruses, have a much larger G_c (108 to 120 kDa) protein than G_n (29 to 41 kDa). GPs have a cystein content of approximately 4 to 7%.

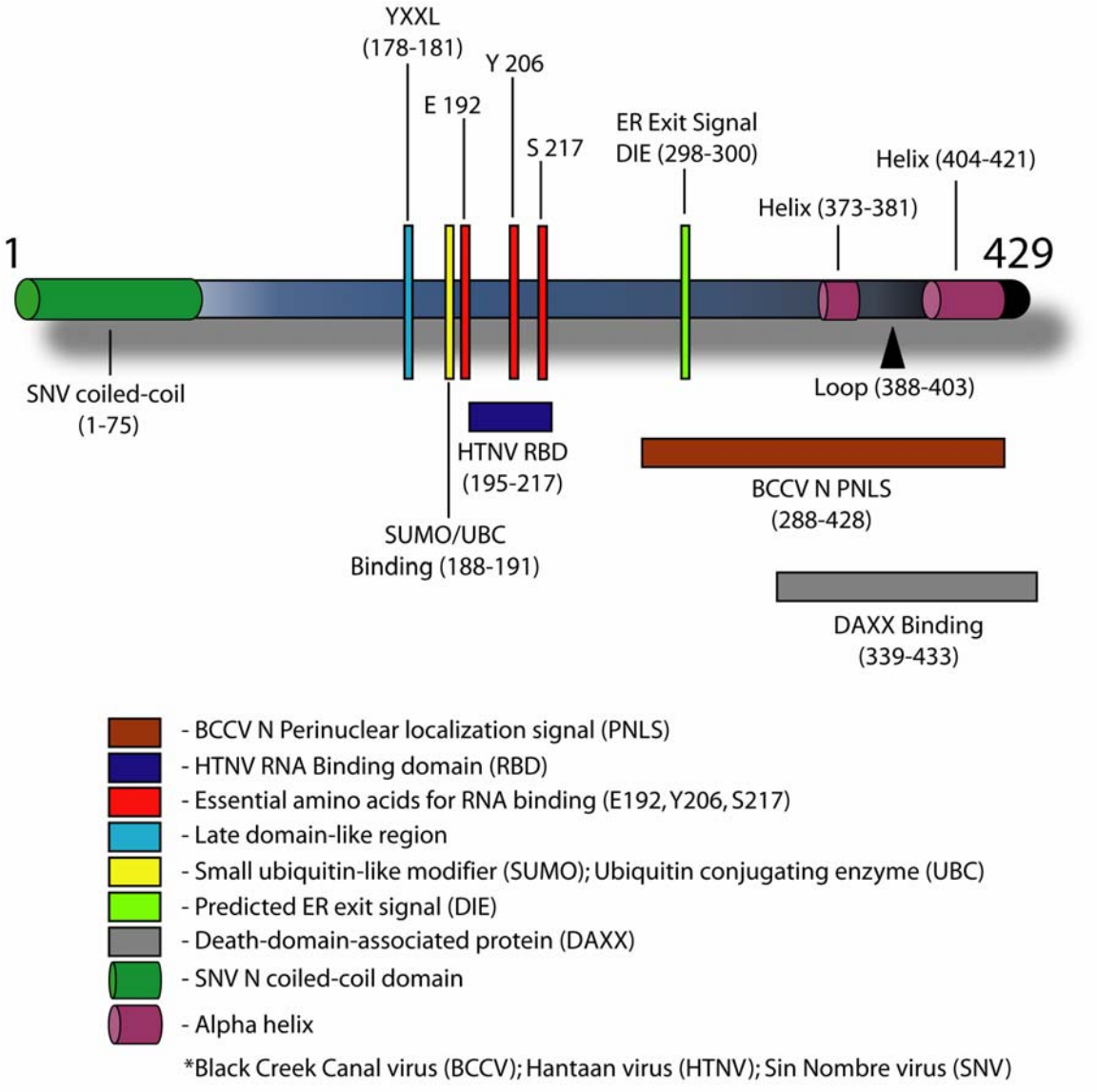

Fig 8: Structure of the N protein and various domain regions relative to its multi-functionality.

The positions of the cystein residues are highly conserved among hantaviruses. This data, and being that their amino acid sequences are approximately 93% in identity, suggest similarities in protein structure between viruses.

Uncleaved GPC has never been detected in virus-infected cells or in cells expressing the M-segment from cDNA (150, 184), however it can be artificially created *in vitro* (212). Both G_n and G_c that facilitate co-translational cleavage of the GPC in the ER (47). Using mutational analysis, a pentapeptide motif (WAASA), highly conserved among hantaviruses, was shown to be the cleavage site for the HTN virus (113). Deletion of this region abrogated cleavage of the GPC. The host proteases that mediate co-translational cleavage of the GPC are not known. Interestingly, although both G_n and G_c are the direct products of the GPC, both posses their own functional signal sequences (183). Unlike the G_c, the exact carboxy-terminus sequence of the G_n is not known for any of the members of this family, with the exception of the snowshoe hare (SSH) virus (46).

GPC polypeptides have variable transmembrane regions and a hydrophobic segment at the carboxy-terminus, which is highly suggestive of a membrane anchor region (Fig. 9). These proteins are regarded as class 1 membrane proteins, where the amino terminus is exposed on the surface of the virion and the coarboxy-terminus is anchored in the virus membrane. Hydropathy plots of the hantavirus M-segment showed similarities between HTN, DOB, SEO, PUU, PH, and SN viruses, despite having small amino acid sequence identities of 34% and 44% for G_n and G_c, respectively (176).

All viruses within this family contain asparagine-linked (N-linked) oligosaccharides. The N-linked oligosaccharides on the two GPs of hantaviruses were found to be made of mannose (180). Examination of these oligosaccharides in orthobunyaviruses revealed a major difference between G_n and G_c. The G_n contains complex oligosaccharides, while G_c has mostly high mannose glycans (152).

RNA-Dependent RNA-Polymerase (RdRp)

The RdRp or L protein is the largest viral protein encoded by the L-segment. The L protein of the *Bunyaviridae* ranges in size from 237 kDa for phleboviruses to 459 kDa for nairoviruses (Fig. 7). Hantavirus L protein is approximately 246 kDa in size (Fig. 7). To date, there are no known post-translational modifications known (214). Although a crystal structure is not available, it has common features similar to other polymerases (94).

The shape of the polymerase is compared to that of a right hand, with fingers, palm, and thumb domains. An X-ray crystal structure of the poliovirus RdRp shows structural conservation, with some differences observed in the thumb and fingers (59). Sequence alignments of several RNA virus polymerases reveals four conserved motifs in the palm region, which have been designated A-D. These conserved regions are shared amongst many viruses, specifically unsegmented and segmented negative-strand RNA viruses, positive strand viruses, and retroviruses (132, 144, 156). Sequence alignments of several members of the family *Bunyaviridae* also show conservation of motifs A-D (72). Motifs A and C are involved in divalent cation use, such as magnesium, while motif A and B may be involved in sugar and nucleoside selection (183). Motif C contains the

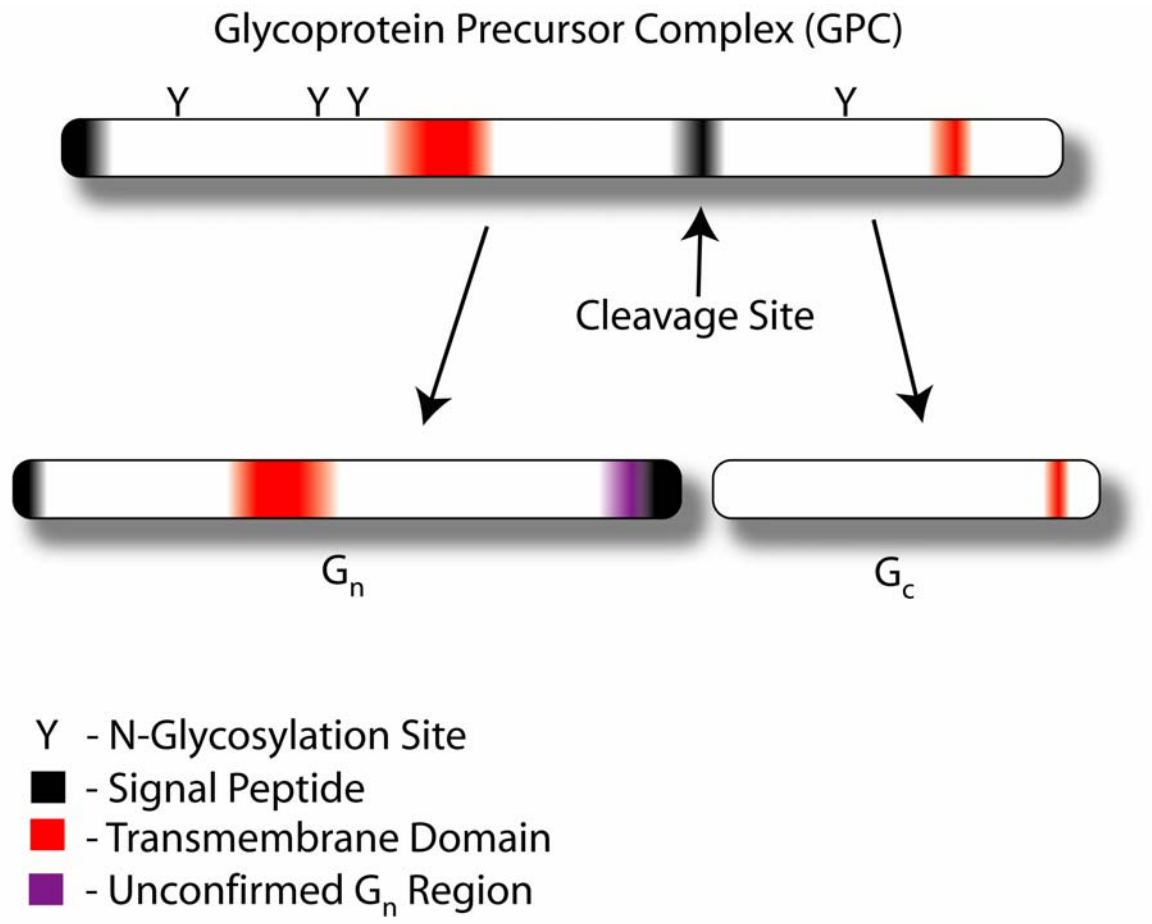

Fig 9: Structure of the glycoprotein precursor complex and the proteolytic processing of G_n and G_c proteins.

catalytic core residues (XDD box) that are essential for polymerase activity, that results in loss of function when mutated (144, 175). Interestingly, site directed mutagenesis of non-conserved amino acids have no effect on polymerase activity.

The viral RdRp is quite complex in that its function must mediate both transcription and replication. The RdRp is multifunctional where it must perform many enzymatic activities and serve as an endonuclease, transcriptase, replicase, and possibly RNA helicase. The function of the RdRp was initially confirmed by expression of L protein from vaccinia virus to transcribe recombinant templates (70). Proofreading capabilities are an unlikely possibility due to hantaviruses having a mutation frequency of $1 \text{ X } 10^{-3}$ (155), which is similar to that of other viral RNA polymerases. This strongly suggests the absence of proofreading or repair mechanisms (39). Endonuclease activity was reported in BUN virus, which demonstrates functional activities of the L protein in providing the capped primers needed for transcription (70).

Virus Life Cycle

Most viruses within the *Bunyaviridae* have a similar life cycle where they enter the cell via receptor mediated endocytosis, and mature and bud from the Golgi apparatus. Some New World Hantaviruses, such as the BCC virus, have been observed to specifically bud from the cell's plasma membrane (163). The stages of the replication process of viruses within the *Bunyaviridae* are outlined below and illustrated in Figure 10:

1. Attachment of virion particle to the cell's surface occurs through interactions between the host's cell surface receptors and the viral glycoprotein.
2. Entry is established through the use of receptor mediated endocytosis; uncoating and release of the viral genomes follows immediately thereafter.
3. Transcription of complimentary RNA from negative-strand vRNA genomes using host-derived primers (5' Cap structure).
4. Using the host machinery, the translation of L and S mRNAs into viral proteins takes place in the cytoplasm and the M mRNA in the ER.
5. Through an unknown mechanism, the virus switches into replication mode. Replication and amplification of viral genome utilizing a cRNA (positive-sense) mediator. Ribonucleocapsids are transported to Golgi apparatus.
6. Assembly of viral proteins and genomic RNA takes place at the Golgi apparatus or plasma membrane (alternative assembly).
7. Viral egress via fusion of the mature virion particles with the plasma membrane.

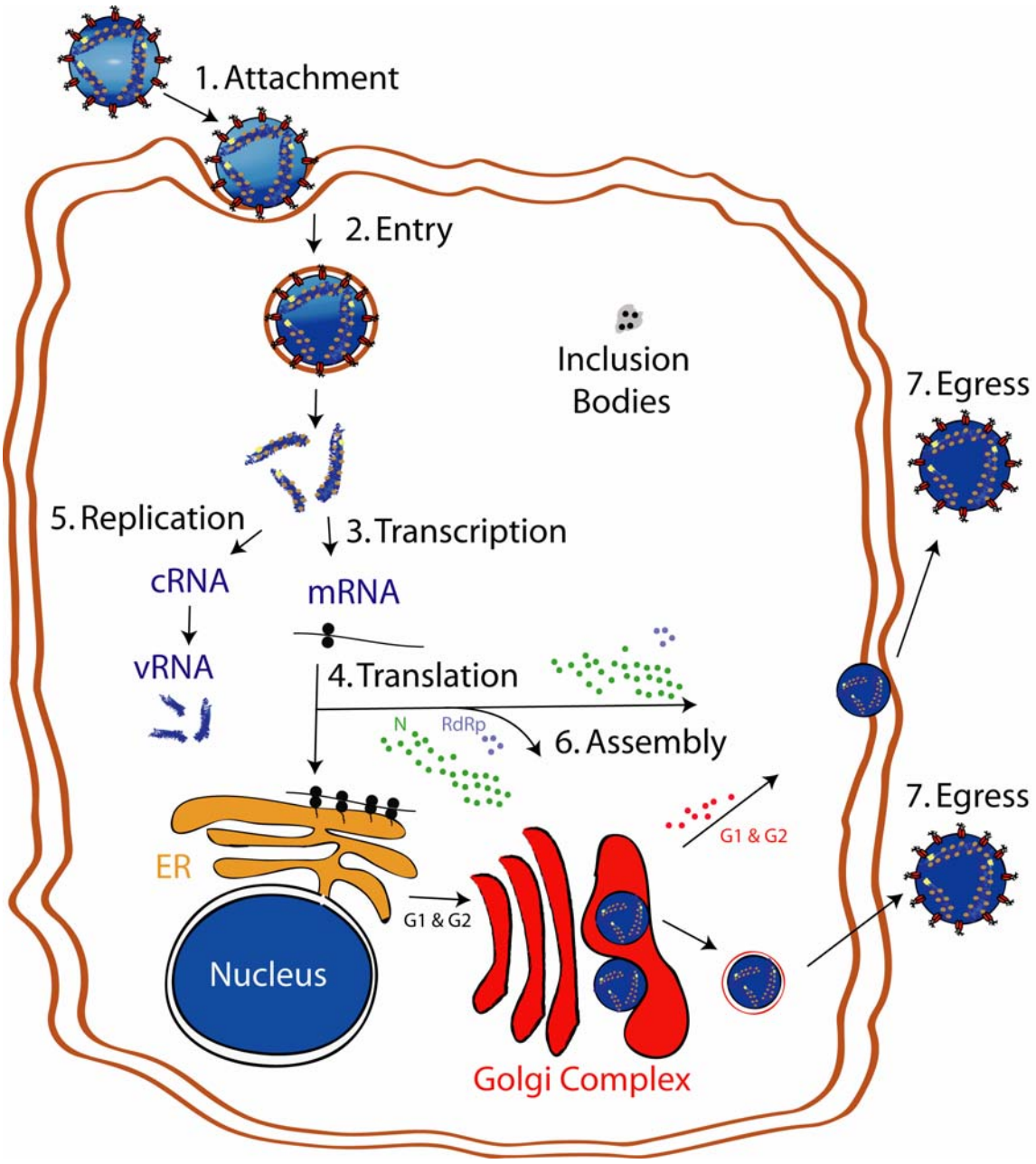

Figure 10: Virus life cycle and intracellular trafficking of viral proteins.

Attachment and Entry

The mechanisms of viral attachment and entry into the cell by members of the family *Bunyaviridae* appear to be very similar to other enveloped viruses. To initiate the entry of the virus particle into the cell, the virus must first interact with the cell's receptors. Evidence demonstrates that pathogenic and non-pathogenic hantaviruses enter host epithelial cells via interaction of the Gn with the host's cell surface receptor(s); β1 and β3 integrins, respectively (50, 51). Although the Gn is the more likely candidate for initiating and facilitating entry, it is very possible that both GPs are involved in the attachment of virus to the host, due to the presence of neutralizing and hemagglutination-inhibiting sites on both the Gn and Gc of hantaviruses (10, 82).

Immediately following attachment, HTN virus entry has been shown to be mediated by clathrin-coated pits (71). Inhibition of entry was observed in cells treated with chlorpromazine, which is a known inhibitor of this endocytic pathway. Furthermore, it was observed that HTN virus proteins co-localized with clatherin in confocal immunofluorescence studies (71). Alternatively, vacuoles were observed to be utilized by members of the *Phlebovirus* and *Nairovirus* genera (45, 173).

After endocytosis, the HTN virus requires transport through acidic compartments such as the transport to early endosomes, and subsequent delivery to late endosomes or lysosomes (71). The use of acidic compartments has been indicated by the reduction of infectivity in cells treated with ammonium chloride, which is known to prevent acidification (57, 169). Similar treatments also abrogated infectivity by the orthobunyavirus, California encephalitis virus, and the UUK virus (57, 169). It is believed that within the endo-lysosomal compartments, the virus is uncoated to liberate

the three RNPs that contain the negative-sense, single-stranded RNA segments that are complexed with both the N protein and RdRp. Immediately after uncoating, the viral genome and the RdRp enter the host's cytoplasm where the RdRp initiates primary transcription. Utilizing a 5' cap structure, primary transcription results in the increased yield of viral mRNA, which gives the initial boost of the replication cycle.

Replication and Transcription

Although the sequence of events that take place immediately after entry and uncoating are not well characterized, there is some literature that outlines a few key events. After uncoating and the release of the viral genome into the cytoplasm, primary transcription of negative-sense vRNA to mRNA is initiated by the L protein and the three RNPs (20) (Fig. 11 and 12). The N protein has been implicated in facilitating transcription initiation, by initiating the dissociation of the RNA panhandle, which frees the 3' terminus for RdRp association (129). The N protein was also suggested to play roles in unfolding the RNA to allow the formation of more suitable structures that facilitate transcription (129). (Fig. 12). The complimentary 3' and 5' terminal sequences are known to form panhandle structures by complementary base-paring (188), and it is believed that the N protein facilitates the unfolding to produce a linear structure (Fig. 12). It has been shown that the 5' termini of the HTN virus S-segment is necessary for interactions with the N protein (185, 188). The region spanning amino acids 175 to 217 of the N protein has been shown to be a central region that binds RNA, specifically several residues such as Glu192, Tyr206, and Ser217 being the crucial residues that facilitate RNA binding (186, 222).

For transcription to initiate, the RdRp requires the use of a suitable primer. The RdRp of hantaviruses has been shown to catalyze an endonucleolytic cleavage of 10-20 nucleotides downstream of the 5' cap of host cell mRNAs that are located in the cytoplasm (49) – termed "cap snatching" (Fig. 13). Cap snatching results in a population of viral mRNAs that contain host-derived 5' primers. Interestingly, to further facilitate transcription, it was found in tospoviruses that newly synthesized mRNAs can serve as cap donors, suggesting a re-snatching mechanism (213).

Host-derived primers with terminal G residues have been shown to be preferred for the initiation of transcription (49). The terminal G residue of the 5' cap aligns and pairs with a C residue at the third nucleotide position of the viral RNA template to initiate transcription (49). After newly synthesized mRNA takes place, the mRNA slips back 3 nucleotides and realigns with the C at the third nucleotide position of the RNA template with terminal sequences of AUCAUCAUC (49). This mechanism has been termed the "prime-and-realign" mechanism. The prime-and-realign model results in a G becoming the first nucleotide of the 5' extension. Transcription results in the production of viral mRNA that lacks the untranslated region (UTR) of the viral genome (Fig. 12).

Following an initial burst of transcription, an uncharacterized signal, possibly accumulation of N proteins in the cytoplasm, prompts the RdRp to switch from transcription to replication (Fig. 11 and 12). Although still speculative for hantaviruses, for other negative-strand viruses such as vesicular stomatitis virus (147) and the influenza virus (7, 64, 189), the N protein has been shown to play roles in providing a means to switch from transcription to replication. In replication mode, the positive-stranded cRNA is synthesized, which is then used as a template for the synthesis of vRNA (Fig. 11). A

similar prime-and-realign model has been proposed for the synthesis of cRNA intermediate. During replication, the entire viral genome is copied, including the UTR (Fig. 12). The mechanism of transcription and replication termination is not known. Although it is believed that encapsidation of the new nascent gene takes place while the gene is copied (Fig. 12), the exact time of encapsidation has not been determined.

Translation and Assembly

Shortly after attachment and entry and synthesis of the viral peptides, the L- and S-segment mRNAs are translated in the cytoplasm on free ribosomes. The M-segment mRNA is translated on membrane-bound ribosomes on the rough ER. The molar quantity of each viral protein varies among species, even within a genus, but overall, the N protein is dominantly expressed. After the M-segment is translated, the GPC is cotranslationally cleaved and processed in the ER to G_n and G_c. Following glycosylation and heterodimerization, the G_n and G_c proteins are transported to the Golgi apparatus where they are retained for assembly. Formation of the RNPs follows after the transport of N and RdRp to the ERGIC or Golgi apparatus. RNPs are packaged into virion particles at the Golgi apparatus, where maturation takes place, followed by egress from the cell via secretory pathways.

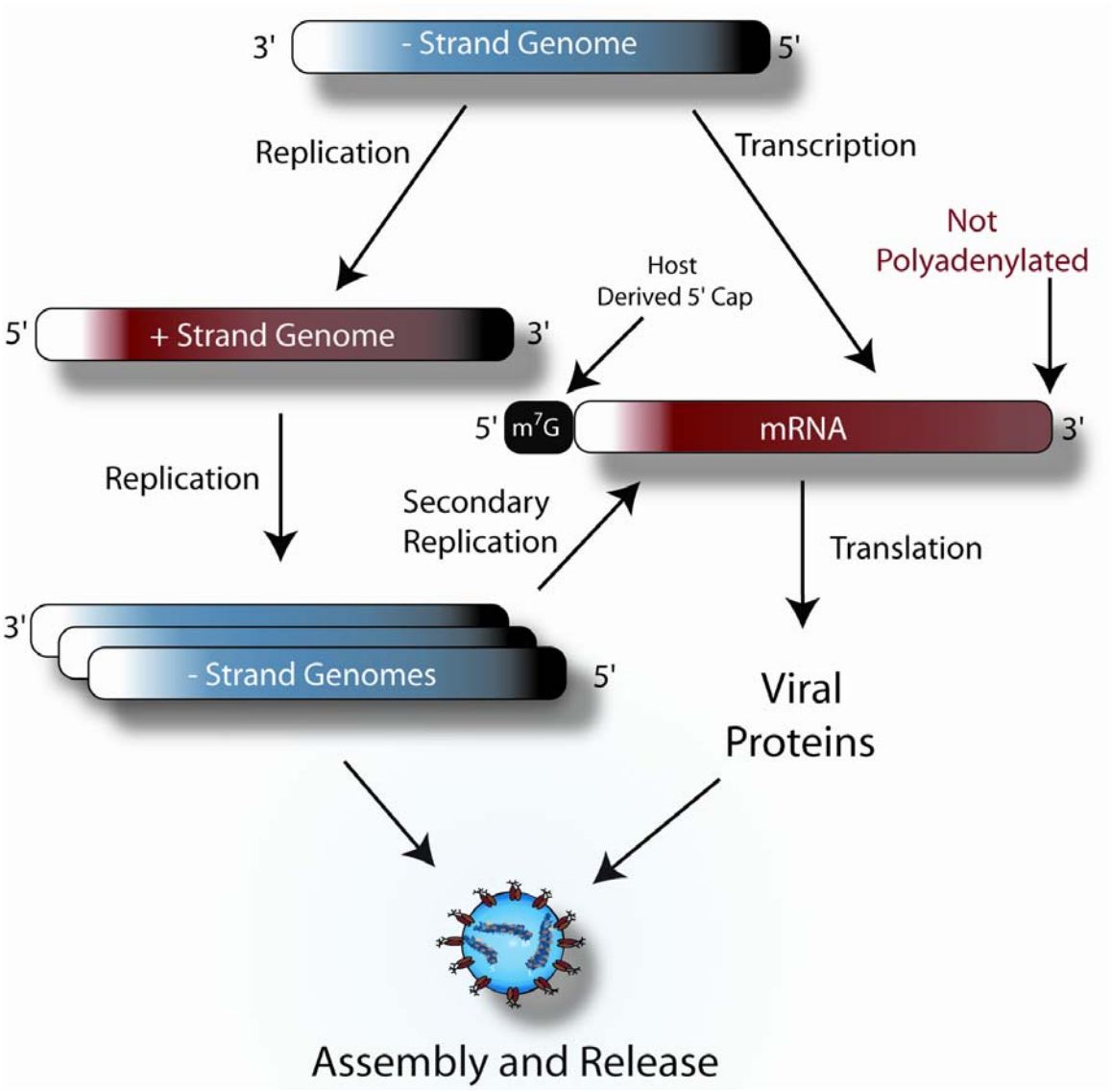

Figure 11: Mechanism of replication and transcription.

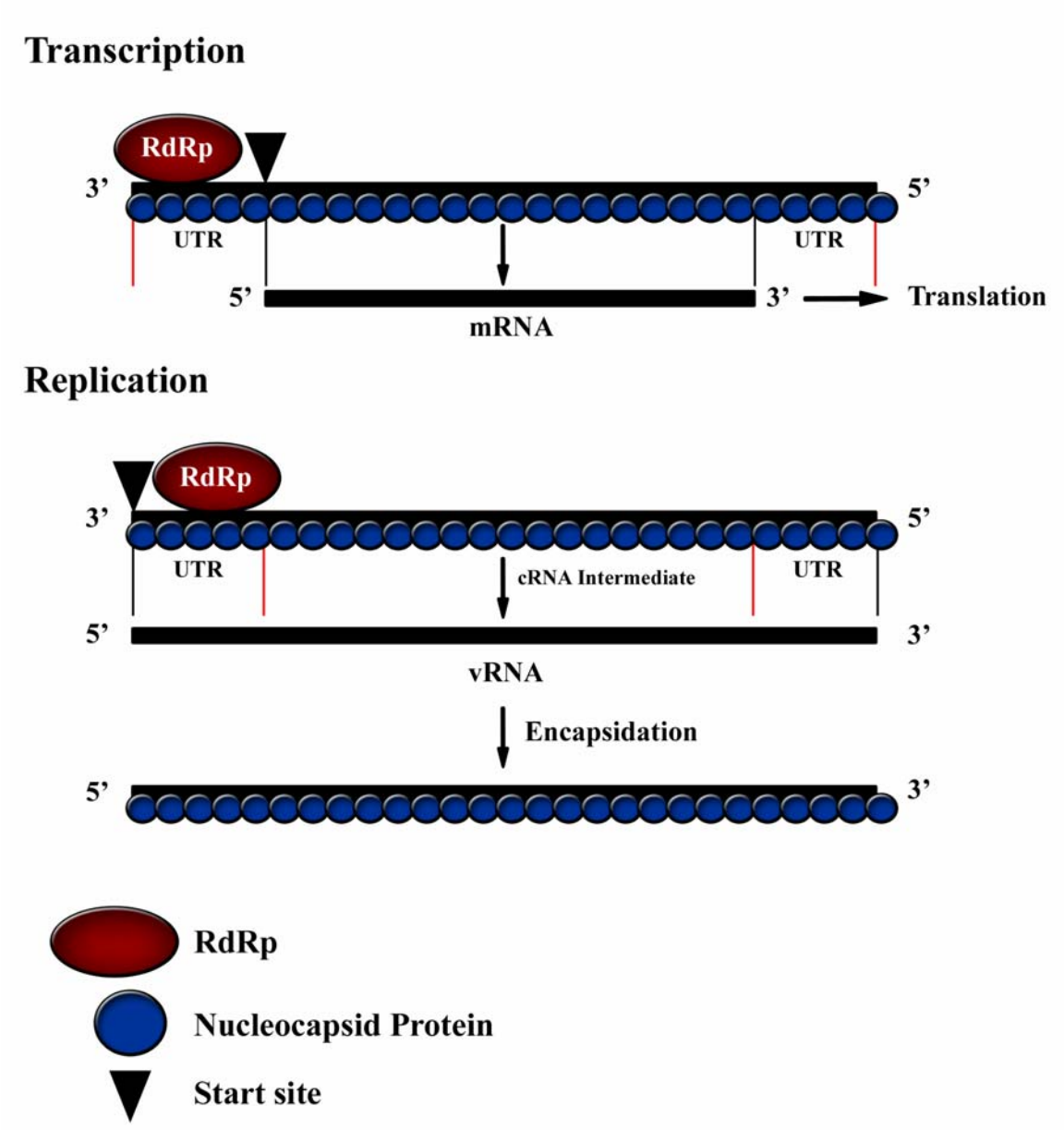

Fig. 12: Replication and transcription products.

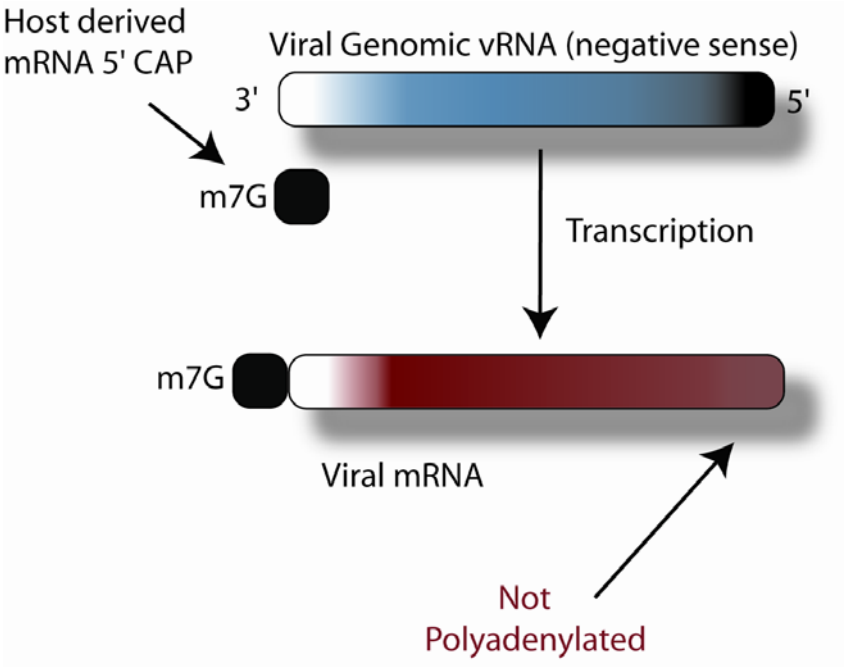

Fig. 13: Mechanism of cap snatching.

Hantavirus Protein Trafficking

Intracellular transport and accumulation of viral proteins is crucial for viral assembly, propagation, and survival. Irrespective of the species or type of virus, all viruses target specific cellular sites where they overtake host machinery for viral protein synthesis. Once the viral proteins have been synthesized, they begin to traffic to specific sites in the cell where viral maturation and assembly may take place. Targeting each viral protein is crucial for the success of the virus so that assembly and budding may occur. Hantaviruses have been known to target the Golgi apparatus.

Targeting of Viral Proteins

One distinct characteristic of virus members of the *Bunyaviridae* is that they mature within the cell by budding at smooth membranes of the Golgi apparatus (9, 66, 164, 172, 181, 183, 216). Most members of this family assemble and bud from the intracellular locations, such as the Golgi apparatus, but budding at other membranes other than the Golgi have been reported for a few viruses. Initially, studies suggested that hantavirus maturation occurred at the cisternae of the ER, while other recent studies showed SN and BCCV viruses preferential budding from the plasma membrane of virus-infected cells (54, 163). Similarly, RVF virus was also found to bud from the plasma membrane, but budding from the Golgi apparatus was also observed (6). Tospoviruses appear to also mature and assemble in the Golgi apparatus, but studies have suggested that Golgi membranes may coalesce around the ribonucleocapsids (88). Although the reasons for maturation of viruses within the *Bunyaviridae* in the Golgi apparatus or at the plasma membrane are not fully understood, it is important to stress that studies of viral

protein transport and retention in the Golgi apparatus have elucidated a portion of this mystery. Overall, it is widely accepted that most hantaviruses mature and bud from the Golgi apparatus (9, 66, 164, 172, 181, 183, 216).

Glycoprotein Trafficking

Since viral maturation within the family *Bunyaviridae* predominates at the Golgi apparatus, it is therefore important to determine whether individual viral proteins helps to define the specific site of maturation. Studies expressing the M-segment of viruses within the *Bunyaviridae* demonstrate that the GPs, G_n and G_c, together are capable of targeting to the Golgi apparatus in the absence of other viral components. The expression of the full-length SN virus GPC has been shown to localize to the Golgi apparatus (196). For some viruses within this family, the G_n is capable of exiting the ER and localizing to the Golgi apparatus, while the G_c remains in the ER when they are expressed alone (14, 122, 149). Conflicting results show that neither GP within the *Hantavirus* was capable of exiting the ER when expressed separately (172). Although it is evident that efficient transport of G_c to the Golgi apparatus does require G_n, the complex formation of G_n and G_c seems to be a significant interaction for targeting and maturation at the Golgi. It seems very reasonable to suggest that GP trafficking could help define the site of maturation at the Golgi apparatus, but further studies would shed some light that can detail more in-depth mechanistic requirements.

To further probe these mechanisms, several studies have attempted to map the Golgi targeting by generating deleted or mutated constructs expressing G_n or G_c, then analyzed their ability to target and retain in the Golgi apparatus. A Golgi targeting signal

was identified and mapped to a transmembrane domain of the G_n within the BUN virus, which demonstrates that the G_n protein is capable of providing the driving force for Golgi targeting (192). Similarly, a Golgi retention signal of PT virus was mapped to the transmembrane domain, which falls within the first 10 amino acids of the cytoplasmic tail of the G_n (122, 123). Furthermore, a study showed that the Golgi localization signal of the UUK virus was also found to be located on the cytoplasmic tail of G_n, but fell within the last 50 amino acids (7). These data help demonstrate that the signal might not be sequence specific, and that G_n protein is the predominant factor in influencing Golgi targeting.

Although G_n provides the driving force, studies done on the HTN virus have shown that the G_n requires the full sequence of G_c for efficient Golgi localization, which suggests that oligomerization of G_n and G_c is significant factor influencing Golgi transport (191). For further validation of how significant oligomerization may be, removal of the transmembrane domain and ctyoplasmic tail of G_n from CCHF virus did not abrogate targeting, and was still capable of dimerizing with G_c during their transport to the Golgi (14). Dimerization of G_n and G_c is essential for the correct transport from the ER to the Golgi apparatus in PT and UUK viruses (25, 151). These studies show the significance of G_n and G_c oligomerization and how it seems to be a dominant factor for effective Golgi targeting and retention.

Although these studies provide some insight as to which viruses within this family target the Golgi and provide mechanistic requirements for Golgi apparatus targeting and retention, they fail to fully justify the reason for Golgi localization. The next step would be to identify the region(s) within the Golgi these viruses are interacting. The Golgi

apparatus comprises several subcompartments, which include the *cis*-, *medial*-, and *trans*-Golgi (114). Studies with the UUK virus have demonstrated that budding may take place on the pre-Golgi intermediate (69) and the involvement of post-Golgi compartments in BUN virus (174). The GPs of Punta Toro (PT) virus were found to localize in the *cis*- and *medial*-Golgi compartments (25). In general, these studies demonstrate the importance of the Golgi apparatus for viral propagation. Further studies will have to be done to help determine the functionality of the Golgi apparatus.

Nucleocapsid Trafficking

For viral assembly and maturation to occur, the N protein must localize to the same intracellular location as G_n and G_c, such as the Golgi apparatus, to help further facilitate protein-protein interactions between N and the GPs. Although the majority of published literature has focused on GP trafficking, this review will discuss the limited aspects of N protein trafficking within the *Hantavirus* genus. Similar studies on the GP trafficking studies have been done to help address questions regarding the localization of the N protein (7, 14, 122, 149, 192, 196)

Studies were performed to determine the localization of the N protein in infected cells. An early study that was trying to determine the accumulation site of virus particles and proteins within the cell showed that the UUK N protein was predominately expressed in the cytoplasm within 5 hours post-infection (93). After 10 hours, the N protein was predominantly observed in the perinuclear region, specifically targeting the Golgi apparatus (93). Similar findings were observed with the SEO virus. Within 2 hours the SEO virus N protein was initially observed to accumulate in cytoplasm in virus-infected

cells (78). Interestingly, the N protein was not observed in the Golgi apparatus within this time-frame. It seemed to reside in regions around the Golgi, but it was eventually detected in the Golgi apparatus after 24 hours (78). It is expected that the N protein of these viruses would initially be found in the cytoplasm, followed by perinuclear targeting, because the N protein is known to play roles in the virus life cycle, including viral transcription (181). The N protein could possibly help facilitate the transcription and translation while it is located in the cytoplasm, but then helps to facilitate assembly once it has reached the perinuclear region. Interestingly, this phenotype has seemed to fit many different virus species within this family, where the N protein was observed to localize to the perinuclear region, in the absence or presence of other viral components (3, 4, 69, 71, 80, 84, 93, 98, 118, 159, 160, 162, 164, 167). Conversely, the LAC virus N protein showed to localize predominately in the cytoplasm in BHK21 cells (162). The disparity observed between perinuclear or cytoplasmic targeting of hantaviruses has been attributed to the difference between Old World and New World hantaviruses, respectively, but this statement was based on the observation of one study.

Since the N protein is known to localize to the perinuclear region, the next studies would be to probe for possible cellular players that help facilitate the trafficking of N protein. Interestingly, the N protein of the BCC virus was observed to form a filamentous pattern, which was found to co-localize with actin microfilaments (164). These filamentous patterns were sensitive to the treatment of CytD, an actin depolymerizing agent (164). They also found actin to co-immunoprecipitate with N protein, which along with their previous data suggests actin to play roles in the transport of N protein to the perinuclear region or the site of assembly. It was also determined that

the BCC virus N protein served as a peripheral membrane-associated protein once the protein was localized to the perinuclear region, which suggests associations with organelle membranes, such as the ER or Golgi apparatus or nearby regions where assembly might take place (162).

Although the N protein of these viruses is known to target the perinuclear region, the specific site is still questionable. The UUK virus N protein has been shown to target the Golgi apparatus in virus-infected cells (93). Using IFA, they found the UUK N protein to colocalize with wheat germ agglutinin (WGA), which is a lectin that binds to the scialic acids of the Golgi apparatus. Although they found the N protein to colocalize with WGA using IFA studies, their electron micrographs were not fully convincible of N protein in the Golgi, because they showed the N protein to predominate in the peri-Golgi region (93). In addition, the BCC virus has also been shown to preferentially localize to the perinuclear region, specifically targeting the Golgi apparatus (162). Using IFA studies, they found the BCC virus N protein to colocalize with the alpha-mannosidase II, a marker for the Golgi apparatus. In contrast, we determined that the HTN virus N protein does not target the Golgi apparatus, but specifically targets the ERGIC (159). Using confocal microscopy, we showed the HTNV N protein did not colocalize with the trans-Golgi, cis-Golgi, early endosomes, or the ER, but was capable of colocalizing with ERGIC-53, a protein found within the ERGIC (159). We also showed that the HTN virus N protein redistributed with ERGIC membranes upon brefeldin A (BFA) treatments, which is known to redistribute ERGIC membranes. Interestingly, using confocal IFA, we observed the HTN virus N protein to be juxtaposed to microtubule filaments and not actin. To probe cytoskeletal association, we treated cells with NOC and CytD, which are

known to depolymerize microtubules and actin, respectively. We showed that NOC, but not CytD, affected the distribution of HTN virus N protein, suggesting trafficking of HTN virus N protein on microtubules to the ERGIC. Furthermore, additional studies on AND, BCC, SEO viruses demonstrate microtubule-dependent trafficking (160). However, distinctions within the early entry events were observed between New World and Old World Hantaviruses. It was demonstrated that the AND virus dependents on intact actin versus microtubules for HTN virus.

The *cis*-acting signal directing the N protein to the perinuclear region has not been identified for viruses within this family. Deletion analysis of N protein gene segments of the BCC virus have demonstrated a possible C-terminal region involved in targeting the protein to the perinuclear region (162). All C-terminal truncated mutant proteins were found to be uniformly distributed in the cytoplasm, while N-terminal deletion mutants varied from perinuclear to cytoplasmic localization, which was dependent on the deletion length from the N-terminus. Deletions beyond amino acid 287 resulted in abrogating perinuclear targeting, which suggests that the C-terminal 141 amino acids are sufficient for directing the perinuclear targeting of the BCC virus N protein. A different location was found within the HTN virus N protein (118). It was determined that deletion of amino acids 188-191 abrogated perinuclear targeting, but it was suggested by the author that the absence of perinuclear targeting was due to the inability of the mutated N protein to interact with the SUMO-1 or with Ubc9.

Viral Assembly and Release

Assembly and maturation of virion particles necessitates that all viral proteins, including RNPs, to be located at the same intracellular space at the same time. It is generally assumed that at least one of each of the L, M, and S-segment RNPs must be packaged into virion particles for full maturation and to be considered infective. Although maturation necessitates at least one RNP of all three genome segments, it is very possible that encased within one virion particle are various molar ratio amounts of each RNP. Studies have suggested that nonequimolar rations of L, M, and S RNA's may constitute a virion particle (66), which may contribute to the various sizes of virion particles that are observed under high magnification (54, 93, 207). The factors that contribute to the selection or negation of RNPs into virion particles have not been determined.

As previously discussed, since viral proteins have been observed to localize to either the Golgi apparatus or the ERGIC, it is generally accepted that maturation takes place at the Golgi apparatus, with a few studies suggesting cell surface maturation (6, 163). How does maturation take place if our studies have shown that the N protein specifically targets the ERGIC (159, 160), while many other studies have shown that the GPs target the Golgi apparatus (14, 122, 149, 172, 192, 196)? What could be the bridging point for these proteins? It has been suggested that MxA, an antiviral protein, and LAC virus N protein localize to β'COP-I-positive membranes (167). COP-I coated vesicles recycle ER proteins from the ERGIC and Golgi stack (215). It is quite a possibility that the N protein is initially routed through the ERGIC, where it physically interacts with either of the GPs (that are being transported from the ER to the Golgi apparatus), then traffic to the Golgi stack, and mature at the trans-Golgi region.

Cellular proteins with which the N protein may associate to facilitate an interaction with the GPs have not been reported. At the Golgi, this could involve Golgi matrix proteins (13)or Golgi transmembrane proteins (112). Both have been shown to cycle between the Golgi and the ERGIC, and could facilitate the coordinated trafficking of N and GPs to the same compartments. Possibly, the GPs may recycle back from the Golgi to the ERGIC or the ER utilizing matrix and transmembrane proteins to increase the probability of its interaction with the N protein (ERGIC) to form complexes required for envelopment. Currently, there is no literature defining the regions of these protein-protein interactions between N protein and GPs. Future studies will have to be done to fully elucidate these interactions, and possibly identify key cellular factors that facilitate the interaction during Golgi apparatus maturation.

Apoptosis

Apoptosis, also called programmed cell death, is the normal physiological response of maintaining the balance between cell proliferation and cell death (203). It is a natural process of self-destruction of living cells that helps regulate cell life span or cells that are damaged. Apoptosis can be induced by a variety of stimuli ranging from physiological to pathological stimuli. Signaling for apoptosis in mammalian cells occurs by utilizing intrinsic or extrinsic factors. Depending on the type of cellular insults, apoptosis can be initiated by cytokines, hormones or viruses (extrinsic factors) that bind death receptors which are located on the cell's plasma membrane. Intrinsic sources such as DNA damage, endoplasmic reticulum stress, or impairment of cell division can also cause cells to undergo apoptosis. Most of the events that lead to cell death are executed

by a group of cystein-dependent aspartate-directed proteases termed caspases that cleave a variety of intracellular polypeptides (43). Caspase activation ultimately leads to cell infrastructure damage and cell death. In addition to cell destruction and apoptosis, a subgroup of a caspase family has been demonstrated to play roles in inflammation by serving as pro-cytokine activators (210). Depending on their function and point of entry into the apoptotic cycle, caspases are classified as initiators or executioners. Initiator caspases are the first caspases that receive a signal for activation from either intrinsic or extrinsic factors such as mitochondrial stress or death receptors, respectively.

Extrinsic Pathway

The extrinsic pathway is responsible for cell removal or elimination of unwanted cells during development or immunosurveillance (17). The extrinsic pathway is activated by a superfamily of known death receptors such as Fas (CD95 or APO-1) or Tumor Necrosis Factor receptor (TNFR) (203), which are known to facilitate the recruitment of procaspase-8 monomers, leading to the dimerization and activation of initiator caspases, such as caspase-8 (11, 17, 40) (Fig. 14). Stimulation of Fas receptor induces an interaction between the cytosolic death domain (DD) of Fas with the adapter molecule Fas-associated protein with death domain (FADD) (135, 136) (Fig. 14). Utilizing the death effector domain (DED) of FADD, pro-caspase-8 is recruited in the formation of the death-inducing signaling complex (DISC), is activated and released into the cytosol (126) (Fig. 14). TNFR is capable of transducing an apoptotic signal by activating caspase-8

similar to Fas, but utilizes TNFR-associated via death domain (TRADD) as a mediator (11, 56) (Fig. 14).

TNF-alpha is known to elicit a wide range of biological responses such as cell proliferation, inflammation, differentiation, and apoptosis through the TNFR. There are two known receptors types of TNFR that are capable of transducing distinct cellular responses: type 1 (TNF-R1; CD120a) and type 2 (TNF-R2; CD120b) (208). These receptors, of the TFNR superfamily, are significantly involved in the maintenance and homeostasis of the immune system. TNF-R1 contains a DD region, with high identity, similar to that of Fas receptor (Fig. 14). Through hetero-association of the homologous DD region, TRADD is capable of directly binding to TNF-R1, followed by the recruitment of FADD, which triggers the activation of caspase-8 and cell death (56, 62, 198) (Fig. 14). Conversely, TRADD can also associate with TNFR-associated factor (TRAF) 2, and receptor interacting protein (RIP) to activate the nuclear factor-κB (NF-κB) (62, 83), which induces the activation of inflammatory genes and anti-apoptotic genes to help protect the cells from an apoptotic response (127) (Fig. 14). Mice that are lacking RIP are unable to activate NF-κB in response to TNFR-1 stimulation, which ultimately leads to TNF-R1 induced apoptosis (83).

Intrinsic Pathway

The intrinsic pathway of caspases is used to eliminate cells due to mitochondrial stress or damage, ionization energy, or certain developmental cues (17). The majority of the signaling cascade of the intrinsic pathway is mitochondrial-initiated by the release of

pro-apoptotic proteins, such as Apaf-1, caspase-9, cytochrome c, and Smac/Diablo. The pro-apoptotic mitochondrial pathway is also known to be negatively or positively regulated by a proteins belonging to the family of Bcl-2 proteins that act as inducers or inhibitors of apoptosis (30, 32, 33). There are three major subfamilies within the Bcl-2 family of proteins. The antiapoptosis subfamily of the Bcl-2 proteins, Bcl-2 and Bcl-xL (mammals), are known to inhibit apoptosis through a variety of methods and distinct mechanisms. Bcl-2 and Bcl-xL are known to inhibit the release of pro-apoptotic proteins from the mitochondria. The other two subfamilies are known inducers of apoptosis. Bax and Bak constitute one subfamily, while BH3 constitutes another. Bax and Bak exist as monomers in the absence of a stimulatory signal, but form homo-oligomers immediately following activation. It is generally accepted that oligomerization of Bax or Bak results in the formation of pores within the mitochondria that help in the release of cytochrome c into the cytosol. Once the mitochondria becomes permeabilized, cytochrome c is released, which facilitates the recruitment and activation of caspase-9. In combination with cytochrome c, the apoptotic protease activating factor 1 (Apaf-1) is capable of directly recruiting caspase-9 through its N-terminal caspase-activation recruitment domain (CARD) (109). It contains a CARD domain that is hidden away when inactive. Upon activation, Apaf-1 serves as a docking protein for both caspase-9 and cytochrome c. Cytochrome c is capable of displacing the CARD domain, which causes the recruitment of caspase-9 in the formation of a complex known as the apoptosome (224). The apoptosome is capable of activating downstream caspases, such as caspase-3.

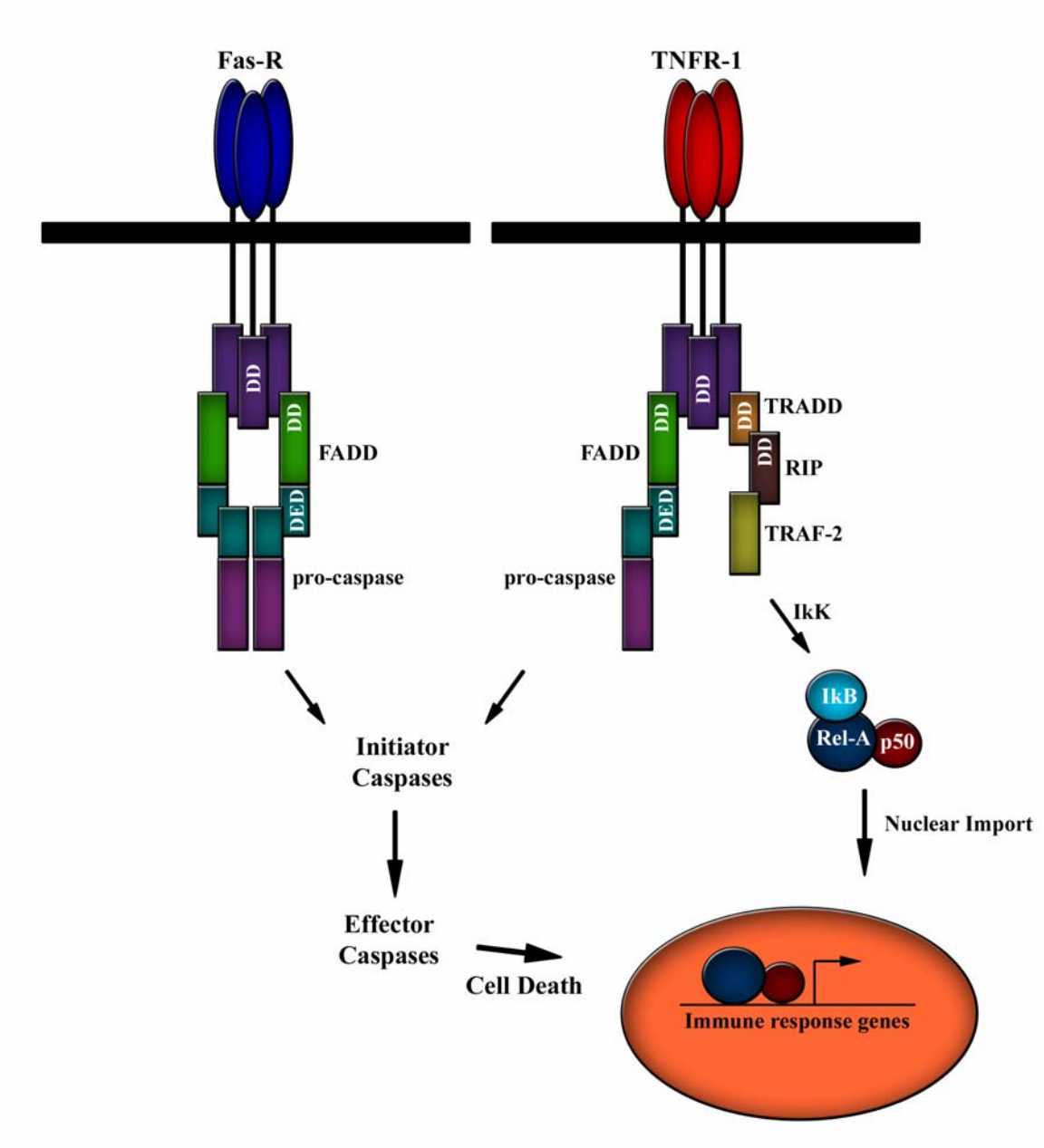

Fig. 14: Intracellular signaling of TNFR-1 and Fas-R.

Caspases

Caspases, or cysteine-aspartic acid proteases, belong to a family of cysteine proteases. They are obligate dimers that contain identical catalytic units, with each unit containing one active site. Each catalytic unit is composed of one large and one small subunit that are separated by a linker region. Caspases share a unique characteristic of being homologous cysteine proteases, which are known to preferentially cleave asparagine residues of target substrates. Caspases are maintained in the cytosol as inactive zymogens. These zymogens are capable of activating themselves by what is termed a homo-activation mechanism, as demonstrated when full-length zymogens were expressed in Escherichia coli that resulted in full caspase activation (201). Increased concentration of full-length zymogens is sufficient to allow homo-activation of caspases. These increased concentrations occur locally at the plasma membrane following activation of clustered death receptors such as Fas-R or TNFR-1. Although most caspases play major roles in dictating programmed cell death, some function as activators of pro-inflammatory cytokines (52, 92, 217). Cleavage of asparagine residues can result in activation or de-activation of target substrates.

Initiator Caspases

Initiator caspases, such as caspase-8, are activated in response to extracellular stimuli, during activation of death receptors. Caspase-10, which is closely related to caspase-8, is also involved in death-receptor-mediated cell death (29). Studies revealed that transient transfections of Jurkat cells with caspase-10 is sufficient for executing the

death-receptor-mediated cascade in cell death (12, 89). These caspases are activated by ligation of a trans-membrane death receptor such as Fas-R or TNFR-1. Immediately following activation of death receptors, aggregates are formed on the cells surface, which facilitate the recruitment of FADD to the cytosolic face of the receptor by utilizing DEDs (5). Once docked, FADD recruits inactive caspase-8 zymogens, which form dimers during DISC formation. After dimerization, homo-activation of caspase-8 is initiated by the removal of N-terminal DEDs, which allow the activated caspase to be released into the cytosol (22). The active forms of initiator caspases are directly capable of activating pro-caspase-3 or 7 with sufficient magnitude to indicate direct processing of apoptosis *in vivo (200)*. Activation of effector caspases results in the cleavage of a number of intracellular proteins leading to the definitive process of apoptosis.

Effector Caspases

Effector (executioner) caspases are the workhorses of the apoptotic process and whose activation has been correlated with cell death (205, 206). The apoptotic action produced by these caspases is an ordered signaling process, which makes it distinct from other forms of cell death. Executioner caspases such as caspase-3 and -7 exist in the cytosol as preformed, inactive dimers, which distinguish them from their initiator counterparts (monomers). Proteolysis within the interdomain linker facilitates the translocation of the activation loops, facilitating the formation of the active site. Once activated, these caspases have a high degree of specificity for their target peptides. Caspases-3 and -7 are capable of cleaving at specific tetrapeptide substrates containing

amino acids DEVD. They are responsible for the proteolytic cleavage of many proteins that results in cell dismantlement, specifically the nuclear enzyme poly(ADP-ribose) polymerase (PARP) (95). The cleavage of PARP may be directed by either of these two caspases or in combination. Although PARP enzyme plays important roles in genomic stability and DNA repair(37, 38), cleaved PARP plays active roles in apoptosis (19). PARP cleavage is a major hallmark of apoptosis.

Caspase Inhibitors

There are several caspase inhibitors that have been discovered, which are categorized under the inhibitors of apoptosis (IAPs) family (35, 36). Some of these inhibitors include proteins such as XIAP, cIAP-1 and cIAP-2. Interestingly, each of these IAPs specifically target executioner caspases, such as caspases-3 and -7 (36, 170). These inhibitors are directly regulated by a transcription factor known as NF-κB (12, 217). Each of these IAPs conatin a κB site located on their promoter region, which serves to help regulate the gene. NF-κB has also been demonstrated to serve as a direct substrate of caspases. Evidence for the cleavage of NF-κB by caspases has been demonstrated in Jurkat T cells (161). Fas-induced apoptosis leads to the caspase-3 dependent, proteolytic cleavage of Rel-A and p50 subunits. Similar results have shown that chicken, mouse, and human c-Rel can serve as a caspase substrate *in vivo* (12).

Hantaviruses and Apoptosis

Although the pathogenesis of a hantavirus infection has been characterized (54, 75), the underlying mechanism of HFRS and HPS is not fully understood. Despite this lack of information, autopsy findings typically reveal vascular leakage or permeability in microvascular beds, suggesting that vascular endothelium is a target for virus infection (54). Hantaviruses replicate in cultured cells with little to no cytopathic effects (CPE). Apoptosis has been observed in Vero E6 cells infected with the HTN virus, despite this evidence, it was not apparent whether infected cells or bystander cells became apoptotic (76). CPE effects and apoptosis have been observed in embryonic kidney cells (HEK293) infected with various hantaviruses, but apoptosis was observed more in bystander cells as apposed to virus infected cells (119). La Crosse virus has been shown to directly induce apoptosis in murine brain (148). In addition, apoptosis has been shown to take place in lymphocytes during HFRS (2). Furthermore, it has been demonstrated that PUU virus N protein directly interacts Daxx, a Fas-mediated apoptosis enhancer (1). In contrast, reports have shown that HFRS causing hantaviruses do not induce apoptosis in either confluent Vero E6 cells or A-549 cells (60). It has also been reported that that Prospect Hill (PH) virus does not cause apoptosis in endothelial cells (85), but PHV is a known hantavirus with no known pathogenicity to humans (177).

Apoptosis has been observed in hantavirus infected HEK293 cells and CPE could be detected cells infected with hantaviruses, such as HTN, SEO and AND viruses early as 3-4 days post-infection (119). Experimental data observed by (76) suggest that apoptosis plays a role in the process of cell death by hantavirus infection. Using subcutaneous injections in mice, experiments demonstrated that programmed cell death is partly responsible for the deterioration of cellular function from La Crosse virus infection (148).

In serum samples from patients infected with PUU virus, elevated levels of lactate dehydrogenase were observed, indicative of cellular damage (90). Furthermore, increased levels of serum perforin, granzyme B and the epithelial cell apoptosis marker cytokeratin-18 were also observed (90), which further suggests the involvement of apoptosis in hantavirus pathology. In contrast, no apoptosis or CPE were induced in fully confluent Vero E6 cells inoculated with HTNV, PUUV, Dobrava hantavirus, or Saarema hantavirus up to 12 days post-infection (60). The literature suggests that hantaviruses may modulate apoptosis depending on the host cell type. Clearly further work on the role of apoptosis in the pathogenesis is important to complete our understanding of hantavirus illness in humans.

MOLECULAR DETECTION OF HUMAN PATHOGENS: HANTAVIRUSES

STEVEN J. ONTIVEROS AND COLLEEN B. JONSSON

Draft [In preparation for] *Encyclopedia of Virology*

Format adapted for dissertation

CHAPTER 2

MOLECULAR DETECTION OF HUMAN PATHOGENS: HANTAVIRUSES

BUNYAVIRIDAE

The family *Bunyaviridae*, which is comprised of a large group of over 300 viruses, each sharing morphogenic and antigenic properties, was established in 1975 (12). There are currently four genera of viruses within the *Bunyaviridae* that contain animal reservoirs (*Orthobunyavirus, Hantavirus, Nairovirus* and *Phlebovirus*) and one genus that contains a plant reservoir (*Tospovirus*) (46). Viruses from the *Bunyaviridae* infect animals, plants, humans and insects. Most viruses are transmitted by arthropods, mosquitoes, ticks, sand flies, or thrips, with the exception of the *Hantavirus* genus, which are rodent-borne (Table 1).

Hantavirus Classification

Hantaviruses are classified into two major groups: Old World and New World, based on their geographic distribution in their rodent hosts (45). Old World hantaviruses, such as the HTN, Puumala (PUU), and Seoul (SEO) viruses cause hemorrhagic fever with renal syndrome (HFRS), while New World hantaviruses, such as SN, Andes (AND) and Black Creek Canal (BCC) viruses cause hantavirus cardiopulmonary syndrome (HCPS) (Table 1). This spectrum of illness varies depending on the virus.

Virion Structure, Morphology and Physical Characteristics

Virions within the *Bunyaviridae* are generally spherical in nature with an average diameter of approximately 80-120 nm (15, 30, 31, 46, 52)(Fig. 1). Due to the large

number of viruses within this family, structures can range between 78-210 nm in diameter (15, 30, 31, 46, 52), and additional morphological shapes may exist, specifically within the hantavirus genus.

The virion particles contain a host-derived lipid bilayer that is approximately 5 to 7 nm thick, which is derived from either of two sources, the cellular plasma membrane or the Golgi apparatus. The outer surface of the lipid bilayer contains glycoprotein (GP) projections that are approximately 5 to 10 nm in length. These GP projections are comprised of heterodimers of the two GPs, G_n (formerly G1) and G_c (formerly G2). Studies on the La Crosse (LAC) virus, family O*rthobunyaviridae*, show that approximately 270 to 1400 GP projections per virion may exist (34). The structure of the virion surface can vary among viruses within the *Bunyaviridae*. A grid-like pattern has been observed primarily in viruses within the *Hantavirus* genus (52).

The interior makeup of a virion particle consists of tightly packed ribonucleocapsids (RNPs). The three negative sense RNA genome segments, S, M, and L, are individually complexed with the N protein to form the three RNP structures (7, 35). These RNP complexes are believed to be the source of the virion's internal filamentous appearance (9). Studies have demonstrated that the Uukuniemi (UUK) virus, family *Phelobovirus*, is comprised of 2% RNA, 58% protein, 33% lipid, and 7% carbohydrate (36). It is presumed that since these viruses lack a matrix protein, the N protein from the three RNPs physically interact with the GP projections on the inner leaf of the lipid membrane.

Hantaviruses share similar physical properties to those of other viruses in the family *Bunyaviridae*. The density of the HTN virus can range from 1.16 to 1.18 g/cm^3 in

sucrose, and 1.20 to 1.21 g/cm^3 in CsCl. Treatment of the HTN virus with non-ionic detergents releases the three RNPs that sediment to densities of 1.18 and 1.25 g/cm^3 in sucrose and CsCl, respectively, using rate-zonal centrifugation methods (42, 44). Treatment of virus particles with lipid solvents or non-ionic detergents results of loss of infectivity in arthropods and mammals (36).

Transmission of hantaviruses is thought to be primarily through the inhalation of rodent excreta. For the virus to be infective, the virus must remain viable in rodent urine, feces, and saliva or in dust aerosols for several days post-excretion. Studies show that the HTN virus can remain viable for 30 min in buffers from pH 6.6 to 8.8, but in the presence of 10% fetal bovine serum (FBS), the virus can remain viable in a larger range of pH 5.8 to 9.0 (41). HTN virus is infectious at temperatures ranging from 4 to 42 °C in the presence or absence of serum, and can remain infectious for 1 to 3 days when at least 10% serum is present in dried samples.

Epidemiology

Old World Hantaviruses

Immediately following the initial discovery of the HTN virus in 1976 (24, 25), epidemiological studies of HFRS significantly progressed. It was initially believed that HFRS only occurred in rural areas of Eurasia, specifically China, Korea, Eastern Russia, and Northern Europe (22), but later findings demonstrated that HFRS could also occur in urbanized cities and in many parts of the world (26). Initially, studies showed that farmers, soldiers and inhabitants of rural regions had highest risk for HFRS, but HFRS can occur in urban areas if the rodent reservoir is present. Three epidemiological patterns

of HFRS have been shown: rural, urban and animal rooms. These are based on the location of the outbreak, and the reservoir hosts of the disease.

The habitat of the striped field mouse, *Apodemus agrarius*, is in rural areas, and is the known rodent reservoir for the HTN virus that causes HFRS (26). This mouse is most common in agricultural fields (3), but is known to invade houses during the winter months in search of food and shelter. Rural cases seem to occur bi-annually, with two seasonal peaks of cases occurring during the late spring and in the fall seasons. There are several factors that could possibly play roles in the increased incidences of HFRS during the fall months, which may be attributed to the harvesting of crops, and possibly the relocation of rodents to indoors in preparation for the winter (19). Furthermore, the number of infected rodents may help to escalate human incidences, since the number of infected *Apodemus agrarius* is high in Asia during the late spring and early fall seasons. Conversely, cases of HFRS in Russia and in the Scandinavian countries are highest during the winter seasons. Most cases of HFRS occur in adult men ranging from 20 to 50 years of age (1, 22). The higher prevalence of HFRS in men than in women directly correlates with the usual duties of men working outside in the fields while most women work in home. A large number of HFRS cases in China may be attributed to the HTN virus, where about 100,000 cases are reported each year. Approximately 300 to 900 annual HFRS cases are estimated to occur each year in Korea and in Eastern Russia. HTN virus related HFRS has been demonstrated to have a mortality rate of 10 to 15%.

Rattus norvegicus and R. rattus, commonly known as the house or domestic rat, are the rodents responsible HFRS cases that occur in urbanized areas (23, 49). The common domestic rat lives in most urban regions throughout the world. Previously

known as the rat virus, SEO virus is the only hantavirus known to cause HFRS in humans in urban areas. Although over 100 cases of HFRS have been reported in large metropolitan areas of Seoul and other larger cities of Korea where patients had direct contact with the domestic rat, SEO virus related HFRS is rare outside of China and Korea. (21). The seasonality of SEO virus outbreaks are somewhat different from the HTN virus, with most outbreaks occurring in the spring and early summer (2).

Nephropathia epidemica is a milder form of HFRS is caused by the PUU virus, which is found throughout Europe. The bank vole, *Clethrionomys glareolus*, has been found to be the primary host of PUU virus. This virus has been found to affect both urban and rural communities of Sweden and Finland. The number of cases in rural areas usually peak in November and January, while most urban cases occur during August. This virus seems to fit the general outbreak pattern of other viruses within this family, because in 1993 an outbreak PUU virus associated-HFRS was recorded in southern Belgium, which directly correlated with high number of bank vole populations (6). Other outbreaks of HFRS have been observed in northeastern France and Germany that also correlate with the increase in the population of bank voles (38).

New World Hantaviruses

After the SN virus outbreak in the Four Corners region of the United States in 1993, much attention and resources were adverted to virus associated-HCPS and New World Hantaviruses. These viruses contain rodent hosts of the *Sigmodontinae* subfamily (Table 1). The SN virus has been found in many parts of the U.S. and Canada, and has been found to be hosted by the rodent *Peromyscus maniculatius*, better known as the deer

mouse. The majority of HCPS-associated cases in both the United States and Canada are caused by the SN virus (33). As of 2001, approximately 280 cases of HCPS have been reported in the United States, spanning 30 states, with the majority of all cases occurring in the southwest. Approximately 35 cases have been reported in western Canada. Deer mice infected with the virus have been detected from Yukon to Mexico and from California to the Appalachian Mountains in the Eastern United States and Canada (32, 33). Similar to Old World Hantaviruses, HCPS disease caused by New World Hantaviruses correlates with increased population of rodent hosts within the region. The majority of all HCPS cases occur in late spring or early summer, which affects human male and females equally (17).

Another New World Hantavirus, BCC virus, was associated with a single event of HCPS in Florida (40). The cotton rat, *Sigmodon hispidus*, was found to be the host of BCC virus (40). Although similar to the SN virus-associated HCPS, BCC virus-associated HCPS seemed to be predominantly pulmonary with less renal involvement (14, 16, 18).

New World Hantaviruses have been found in other regions such as Central and South America. Over 300 HCPS cases were identified in various parts of South America spanning a region from Argentina, Chile, Paraguay, Brazil, and Uruguay, and also in Central America locations such as Panama (51). Similar to other hantaviruses, transmission is usually through infected rodents with the exception of an outbreak that occurred in Patagonia. The outbreak in Patagonia was caused by the AND virus, which is hosted by *Olygoryzomys longicaudatus* (28). Investigations of the AND virus outbreak in Patagonia suggested a human-to-human transfer between a doctor and an infected patient

(37, 51). Extensive consideration should be taken when dealing with AND virus infected patients since the AND virus has a high mortality rate of approximately 50%.

Hantavirus Pathogenesis

World-wide, approximately 150,000 to 200,000 cases of HFRS are reported each year, with more than half occurring in China (10). Depending on which virus strain that is causing disease, variations of mortality may occur. Death occurs in less than 0.1% in patients infected with the PUU virus. Fatalities as high as 15% have been observed for HFRS caused by the HTN virus. More than 250 cases of HCPS have been reported throughout North and South America. Fatality rates also vary for HCPS related deaths, ranging from 30 to 50% for disease caused by SN and AND viruses, respectively. Other hantaviruses from South America, such as Laguna Negra, have death rates ranging from 5 to 15%.

Human Infections

The effects of a hantavirus infection in humans is different to what is observed in their natural rodent hosts. The progression of a diseased state, either HFRS or HCPS, is usually the end result of a human infection, depending on the type of hantavirus. Following exposure, an incubation period of approximately 7 to 21 days takes place before the development of illness. Clinical progression and manifestations of disease caused by HFRS and HCPS is outlined by five overlapping stages: febrile, hypotensive (HFRS) or cardiopulmonary (HCPS), oliguric, diuretic, and convalescent (21, 39, 48).

Disease begins with influenza-like symptoms, headache, backache, fever and chills. Once the infection has entered the febrile phase, lasting approximately 3 to 6 days for both HFRS and HCPS, slight hemorrhage manifestations are evident in the conjunctiva. This stage is characterized by headache, fever, vertigo, nausea, and myalgia. The clinical symptoms of the febrile stage are eventually augmented to the hypotensive (HFRS) or cardiopulmonary (HCPS) stage. Both stages are characterized by thirst, restlessness, nausea and vomiting, each lasting hours or days. Approximately one third of all patients suffering during the hypotensive stage of HFRS develop shock and mental confusion (20). Symptoms of vascular leakage, abdominal pain and tachycardia are observed within this stage. Shock, pulmonary edema and hypotension are observed in patients suffering from HCPS during the cardiopulmonary stage. The oliguric phase lasts from 1-16 days for HFRS or 4 to 24 hours for HCPS. Conjuctival, cerebral and gastrointestinal hemorrhage occurs in about one third of all patients (20). The oliguric stage accounts for approximately one-half of all hantavirus related deaths (29). Although a patient may completely recover from HFRS or HCPS, which may take from several weeks to months, renal or pulmonary dysfunction may persist for the life of the patient. Although there is currently no effective treatment for disease caused by hantaviruses, ribavirin could serve as a possible candidate for treatment (47).

Diagnosis

Four basic technology platforms exist for detection of infectious agents in humans, animals and the general environment. These include those based on the immunoflouresence assays (IFA), polymerase chain reaction (PCR), ELISA and lateral-

flow immunoassay. The development of a rapid field test and laboratory systems for detection of infection in humans is critical for outbreaks of pathogens, standard clinical laboratories as well as ecological and epidemiological surveys. These technologies have a broad technical impact in that they can be used in clinical laboratories for routine diagnosis, in animal laboratories interested in ascertaining if animals have infection prior to or during the course of a study, in clinical laboratories in outbreak areas around the globe, in military settings where soldiers are at high risk for exposure, in the evaluation of vaccines for clinical trials for human use, and finally in research laboratories focused on epidemiology or ecology of the virus in humans or rodents. Herein, we seek to review the available systems and the strengths and weaknesses of each. Importantly, each system has strengths and weaknesses according to the laboratory setting, the demands on the laboratory for processing samples and the level of accuracy demanded (clinical versus research).

Conventional Techniques

Clinical cases of HFRS/HPS are confirmed by a variety of laboratory analysis, and because of the rapid progression of disease, there is a significant necessity for a rapid diagnostic test. Confirmation of HFRS/HPS is established through the presence of specific hantavirus antibodies, or viral antigens, or viral RNA. Each can be demonstrated by immunoassays, immunohistochemistry (IHC), and RT-PCR, respectively. Specific antibodies to hantavirus are consistently present in acute HFRS/HPS patients as well as in HPS convalescents and survivors. Due to this fact, immunoassays have become the pillar in laboratory diagnosis.

IHC is a very simple confirmatory test that permits visual identification of viral antigens in tissues utilizing a specific antibody, but these tests can only be performed in post-mortem individuals. Although this tool has been proven to be very useful, IHC cannot identify the specific hantivirus present, due to the cross-reactivity between closely related hantavirus N proteins (17). Virus-specific diagnosis can be confirmed by IHC, but the test requires the use of hantavirus monoclonal antibodies.

Rapid serological tests to facilitate diagnosis are usually in urgent need due to the quick progression of the disease. Enzyme-linked immunosorbent assay (ELISA) and/or western blotting (WB) have being widely used in reference laboratories, although ELISA has found greater acceptance worldwide. For both assays, the N protein is most commonly used in these serologic formats for hantaviruses since it has been proven to be the most antigenic and cross-reactive of the four hantaviral proteins. ELISA tests are being used extensively for routine diagnosis of HFRS/HPS. A rapid IgM capture ELISA for hantaviruses has been developed and proven to be sensitive for detection of HFRS and HPS patients by USAMRIID and the Center for Diseases Control and Prevention (11). At the onset of symptoms, virtually all patient confirmed cases of HPS contain IgM and IgG antibodies to the H protein. Although this test is highly sensitive, false-positive reactions in malaria-positive individuals have been detected. Other disadvantages of ELISA are the requirement for specialized equipment, personnel and incubation conditions that most often are not present in field or satellite laboratories.

A more recent method, the strip immunoblot assay (SIA), that competes with the ELISA in sensitivity and specificity, has been developed. This format has great advantages over WB and ELISA, as it requires minimum amount of effort, equipment,

expertise and can easily be performed in field conditions. From one single run, the assay can analyze reactivities to multiple homologous antigens, which is ideal when dealing with minute quantities of sample. Therefore, it can be designed to be highly specific and confers the formidable advantage of distinguishing distinct hantavirus serotypes by analysis of band intensities and titer. Although the SIA assay has been proven to be very sensitive, a major disadvantage is the antigens required for the test must be highly purified. Specifically, all possible traces of E.coli proteins must be removed to decrease the possibility of false positives due to nonspecific antibody reaction to these contaminants. In such a case that traces amounts of E. coli interfere with the SIA assay, the coding regions of the cloned proteins will be moved and expressed in the baculovirus system as previously described. Another disadvantage is the length of time required to conduct the test which can be as long as 8 hours.

Lateral-flow assays have been considered an ideal field-usable diagnostic platform since they are simple-to-perform, rapid, stable at field conditions and portable. Rapid, membrane based methods where the reactants move by capillary action along a narrow rectangular strip. The sample is applied at one end and traverses the strip, coming into contact first with detecting antigen and subsequently with capture antibodies that have been dried onto the membranes. If the sample contains the hantavirus antibodies it will form visible lines as it accumulates at the position of the detecting antigen and capture antibodies. If the sample does not contain hantavirus antibody it will form a visible line only at the position of capture antibody. This assay promises to be easy to perform in field settings, economic and highly sensitive for detection of HFRS and/or HPS acute patients (G. Ludwig, USAMRIID personal communication). Currently, the

system has been shown to be useful for detection of IgG; however, as mentioned above, the test suffers from high background reactivity in tests for IgM (G. Ludwig, personal communication). It is likely that the background is caused by residual E. coli proteins in the preparation. The antigen production and purification scheme developed in this proposal, employing plant expressed recombinant proteins, should eliminate those contaminants and provide abundant and affordable antigen suitable for the lateral flow assay format or other applications.

Plaque reduction neutralization test (PRNT) is the most definitive method to facilitate the identification and differentiation of hantaviruses (5, 43). It is a specific test that can detect and measure neutralizing antibodies. Cross-PRNT has permitted serotypic classification of hantavirus infection in rodents and humans (4, 5, 27). Although the assay is highly specific and is capable of distinguishing hantaviruses with serum from experimentally infected animals, it was shown to be less specific when human convalescent sera from HFRS and HPS patients were used (4). A major disadvantage of PRNT is that its use is confined to very specialized research laboratories. PRNT necessitates the need for a biosafety level 3 containment laboratories due to the hazardous nature of hantaviruses, and the specialized training of staff that mandate the use of such a facility. In addition, the amount of time and effort to perform these tests requires the expertise of highly trained personnel, and are not amenable for diagnostic. Furthermore, PRNT necessitates the existence of a virus that can be propagated in cell culture, and hantaviruses are known to have a slow growth rate, which present low titers when grown in these conditions. In order to visualize the plaques, isolates must be generally passed several times in cell culture and require careful optimization of plaque assays parameters.

The PRNT is not a practical model for diagnostic purposes due to the length of time required to perform a test, but should be used to help validate other methods.

Molecular Techniques

The Real-Time Polymerase Chain Reaction (RT-PCR) has been a very useful and efficient tool, which proved to be a cornerstone of the diagnosis of severe acute respiratory syndrome once the SARS viral sequence was obtained. The Real-Time Polymerase Chain Reaction (PCR) allows the ability to monitor the progress of the PCR as it occurs. This type of platform has proved exceptional for a number of pathogens for which the pathogen is present upon patient entry into the hospital.

RT-PCR is a very sensitive confirmatory method that permits the genetic identification of the virus associated with the HPS. Through the course of disease, patients under the early acute phase have suitable detectable levels of viral RNA at the onset of pulmonary edema, but afterward clear virus rapidly from circulation (13, 50). Therefore, this method is *only* effective in patients with acute HPS. RT-PCR reactions are characterized by the point in time during cycling when amplification of a target is first detected rather than the amount of target accumulated after a fixed number of cycles. The detection of fluorescence signal generated by the RT PCR reaction will be proportional to the known amount of targets that will be added to the reaction mixture. All data obtained from real time detection will be able to be displayed and evaluated after the reaction is completed. The following criteria are tested and analyzed in launching any RTPCR diagnostic: the Ct value, linear range, accuracy and precision, limits of detection, efficiency and the specificity of the method.

The PCR-Enzyme Immunoassay (PCR-EIA) is a colorimetric hybridization assay that is simple, and a highly sensitive and specific method for detecting and differentiating hantaviruses (8). It is highly useful, because it combines the specificity of PCR with the sensitivity of enzymatic detection. Within this assay, digoxigenin-labeled PCR products are amplified with degenerate primers that correspond to a highly conserved sequence of viral S-segment. The amplicons are mixed with biotinylated type-specific probes that permit the binding of the probe-DNA hybrids to streptavidin plates. Subsequently, hybrids are detected colorimetrically as in ELISA. This assay has proven to be highly sensitive; as little as 1.5 PFU of virus produced a positive signal. The assay is highly specific and can correctly identify virus types with no cross-reactivity. Although this test is highly promising and could replace PRNT for typification of hantaviruses, specific capture probes must be available. This is a major disadvantage, because as the number of discovered hantaviruses increases, additional capture probes will need to be designed and added to the panel. Overall, the procedure of PCR-EIA is definitely much simpler and faster than PRNT, and shows equal potential for typing hantaviruses in cell cultures, rodent samples and clinical samples.

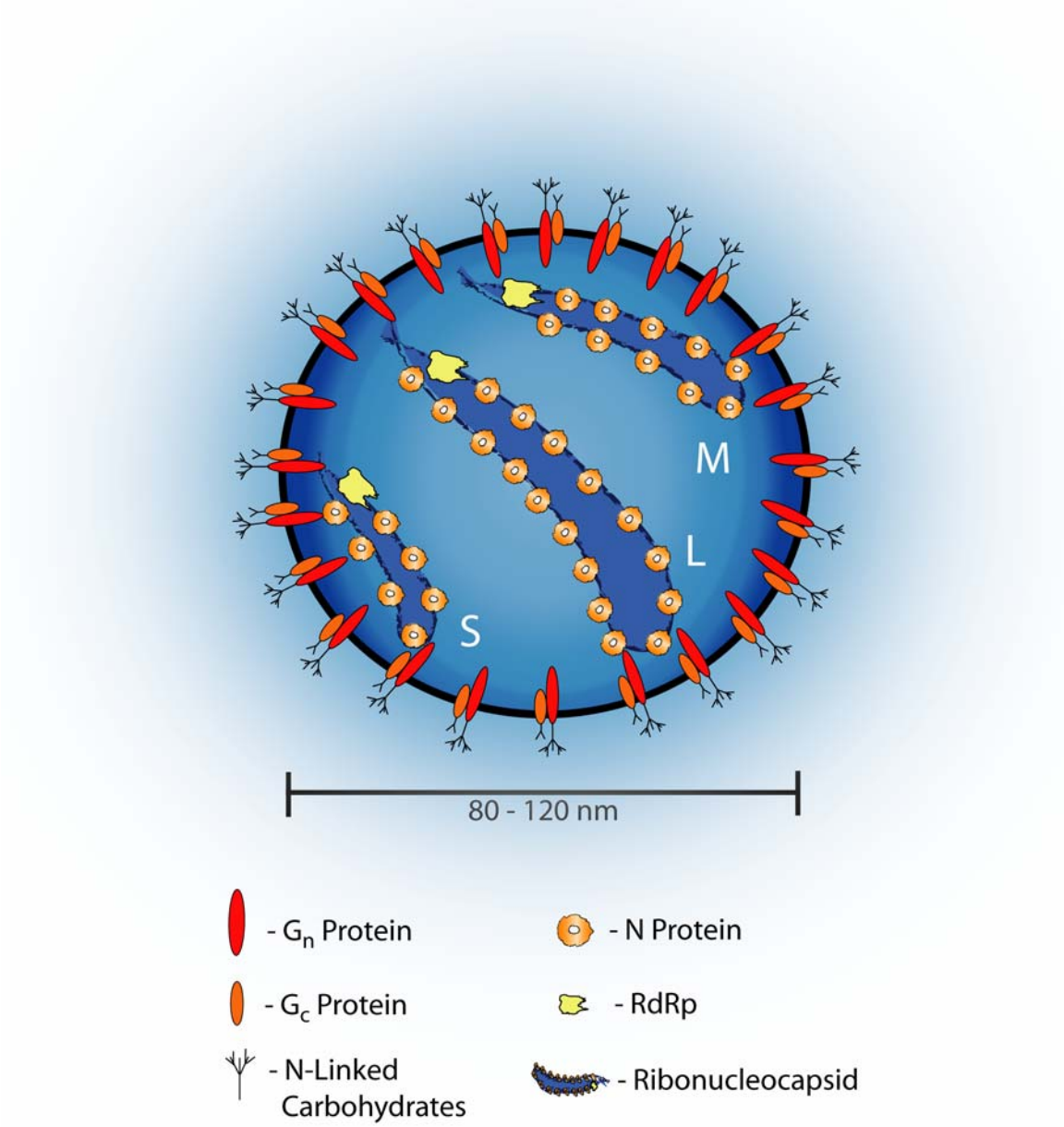

Figure 1: Schematic illustration of a virion particle showing glycoprotein projections at the surface and the internal tripartite genomic structure of the ribonucleocapsids.

Table 1: Representative viruses of the family *Bunyaviridae* (46)

Genus	Notable virus Members	Geographic Distribution	Vector	Disease
Orthobunyavirus	Bunyamwera	Africa	Mosquitoes	Human
	Cache Valley	North America	Mosquitoes	Sheep, cattle, humans
	Germiston	Africa	Mosquitoes	Human
	Bwamba	Africa	Mosquitoes	Human
	Apeu	South America	Mosquitoes	Human
	La Crosse	North America	Mosquitoes	Human
	Jamestown Canyon	North America	Mosquitoes	Human
Phlebovirus	Punta Toro	North and South America	Phlebotomine flies	Human
	Rift Valley fever	Africa	Mosquitoes	Human, cattle
	Sandlfly fever	Europe, Africa, Asia	Phlebotomine flies	Human
	Toscana	Europe	Phlebotomine flies	Human
	Uukuniemi	Europe	Ticks	Seabirds
Nairovirus	Crimean-Congo HF	Africa, Asia, Europe	Ticks	Human
	Hughes	North and South America	Ticks	Seabirds
Tospovirus	Tomato spotted wilt	World wide	Thrips	Plants

Table 1: Continued

Genus	Notable virus Members	Geographic Distribution	Vector	Disease
Hantavirus				
Old World	Hantaan	Asia	Rattus	Human
	Dobrava	Europe	Apodemus flavicollis	Human
	Seoul	Asia	Rattus	Human
	Puumala	Europe, Asia and Americas	Clethrionomys	Human
New World	Sin Nombre	North America	Peromyscus maniculatus	Human
	Bayou	North America	Otyzomys palustris	Human
	Black Creek Canal	North America	Sigmodon hispidus	Human
	Andes	South America	Oligoryzomys palustris	Human
	Laguna Negra	South America	Calomys laucha	Human
	Araraquara	South America	Bolomys lasiurus	Human

References

1. **Chen, H. X., and F. X. Qiu.** 1993. Epidemiologic surveillance on the hemorrhagic fever with renal syndrome in China. Chin Med J (Engl) **106:**857-63.

2. **Chen, H. X., F. X. Qiu, B. J. Dong, S. Z. Ji, Y. T. Li, Y. Wang, H. M. Wang, G. F. Zuo, X. X. Tao, and S. Y. Gao.** 1986. Epidemiological studies on hemorrhagic fever with renal syndrome in China. J Infect Dis **154:**394-8.

3. **Chernukha, Y. G., O. A. Evdokimova, and A. V. Cheechovich.** 1986. Results of karyologic and immunobiological studies of the striped field mouse (Apodemus agrarius) from different areas of its range. Zool J **65:**471-475.

4. **Chu, Y. K., G. Jennings, A. Schmaljohn, F. Elgh, B. Hjelle, H. W. Lee, S. Jenison, T. Ksiazek, C. J. Peters, P. Rollin, and et al.** 1995. Cross-neutralization of hantaviruses with immune sera from experimentally infected animals and from hemorrhagic fever with renal syndrome and hantavirus pulmonary syndrome patients. J Infect Dis **172:**1581-4.

5. **Chu, Y. K., C. Rossi, J. W. Leduc, H. W. Lee, C. S. Schmaljohn, and J. M. Dalrymple.** 1994. Serological relationships among viruses in the Hantavirus genus, family Bunyaviridae. Virology **198:**196-204.

6. **Clement, J., P. Colson, and P. McKenna.** 1994. Hantavirus pulmonary syndrome in New England and Europe. N Engl J Med **331:**545-6; author reply 547-8.

7. **Dahlberg, J. E., J. F. Obijeski, and J. Korb.** 1977. Electron microscopy of the segmented RNA genome ofLa Crosse virus: absence of circular molecules. J Virol **22:**203-9.

8. **Dekonenko, A., M. S. Ibrahim, and C. S. Schmaljohn.** 1997. A colorimetric PCR-enzyme immunoassay to identify hantaviruses. Clin Diagn Virol **8:**113-21.

9. **Donets, M. A., M. P. Chumakov, M. B. Korolev, and S. G. Rubin.** 1977. Physicochemical characteristics, morphology and morphogenesis of virions of the causative agent of Crimean hemorrhagic fever. Intervirology **8:**294-308.

10. **Duchin, J. S., F. T. Koster, C. J. Peters, G. L. Simpson, B. Tempest, S. R. Zaki, T. G. Ksiazek, P. E. Rollin, S. Nichol, E. T. Umland, and et al.** 1994. Hantavirus pulmonary syndrome: a clinical description of 17 patients with a newly recognized disease. The Hantavirus Study Group. N Engl J Med **330:**949-55.

11. **Feldmann, H., A. Sanchez, S. Morzunov, C. F. Spiropoulou, P. E. Rollin, T. G. Ksiazek, C. J. Peters, and S. T. Nichol.** 1993. Utilization of autopsy RNA for the synthesis of the nucleocapsid antigen of a newly recognized virus associated with hantavirus pulmonary syndrome. Virus Res **30:**351-67.

12. **Fenner, F.** 1975. The classification and nomenclature of viruses. Summary of results of meetings of the International Committee on Taxonomy of Viruses in Madrid, September 1975. Intervirology **6:**1-12.

13. **Hjelle, B., C. F. Spiropoulou, N. Torrez-Martinez, S. Morzunov, C. J. Peters, and S. T. Nichol.** 1994. Detection of Muerto Canyon virus RNA in peripheral blood mononuclear cells from patients with hantavirus pulmonary syndrome. J Infect Dis **170:**1013-7.

14. **Hjelle, B., N. Torrez-Martinez, and F. T. Koster.** 1996. Hantavirus pulmonary syndrome-related virus from Bolivia. Lancet **347:**57.

15. **Hung, T., Z. Y. Chou, T. X. Zhao, S. M. Xia, and C. S. Hang.** 1985. Morphology and morphogenesis of viruses of hemorrhagic fever with renal syndrome (HFRS). I. Some peculiar aspects of the morphogenesis of various strains of HFRS virus. Intervirology **23:**97-108.

16. **Khan, A. S., M. Gaviria, P. E. Rollin, W. G. Hlady, T. G. Ksiazek, L. R. Armstrong, R. Greenman, E. Ravkov, M. Kolber, H. Anapol, E. D. Sfakianaki, S. T. Nichol, C. J. Peters, and R. F. Khabbaz.** 1996. Hantavirus pulmonary syndrome in Florida: association with the newly identified Black Creek Canal virus. Am J Med **100:**46-8.

17. **Khan, A. S., R. F. Khabbaz, L. R. Armstrong, R. C. Holman, S. P. Bauer, J. Graber, T. Strine, G. Miller, S. Reef, J. Tappero, P. E. Rollin, S. T. Nichol, S. R. Zaki, R. T. Bryan, L. E. Chapman, C. J. Peters, and T. G. Ksiazek.** 1996. Hantavirus pulmonary syndrome: the first 100 US cases. J Infect Dis **173:**1297-303.

18. **Khan, A. S., C. F. Spiropoulou, S. Morzunov, S. R. Zaki, M. A. Kohn, S. R. Nawas, L. McFarland, and S. T. Nichol.** 1995. Fatal illness associated with a new hantavirus in Louisiana. J Med Virol **46:**281-6.

19. **LeDuc, J. W.** 1987. Epidemiology of Hantaan and related viruses. Lab Anim Sci **37:**413-8.

20. **Lee, H. W.** 1989. Clinical Manifestations of HFRS, p. 19-38, Manual of Hemorrhagic Fever with Renal Syndrome, Lee, H. W. Dalrymple, J. M. ed, Seoul.

21. **Lee, H. W.** 1989. Hemorrhagic fever with renal syndrome in Korea. Rev Infect Dis **11:**S864-S867.

22. **Lee, H. W.** 1982. Korean hemorrhagic fever. Prog Med Virol **28:**96-113.

23. **Lee, H. W., L. J. Baek, and K. M. Johnson.** 1982. Isolation of Hantaan virus, the etiologic agent of Korean hemorrhagic fever, from wild urban rats. J Infect Dis **146:**638-44.

24. **Lee, H. W., and K. M. Johnson.** 1976. Korean hemorrhagic fever: Demonstration of causative antigen and antibodies. Jorean J. Intern. Med **19:**371.

25. **Lee, H. W., P. W. Lee, and K. M. Johnson.** 1978. Isolation of the etiologic agent of Korean Hemorrhagic fever. J Infect Dis **137:**298-308.

26. **Lee, H. W., and G. van der Groen.** 1989. Hemorrhagic fever with renal syndrome. Prog. Med Virol **36:**62.

27. **Lee, P. W., C. J. Gibbs, Jr., D. C. Gajdusek, and R. Yanagihara.** 1985. Serotypic classification of hantaviruses by indirect immunofluorescent antibody and plaque reduction neutralization tests. J Clin Microbiol **22:**940-4.

28. **Lopez, N., P. Padula, C. Rossi, M. E. Lazaro, and M. T. Franze-Fernandez.** 1996. Genetic identification of a new hantavirus causing severe pulmonary syndrome in Argentina. Virology **220:**223-6.

29. **Lukes, R. J.** 1954. The pathology of thirty-nine fatal cases of epidemic hemorrhagic fever. Am J Med **16:**639-50.

30. **Martin, M. L., H. Lindsey-Regnery, D. R. Sasso, J. B. McCormick, and E. Palmer.** 1985. Distinction between Bunyaviridae genera by surface structure and comparison with Hantaan virus using negative stain electron microscopy. Arch Virol **86:**17-28.

31. **McCormick, J. B., D. R. Sasso, E. L. Palmer, and M. P. Kiley.** 1982. Morphological identification of the agent of Korean haemorrhagic fever (Hantaan virus)as a member of the Bunyaviridae. Lancet **1:**765-8.

32. **Mills, J. N., J. M. Johnson, T. G. Ksiazek, B. A. Ellis, P. E. Rollin, T. L. Yates, M. O. Mann, M. R. Johnson, M. L. Campbell, J. Miyashiro, M. Patrick, M. Zyzak, D. Lavender, M. G. Novak, K. Schmidt, C. J. Peters, and J. E. Childs.** 1998. A survey of hantavirus antibody in small-mammal populations in selected United States National Parks. Am J Trop Med Hyg **58:**525-32.

33. **Monroe, M. C., S. P. Morzunov, A. M. Johnson, M. D. Bowen, H. Artsob, T. Yates, C. J. Peters, P. E. Rollin, T. G. Ksiazek, and S. T. Nichol.** 1999. Genetic diversity and distribution of Peromyscus-borne hantaviruses in North America. Emerg Infect Dis **5:**75-86.

34. **Obijeski, J. F., D. H. Bishop, F. A. Murphy, and E. L. Palmer.** 1976. Structural proteins of La Crosse virus. J Virol **19:**985-97.

35. **Obijeski, J. F., D. H. Bishop, E. L. Palmer, and F. A. Murphy.** 1976. Segmented genome and nucleocapsid of La Crosse virus. J Virol **20:**664-75.

36. **Obijeski, J. F., and F. A. Murphy.** 1977. Bunyaviridae: recent biochemical developments. J Gen Virol **37:**1-14.

37. **Padula, P. J., A. Edelstein, S. D. Miguel, N. M. Lopez, C. M. Rossi, and R. D. Rabinovich.** 1998. Hantavirus pulmonary syndrome outbreak in Argentina: molecular evidence for person-to-person transmission of Andes virus. Virology **241:**323-30.

38. **Pilaski, J., H. Feldmann, S. Morzunov, P. E. Rollin, S. L. Ruo, B. Lauer, C. J. Peters, and S. T. Nichol.** 1994. Genetic identification of a new Puumala virus strain causing severe hemorrhagic fever with renal syndrome in Germany. J Infect Dis **170:**1456-62.

39. **Powell, G. M.** 1954. Hemorrhagic fever: a study of 300 cases. Medicine (Baltimore) **33:**97-153.

40. **Ravkov, E. V., P. E. Rollin, T. G. Ksiazek, C. J. Peters, and S. T. Nichol.** 1995. Genetic and serologic analysis of Black Creek Canal virus and its association with human disease and Sigmodon hispidus infection. Virology **210:**482-9.

41. **Schmaljohn, C.** 1996. Molecular Biology of Hantaviruses, p. 63-90. *In* R. Elliot (ed.), *The Bunyaviridae.* Plenum Press, New York.

42. **Schmaljohn, C. S., and J. M. Dalrymple.** 1983. Analysis of Hantaan virus RNA: evidence for a new genus of bunyaviridae. Virology **131:**482-91.

43. **Schmaljohn, C. S., S. E. Hasty, J. M. Dalrymple, J. W. LeDuc, H. W. Lee, C. H. von Bonsdorff, M. Brummer-Korvenkontio, A. Vaheri, T. F. Tsai, H. L. Regnery, and et al.** 1985. Antigenic and genetic properties of viruses linked to hemorrhagic fever with renal syndrome. Science **227:**1041-4.

44. **Schmaljohn, C. S., S. E. Hasty, S. A. Harrison, and J. M. Dalrymple.** 1983. Characterization of Hantaan virions, the prototype virus of hemorrhagic fever with renal syndrome. J Infect Dis **148:**1005-12.

45. **Schmaljohn, C. S., and J. W. Hooper.** 2001. *Bunyaviridae*: The viruses and their replication., p. 1581-1602. *In* K. D. Fields BN, Howley PM. (ed.), Virology, 4 ed, vol. 2. Lippincott-Raven, Philadelphia.

46. **Schmaljohn, C. S., and S. T. Nichol.** 2006. *Bunyaviridae*, p. 1741-1789. *In* D. Knipe (ed.), Virology, vol. 2. Lippincott-Raven, Philadelphia.

47. **Severson, W. E., C. S. Schmaljohn, A. Javadian, and C. B. Jonsson.** 2003. Ribavirin causes error catastrophe during Hantaan virus replication. J Virol **77:**481-8.

48. **Sheedy, J. A., H. F. Froeb, H. A. Batson, C. C. Conley, J. P. Murphy, R. B. Hunter, D. W. Cugell, R. B. Giles, S. C. Bershadsky, J. W. Vester, and R. H. Yoe.** 1954. The clinical course of epidemic hemorrhagic fever. Am J Med **16:**619-28.

49. **Sugiyama, K., S. Morikawa, Y. Matsuura, E. A. Tkachenko, C. Morita, T. Komatsu, Y. Akao, and T. Kitamura.** 1987. Four serotypes of haemorrhagic fever with renal syndrome viruses identified by polyclonal and monoclonal antibodies. J Gen Virol **68 (Pt 4):**979-87.

50. **Terajima, M., J. D. Hendershot, 3rd, H. Kariwa, F. T. Koster, B. Hjelle, D. Goade, M. C. DeFronzo, and F. A. Ennis.** 1999. High levels of viremia in patients with the Hantavirus pulmonary syndrome. J Infect Dis **180:**2030-4.

51. **Wells, R. M., S. Sosa Estani, Z. E. Yadon, D. Enria, P. Padula, N. Pini, J. N. Mills, C. J. Peters, and E. L. Segura.** 1997. An unusual hantavirus outbreak in southern Argentina: person-to-person transmission? Hantavirus Pulmonary Syndrome Study Group for Patagonia. Emerg Infect Dis **3:**171-4.

52. **White, J. D., F. G. Shirey, G. R. French, J. W. Huggins, O. M. Brand, and H. W. Lee.** 1982. Hantaan virus, aetiological agent of Korean haemorrhagic fever, has Bunyaviridae-like morphology. Lancet **1:**768-71.

CHAPTER 3

SPATIO-TEMPORAL DISTRIBUTION OF THE HANTAAN VIRUS NUCLEOCAPSID PROTEIN AND TRANSPORT TO THE ENDOPLASMIC RETICULUM-GOLGI INTERMEDIATE COMPARTMENT

Abstract

The pathways of assembly for the Old and New World hantaviruses are under active investigation. While it is generally accepted that Old World hantaviruses assemble and bud into the Golgi complex, the assembly site for the New World hantaviruses remains controversial. To gain insight into assembly pathways of Old World hantaviruses, we examined the spatial and temporal distribution of the N protein of the Hantaan virus (HTNV) in Vero E6 cells. We show progressive redistribution of HTNV N protein from cell periphery to the perinuclear region during infection. At the perinuclear region, the HTNV N protein was observed to co-localize at the endoplasmic reticulum-Golgi intermediate compartment (ERGIC). We did not observe co-localization of the N protein with actin microfilaments, suggesting that the targeting of the N protein is unlikely to be dependent on actin cytoskeleton. Expression of HTNV N protein in Vero E6 cells independent of other viral components shows the N protein localized to the peri-nuclear region similar to that of virus-infected cells. This suggests the N proteins have autonomous signals sufficient for subcellular targeting. Fractionation of cells expressing HTNV N protein showed a small portion of N protein associated with microsomal membranes. This suggests that association of the N protein with host's cellular membranes may play a role in virus assembly.

Introduction

Numerous hantaviruses have been identified in discrete parts of the world. Hantaviruses are classified as Old World and New World based on their geographic distribution and their ability to in induce distinct illnesses in humans (38). Old World hantaviruses (Hantaan virus, HTNV) are found in Eurasia and cause hemorrhagic fever with renal syndrome (HFRS), while New World hantaviruses (Andes virus, ANDV) are found in the Americas and cause hantavirus pulmonary syndrome (HPS) (24). Despite their differences in pathogenesis, the Old World and New World hantaviruses share high homology in the organization of their nucleic sequences, and exhibit similar aspects of their life cycle.

Hantaviruses enter host epithelial cells via interaction of the larger viral glycoprotein (G1) with the host's cell surface receptor(s); β1 and β3 integrins (8, 9). HTNV entry has been shown to be mediated by clathrin-coated pits, followed by movement to early endosomes, and subsequent delivery to late endosomes or lysosomes (15). Within the endo-lysosomal compartments, the virus is uncoated to liberate the three nucleocapsids that contain the negative-sense, single-stranded RNA segments complexed with N protein and RNA dependent RNA polymerase (RdRp). After uncoating, the viral genome and the RdRp enter host cytoplasm and the RdRp initiates primary transcription to give rise to viral mRNA.

The transcripts of the large (L; encoding RdRp), medium (M: encoding glycoproteins G1/G2), and small (S; encoding nucleocapsid N protein) segments of the viral genome are then translated on host's ribosomes (37). The RdRp and N proteins lack

transmembrane domains and are presumed to be translated on free ribosomes and remain within the cytoplasm. The glycoprotein G1/G2 precursor is translated on membrane-bound ribosomes and co-translationally inserted into rough endoplasmic reticulum (ER). The precursor is proteolytically processed into two transmembrane polypeptides, G1 and G2 during import into the ER (33, 42). In HTNV, a conserved amino acid motif, WAASA, located at the end of G1 is presumed to be the proteolytic cleavage site (22). The G1 and G2 proteins are core glycosylated in the ER and subsequently transported to the Golgi complex (3, 28, 33, 37, 46).

At a point after infection determined by an unknown mechanism, the virus switches from transcription to replication of the viral genomic RNA (vRNA) to viral complementary RNA (cRNA) and vice versa. When sufficient levels of protein and nucleic acid components are produced, packaging and assembly of viral particles occurs. The newly synthesized vRNAs and RdRp are encapsidated by N proteins to form the ribonucleocapsids (RNPs) (38). The RNPs are then enveloped by membranes containing G1/G2 to produce hantavirus particles.

It has been suggested that Old World hantaviruses assemble and mature at the Golgi complex (12, 38), while New World hantaviruses assemble and mature at the plasma membrane (26). This is largely based on the observation that intracellular particles were not observed in cells infected with the Sin Nombre virus (SNV) and the Black Creek Canal virus (BCCV), suggesting that they bud at the PM. However, the N and G1/G2 proteins of BCCV accumulate in the Golgi region, suggesting that Golgi events may be important for virus assembly.

To further explore possible pathways in the assembly process of Old World hantaviruses, we analyzed the temporal-spatial distribution of N proteins of the HTNV during infection. We used an immunofluorescence approach to characterize the localization of the HTNV N proteins in Vero E6 cells from day 1 to day 7 post-infection. Herein, we show that over the course of the infection, the HTNV N protein progressively relocates from peripheral cellular regions to the perinuclear region. We have identified that the HTNV N protein target endoplasmic reticulum-Golgi intermediate compartment (ERGIC). Although, previous studies have suggested the involvement of the actin cytoskeleton in hantavirus assembly, we have not detected association of HTNV N protein with actin at any time post-infection, suggesting that the actin cytoskeleton is not the major determinant of HNTV protein targeting. We also report that HTNV N protein targets the peri-nuclear region when expressed in cells without other viral components, and stably associate with cellular membranes. These findings suggest that the peri-nuclear distribution is at least partially due to HTNV N protein binding to membranes on peri-nuclear compartments. It is likely that this association plays a significant role in the assembly pathway of the HTNV.

Results

Spatial and temporal distribution of HTNV N protein in Vero E6 cells

To address the trafficking of the HTNV, we examined the spatial and temporal patterns of HTNV at days 1, 3, 5, and 7 days post-infection of Vero E6 cells. The temporal distribution of this virus over course of 7 days was followed by the N protein.

On day 1 post-infection, the HTNV N protein was predominantly detected in small punctate structures dispersed throughout the cell (Fig. 1, day 1). Some of the structures were near the perinuclear region, but the majority was more peripheral. While an enlarged image of a single cell is shown in figure 1, an analogous punctate pattern of N protein localization was observed in the majority of virus-infected cells (data not shown).

A significant change in the distribution of N proteins was observed 3 days post-infection. At that time, the majority of the punctate structures containing HTNV N protein were clustered in the perinuclear region, with less N protein remaining in cell periphery (Fig. 1, day 3). This trend continued, and at 5 and 7 days post-infection the vast majority of the N protein was observed at the peri-nuclear region (Fig 1, day 5 and 7). At day 7, the HTNV N protein was localized exclusively within the perinuclear region in what appears like a continuous structure surrounding one side of the nucleus. Interestingly, cells epressing GFP tagged N protein had a similar expression profile as in virus-infected cells.

HTNV N protein targets peri-Golgi compartments in virus-infected Vero E6 cells

Members of the *Bunyaviridae* family have been shown to assemble and bud at the Golgi complex. The Golgi complex is the main peri-nuclear compartment in mammalian cells. The perinuclear localization of the HTNV N protein in infected cells suggested possible targeting to the Golgi complex. We therefore examined the distribution of HTNV N protein relative to the Golgi complex over a 7 day period after infecting Vero E6 cells with the the HTNV (Fig. 2). In these experiments, the Golgi complex was

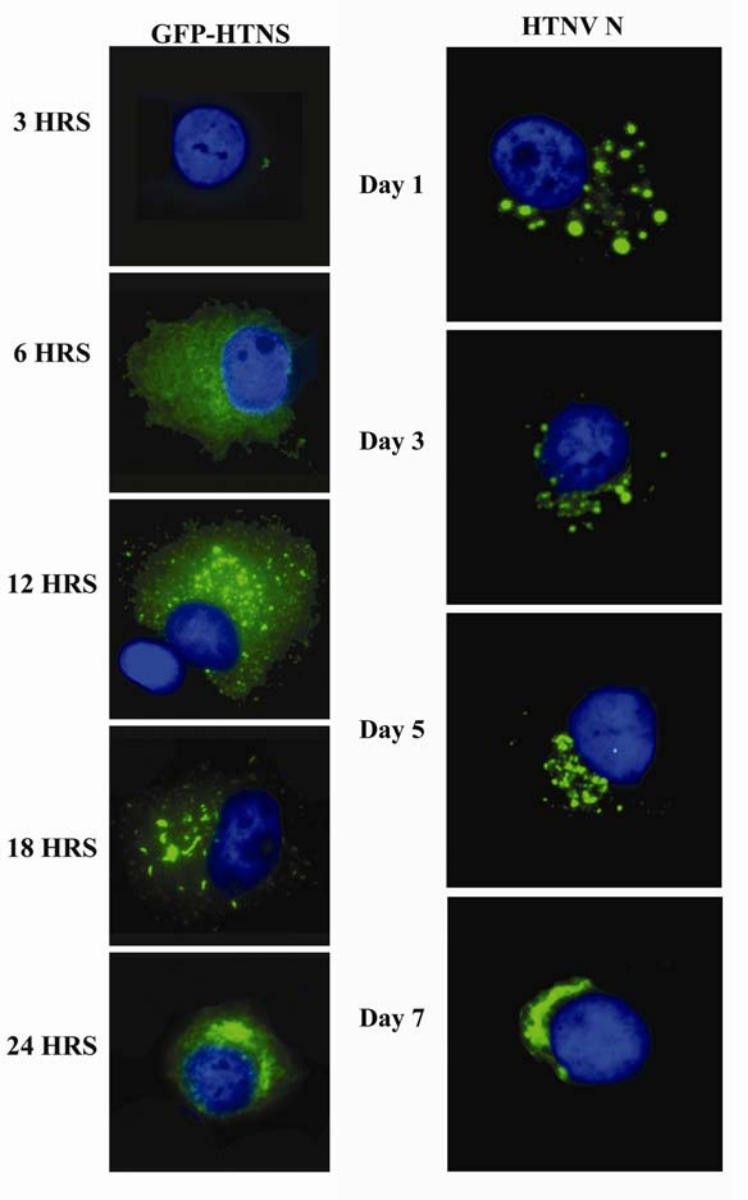

Figure 1: Spatio-temporal redistribution of HTNV N protein in virus-infected or transfected cells. Vero E6 cells were infected with HTNV at MOI 1.0 or transfected with 1 μg of plasmid DNA expressing GFP-HTNS. The cells were examined by immunofluorescence at the indicated time points post-infection, using monoclonal antibodies against HTNV N protein, or by GFP expression in transfected cells.

detected using Wheat Germ Agglutinin (WGA) coupled to Alexa-594. WGA is a lectin specific for complex type oligosaccharide present on Golgi-localized proteins, and has been used extensively to label the Golgi complex in a variety of mammalian cells.

Partial co-localization of the HTNV N protein with the Golgi marker was observed at 1 to 7 days post-infection. At day 1, HTNV-infected cells show limited co-localization of N protein with WGA at the Golgi complex (Fig. 2, day 1). This is consistent with data in Figure 1 showing predominantly peripheral localization of the N proteins at that time. At day 3, a higher proportion of HTNV N protein co-localized with the WGA marker at the Golgi complex (Fig 2, day 3).

The proportion of HTNV N protein co-localized with the WGA at the Golgi complex increased steadily from day 5 through day 7 post-infection (Fig. 2). At day 7, the majority of the HTNV N protein was observed at the Golgi complex (Fig. 2, day 7). Significantly, even 7 days after infection, at a time of maximal co-localization of HTNV N protein with the Golgi complex, a proportion of the N proteins targeted to the peri-nuclear region did not co-localize with the Golgi. This lack of complete co-localization with the Golgi complex suggests that the N proteins may be indirectly targeted to the Golgi complex through other compartments, or that they have additional biological activities that warrant trafficking to non-Golgi perinuclear compartments.

HTNV N proteins target ER in virus-infected Vero E6 cells

The incomplete co-localization of the HTNV N protein with the Golgi complex suggested the N proteins associate with other peri-nuclear compartments. Another cellular compartment concentrated in the peri-nuclear region of Vero E6 cells is the

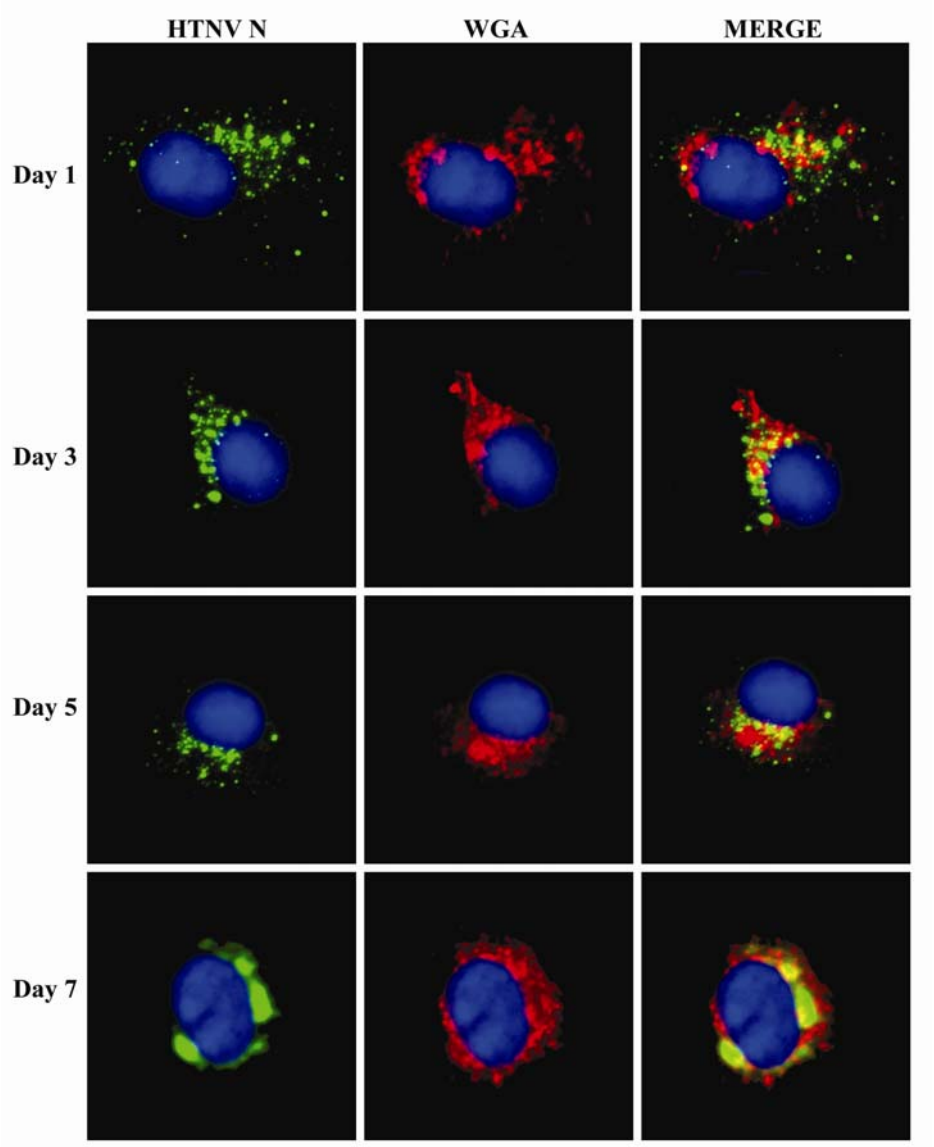

Figure 2: HTNV N protein partially localizes to the Golgi complex in virus-infected cells. Vero E6 cells were infected with HTNV at MOI 1.0. Cells were examined by immunofluorescence at the indicated time points post-infection, using monoclonal antibodies against HTNV N protein. The Golgi complex was labeled with WGA.

endoplasmic reticulum (ER). While the ER extends to the periphery of the cells, ER is also concentrated in the peri-nuclear region of cells. We therefore performed immunofluorescence studies to examine the targeting of the HTNV N protein to the ER. The ER was detected using the resident protein PDI as a marker. The HTNV N protein extensively co-localized with PDI at 1 day post-infection (Fig. 3, day 1). Interestingly, the co-localization was apparent in the peri-nuclear region as well as in more peripheral punctate structures (Fig. 1, day 1). HTNV N protein showed partial co-localization with the ER through 7 days post-infection (Fig. 3).

The localization of the HTNV N protein at the ER suggests that the ER could play a significant role in facilitating the maturation of virus particles. The incomplete localization of N protein to the ER (Figure 3), and to the Golgi complex (Fig. 2) suggests that the HTNV N protein may target to additional peri-nuclear compartments.

HTNV N protein does not co-localize with actin filaments in virus-infected Vero E6 cells

The three predominant cytoskeletal systems of mammalian cells are composed of microtubules, actin microfilaments, and intermediate filaments. Microtubules and actin microfilaments have been shown to have important roles in protein traffic (45). Recently, actin microfilaments were suggested to play a significant role in the trafficking of the N proteins of the Crimean Congo Hemorrhagic Fever Virus (CCHFV) (2) and the New World hantavirus Black Creek Canal Virus (BCCV) (28). We therefore explored the relationship between actin cytoskeleton and the HTNV N protein in virus-infected cells.

The actin content was detected with phalloidin conjugated to Alexa-594. The actin cytoskeleton in Vero E6 cells consists of organized filaments, stress fibers, and

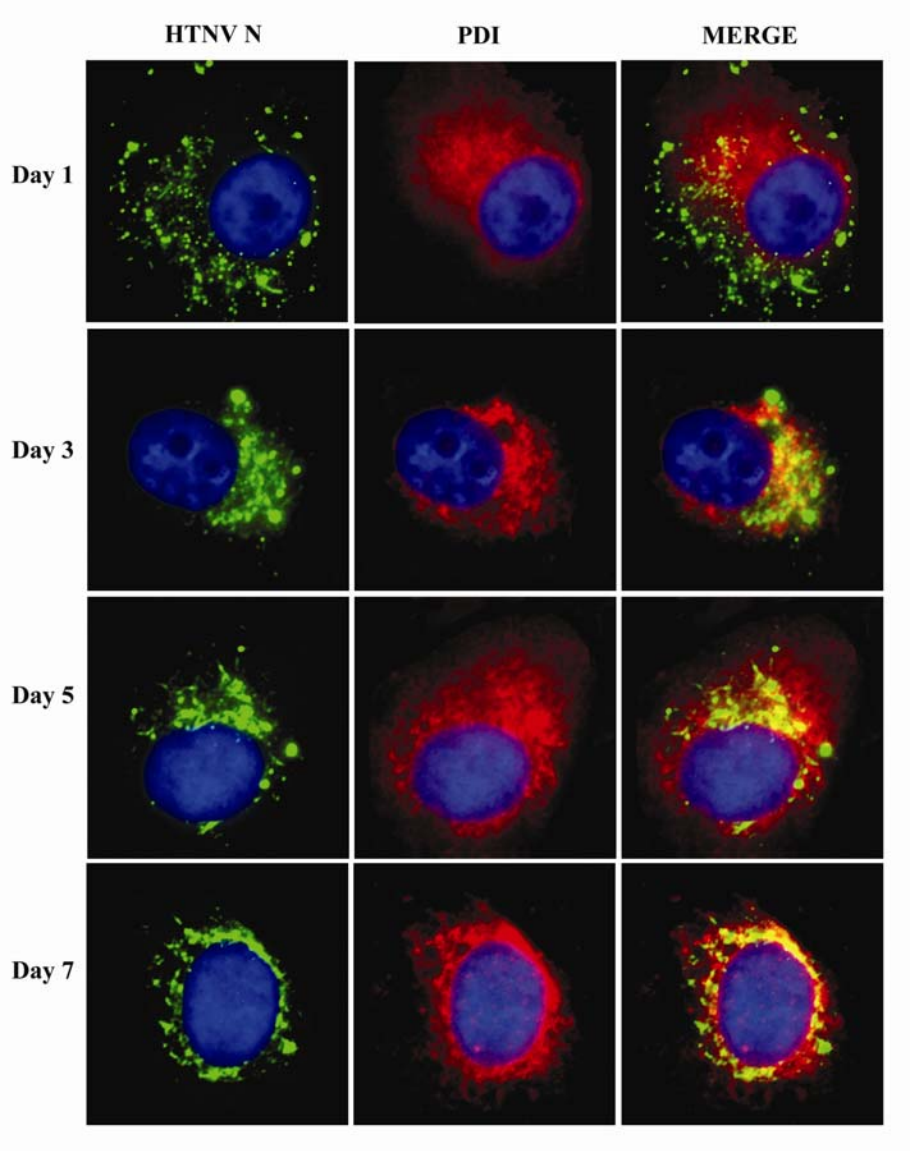

Figure 3: HTNV N protein partially localize to the ER in virus-infected cells. Vero E6 cells were infected with HTNV at an MOI 1.0. The cells were examined by double-label immunofluorescence at the indicated time points post-infection, using monoclonal antibodies against HTNV N protein and polyclonal antibodies against calreticulin. The HTNV N protein shows co-localization with the ER, especially at early time points post-infection.

subcortical actin. Unexpectedly, in virus-infected cells (Fig. 4), the pattern of actin microfilaments differed as compared to uninfected cells. Instead of organized filaments and stress fibers, the infected cells had diffuse cytoplasmic staining and short disorganized fibers. We did not detect co-localization of HTNV N protein with actin microfilaments at any time post infection (Fig. 4, day 1-7). Our results contrast with the CCHFV and BCCV studies, and suggest that different members of the *Bunyaviridae* may utilize distinct mechanisms to position their respective N protein within the cell.

HTNV N protein expressed in Vero E6 targets the peri-nuclear region in the absence of other viral components

The BCCV N protein has been shown to target to the perinuclear region in the absence of other viral components (26). We therefore explored whether HTNV N protein can target to peri-nuclear compartments independently of other viral components. Plasmids encoding HTNV N protein were transfected into Vero E6 cells. After 24 hours, the cells were processed by immunofluorescence to examine the distribution of the N proteins relative to Golgi and ER markers.

The HTNV N protein only partially co-localized with the WGA Golgi marker in cells expressing N protein (Fig. 5A). Importantly, the patterns observed in transfected cells parallel those observed in virus-infected cells (Fig. 2). This indicates that the trafficking of HTNV N protein to the Golgi complex is defined by an intrinsic molecular characteristic and is not determined by other viral components.

The HTNV N protein also co-localized with the ER marker protein disulfide isomerase (PDI) (Fig. 5B). The localization of the N proteins to the Golgi and the ER in

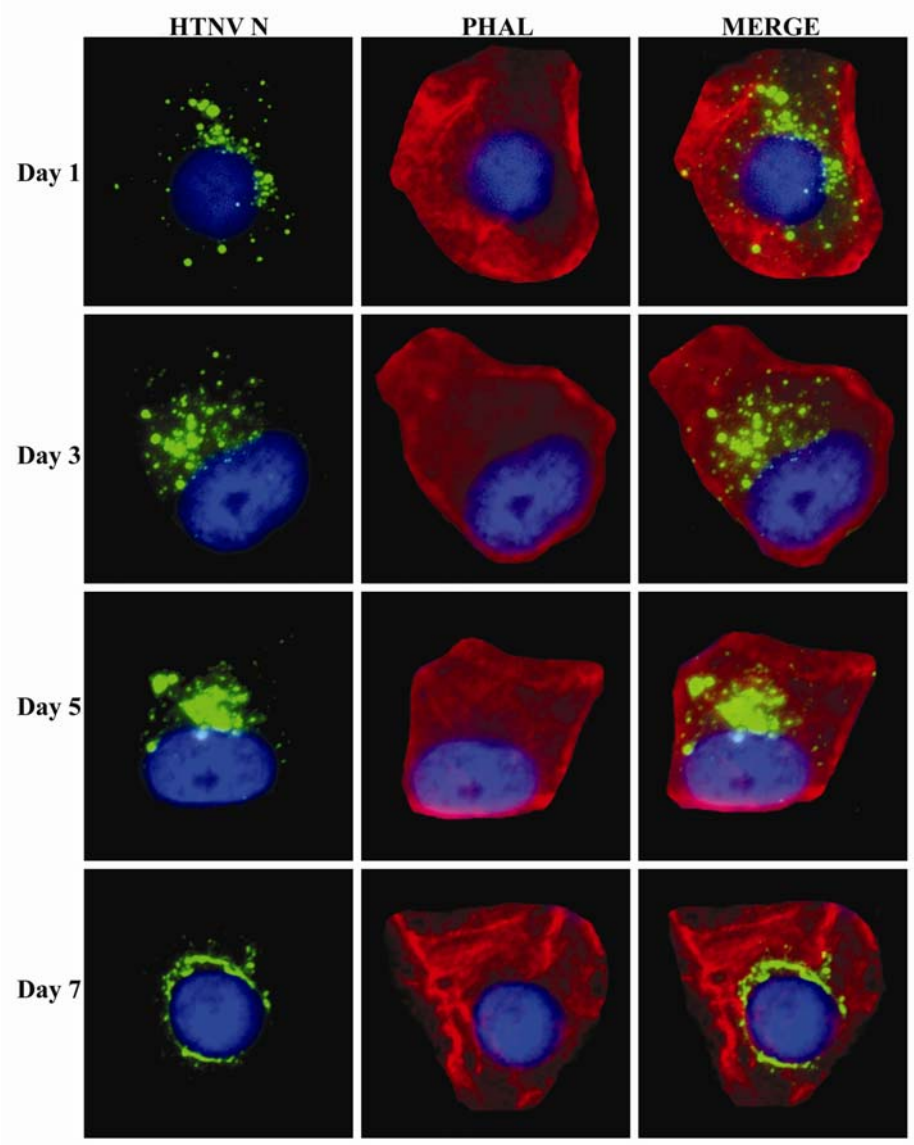

Figure 4: HTNV N protein does not co-localize with actin in virus-infected cells. Vero E6 cells were infected with HTNV at an MOI 1.0. The cells were examined by immunofluorescence at the indicated time points post-infection, using monoclonal antibodies against HTNV N protein. The actin cytoskeleton was labeled with phalloidin conjugated to Alexa-594.

the absence of other viral components suggests the N proteins have autonomous localization signals sufficient for delivery to the peri-nuclear region.

The actin disruption observed in virus-infected cells (Fig. 4) may be the direct result of accumulation of any of the viral components. To explore whether the HTNV N protein contributed to the actin phenotype, we analyzed actin architecture in cells expressing only N protein. Like in cells infected with HTNV, we observed disruption of actin filaments in cells expressing only the N protein (compare Fig. 4 and 5C). The apparent change in the actin cytoskeleton in the presence of HTNV N protein suggests that actin architecture may be remodeled (directly or indirectly) by the N protein. Furthermore, in accordance with our results in virus-infected cells (Fig. 4), HTNV N protein did not co-localize with actin microfilaments in cells expressing N protein alone (Fig. 5C).

HTNV N protein colocalizes with ERGIC-53

Since we had observed only partial co-localization with Golgi and ER using non-confocal imaging analysis, we decided to test whether the N protein also associated with other peri-nuclear compartments, such as ERGIC, using confocal microscopy. To help identify the compartment that is being targeted by the N protein, we utilized dual-immunofluorescence labeling techniques with confocal laser-scanning microscopy of HTN virus-infected Vero E6 cells using specific antibodies against HTN virus N protein and various subcellular organelles, such as early endosomes (EE), Golgi apparatus, ER, and ERGIC. We used EEA1 as a marker for EE and examined the distribution of HTN virus N protein relative to the EE in infected cells. At 72 h post-infection, the N protein

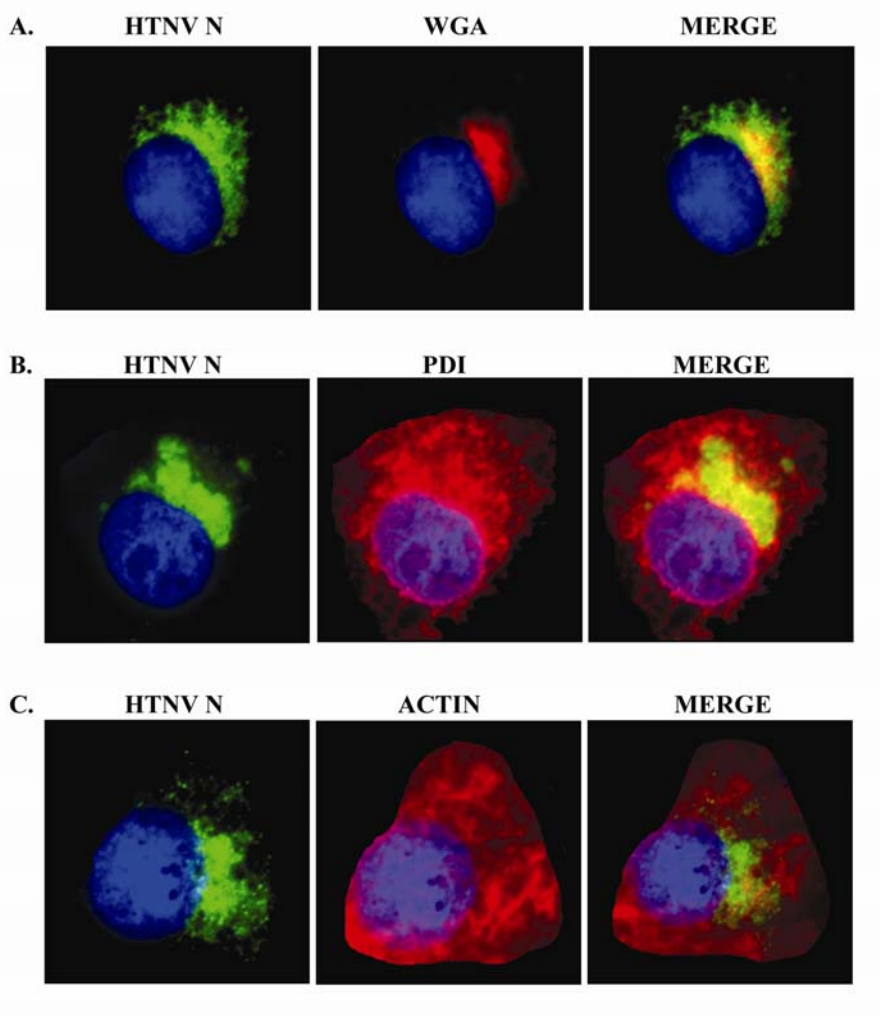

Figure 5: HTNV N protein targets the perinuclear region independent of other viral components. Vero E6 cells transfected with plasmids encoding the N protein from HTNV (A, B, C) were examined by immunofluorescence 24 hours post-transfection using monoclonal antibodies against HTNV N protein. The Golgi was labeled with WGA conjugated to Alexa-594 (panels A). The ER was labeled with antibodies against PDI (panel B). Actin filaments were labeled with phalloidin conjugated to Alexa-594 (panels C).

accumulated as we previously demonstrated, but did not observe any co-localization with EEA1 (Fig. 6A). Since we observed the N protein to associate with the Golgi apparatus using non-confocal imaging analysis, we decided to test this compartment using confocal microscopy. In these experiments, the *trans*-Golgi complex was detected using WGA coupled to Alexa-594 (Fig. 6B). We also labeled the *cis*- and *medial*-Golgi compartments with Mann II (Fig. 6C). To our surprise, we observed no colocalization of N protein with WGA or Mann II (Fig. 6B and C) as we had in non-confocal studies (Fig. 2). This was an unusual finding, because we had initially expected the N protein to localize to the Golgi apparatus since the based on our previous findings and because the viral glycoproteins are known to target this organelle.

Our results demonstrating that the N protein did not co-localize with the Golgi apparatus in confocal studies suggests other perinuclear compartments to be involved. Furthermore, this demonstrates that non-confocal microscopy should not be used in co-localization studies, because it can produce artificial results. Since we observed artificial co-localization between N protein and WGA in non-confocal studies, possibly the association we observed with ER could also be an artifact. We therefore performed similar confocal microscopy studies to examine the targeting of the HTN virus N protein to the ER by using the resident protein PDI of the ER as a marker. Interestingly, our results reveal that the N protein did not target the ER (Fig. 6D), as it had in non-confocal imaging (Fig. 4), but was observed to significantly co-localize with ERGIC-53 as indicated by the yellow signal in the merged image (Fig. 6E).

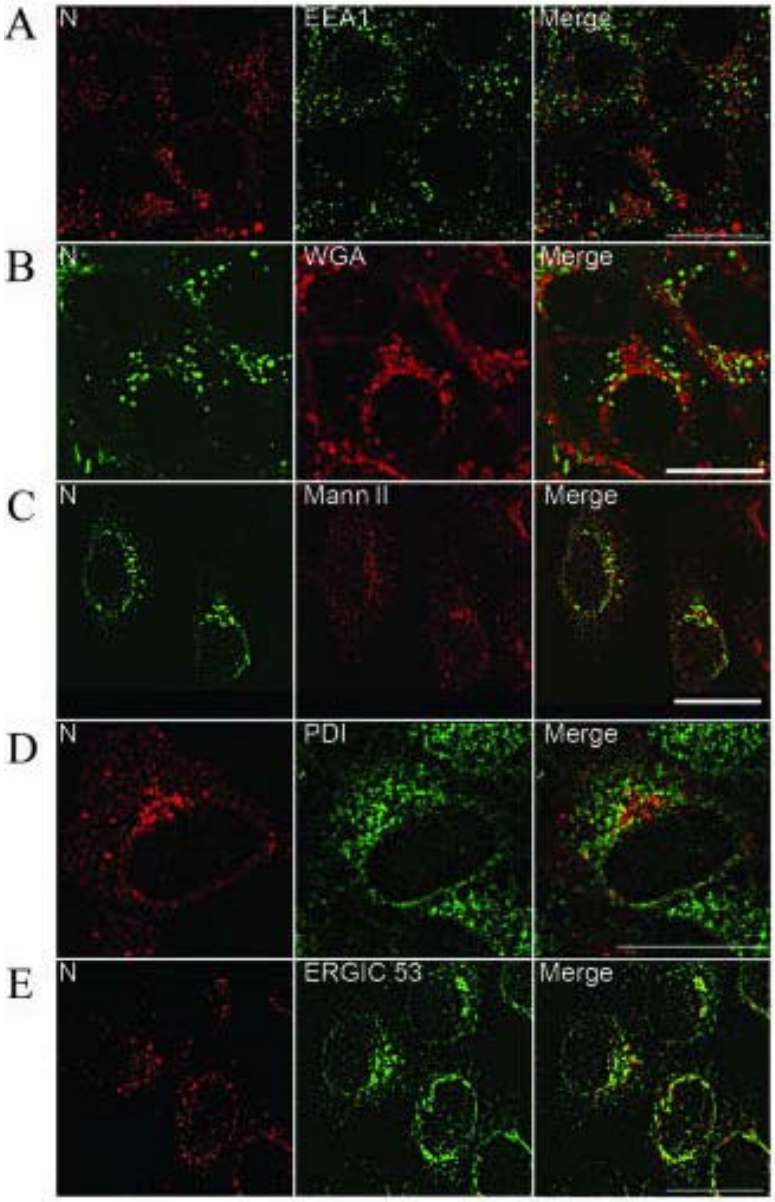

Figure 6: Colocalization of HTNV N protein with ERGIC-53. Vero E6 cells were infected with HTNV at MOI 0.1. Cells were examined by immunofluorescence at 3 days post-infection using antibodies against HTNV N protein. Various subcellular organelle markers were were detected to label label the early endosomes (A), *trans*-Golgi complex (B), *cis*-Golgi complex (C), ER (D), or ERGIC (E).

HTNV N protein associates with microsomal membranes

The co-localization between N protein and ERGIC suggests that the N protein may associate with compartmental membranes. To further explore this possibility, Vero E6 cells expressing the HTNV N protein were subjected to subcellular fractionation. Cells were homogenized and the homogenates were separated into microsomal and cytosolic fractions by ultra-centrifugation. The association of HTNV N protein with the microsomal and the cytosolic fractions was analyzed by Western blot (Fig. 7A). Interestingly, the HTNV N protein was predominantly associated with the microsomal fraction.

The fractions also were probed with antibodies to calnexin and ß-tubulin (Fig. 7B). Calnexin is a transmembrane protein that functions as a marker for cellular membranes, and ß-tubulin is a cytosolic protein that functions as a cytosolic marker. The recovery of each marker only in their cognate fraction confirms the efficiency of the fractionation. . Although the majority of N protein was observed to reside within the membrane fraction (Fig. 7A), only a small amount of N protein was observed within the membrane-containing fractions in extracts subjected to discontinuous sucrose gradient analysis (Fig. 7C, fractions 2-3). Based on these results, we conclude that only a small fraction of N protein can associate with cellular membranes.

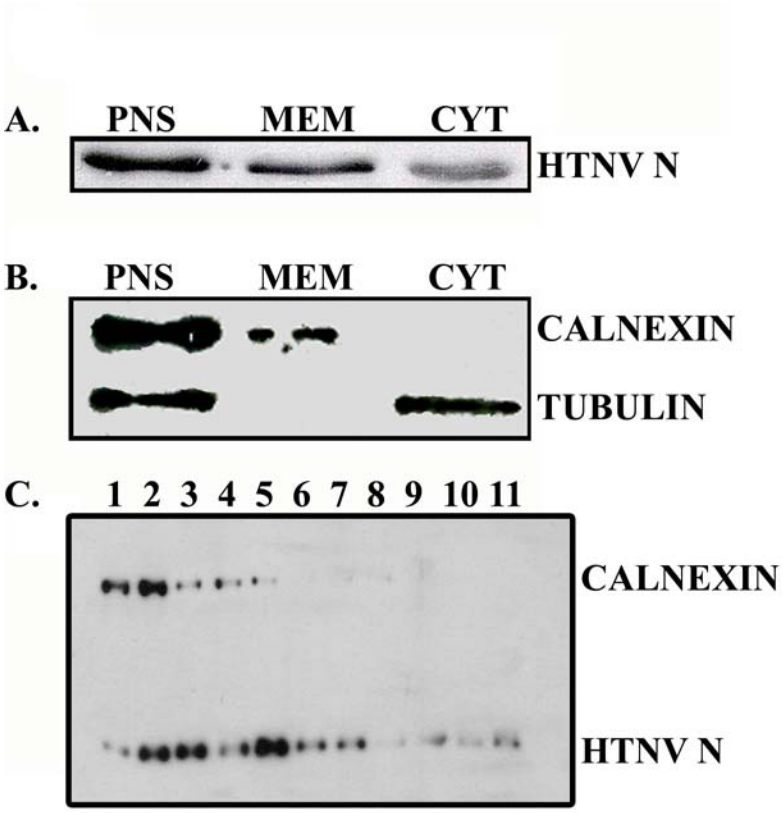

Figure 7: HTNV N protein partially associates with microsomal membranes. Vero E6 cells were transfected with plasmids encoding HTNV N protein, and harvested 24 hours later. Cells were disrupted by passing through an 18 gauge needle. (A)The homogenate was fractionated to obtain the post nuclear supernatant (PNS), the microsomal membranes (MEM) and the cytosol (CYT). An aliquote of each fraction was processed by SDS-PAGE and the gel transferred to NC filter. The filter was Western blotted with antibodies against HTNV N protein (A), or a mixture of anti-β-tubulin and anti-calnexin antibodies (B) as quality controls of MEM and CYT fractions. (C) Sucrose gradient analysis of cell extracts expressing HTNV N protein. Calnexin served as a control to detect membrane fraction.

Discussion

The pathway towards assembly and maturation is essential for viral propagation. The replication of RNA viruses is distinct from other viruses and their sites of assembly have been shown to vary from species to species. It appears that the N protein plays a key role in facilitating viral assembly within the host cell. For the negative stranded RNA enveloped viruses such as the rhabdoviruses and paramyxoviruses, assembly has been shown to take place at the plasma membrane. In those viruses, the N protein is expressed in the cytoplasm and is polymerized on the nascent vRNA during RNA synthesis to form the RNP (14, 44). In rhabdoviruses, the N protein is associated with a phosphoprotein (P), that serves as a chaperone to facilitate the solubility of the N protein prior to RNP formation (14). RNP complexes localize to the plasma membrane via interactions with the matrix protein (MP) (14, 44). For the Influenza A virus, from the *orthomyxoviridae*, RNPs are synthesized in the nucleus and shuttled out to the cytoplasm (21). The N protein of Influenza A virus is capable of localizing to and shuttling between the nucleus and the cytoplasm when expressed alone, without other viral components (47, 48). The N protein of the Marburg virus, family *Filoviridae*, has been visualized by electron microscopy to accumulate in the cytoplasm (18). The N protein of positively stranded viruses, such as the coronaviruses, from the *Nidovirales*, localizes to both the cytoplasm and the nucleolus (11, 49).

Questions remain regarding the assembly pathway for Old World and New World hantaviruses in the *Bunyaviridae,* following entry and replication. It has been suggested that the pathway of assembly and maturation for New World viruses differs from Old World hantaviruses (26). Localization of the N, G1, and G2 proteins at the Golgi has

been observed in both New World and Old World hantaviruses (25, 26, 43). Viral proteins and virion particles of other member of the *Bunyaviridae* family such as Ukuniemi (UUK) (7, 13, 19) and Bunyamwera (BUN) (35) have also been observed to accumulate at the Golgi complex. In contrast to Golgi maturation, BCCV is thought to mature at the cells apical surface (27), similar to Sin Nombre Virus (SNV) (10).

To probe the trafficking of Old World hantaviruses, we have examined the temporal and spatial expression of the HTNV N protein. The N protein is the most abundant viral protein synthesized early in infection (38) and plays key roles in several important steps in the virus life cycle (16) including assembly and packaging. We show that the HTNV N protein accumulates at the perinuclear region in the presence and absence of other viral components, suggesting that the N protein may help to direct the assembly pathway. Using antibodies to various subcellular compartments, we show that the N protein colocalized with ERGIC but not with the Golgi and ER compartments, F-actin, or EE. These data suggest that N protein directly targeted the ERGIC prior to movement to the Golgi compartments and imply that once HTNV N protein traffics to the Golgi compartments, it rabidly assembles into the virion. UUKV N protein has been shown to associate with *cis*-Golgi elements and accumulate in periphery that could also include the ERGIC (13). The ERGIC and Golgi complex have been shown to fragment after BUNV infection in Vero E6 cells, although they remain functional for virus maturation (35). This fragmentation of the ERGIC and Golgi complex could facilitate rapid flux of viral N protein through the ERGIC-Golgi interface. The ERGIC constitutes and independent structure that is not continuous with the ER or the *cis*-Golgi compartment (5, 17, 39). ERGIC is maintained by a continuous flow membranes

mediated by molecular motor proteins that include the microtubule protein dynein, the motor kinessin, microtubules, actin, and various RAB GTPases. Together, they carry intracellular cargo bidirectionally to the ER and to the *cis*-Golgi compartment from ERGIC (4, 32). ERGIC has been show to play roles in the biogenesis of several viruses (17, 23, 30, 31, 34, 36, 41) .

Although there is no evidence so far for any kind of membrane-associated, posttranslational modifications of N protein (38), the N protein of the UUK virus (13) and BCC virus (26) and the L protein of the Tula virus (20) have been shown to associate with microsomal membranes. Furthermore, our studies show that the HTNV N protein is somewhat associated with microsomal membranes, but only a small fraction was found to be membrane bound. Due to this minute association with membranes, it would be difficult to determine the composition of the membranes in the fraction that associated with N protein. The Golgi compartment membranes could serve as the best candidates.

The actin cytoskeleton plays essential roles in cellular functions including cell survival, maintenance and interactions with the extracellular matrix, cell motility, compartment positioning within the cell and vesicular transport (6). Actin microfilaments are extensively regulated by signaling cascades involving the Rho subfamily of GTPases (29). Actin cytoskeleton has been shown to play roles in viral morphogenesis, as exemplified by actin filament involvement in the life cycle of the BCC and Crimean-Congo hemorrhagic fever viruses (1, 28). Specifically, the N protein of BCCV (after infection or transfection of cells) localizes in a filamentous pattern analogous to that of actin microfilaments (28). Such pattern of staining was not observed

in HTNV-infected or transfected cells in our studies. These findings suggest other cytoskeletal elements are involved in trafficking of the HTNV N protein to the ERGIC.

In summary, we show that HTNV N protein localizes to the peri-nuclear region following infection and during a time period of active viral production. The N protein strongly co-localized with ERGIC. We also demonstrate that the N protein is able to localize to the peri-nuclear compartments independently of other viral components and associate with cellular membranes, which suggests the N protein has an autonomous directionality sequence that is sufficient for its subcellular targeting. Our future studies will focus on characterizing the signals that target the N proteins to cellular compartments.

Materials and Methods

Construction of Plasmids

The plasmid pSRI-51 was generated by ligating the coding region of the S-segment from HTNV 76-118 into pcDNA4/TO (Invitrogen™, Carlsbad, CA). The coding region was PCR-amplified from the vector pGEM1-HTNVS (gift of Connie Schmaljohn, Virology Division, USAMRIID, GenBank #M14626) with oligonucleotides synthesized by Integrated DNA Technologies (IDT, Coralville, Iowa). We engineered 5′ *Eco*RI and 3′ *Xho*I sites (underlined) in the forward (5′-GCGGAATTCACGATGGCAACTATGGAGGAATTAC-3′) and reverse primers (5′-GCGCTCGAGTTAGAGTTTCAAAGG CTCTTGG-3′) respectively. The PCR product and pcDNA4/TO were digested with *Eco*RI and *Xho*I (New England Biolabs®, Beverly, MA), gel purified and ligated using Quick Ligase (New England Biolabs®, Beverly, MA). The nucleotide sequences of the were confirmed by bidirectional sequencing using the pcDNA4/TO CMV forward and BGH reverse sites by the Heflin Center for Human Genetics Sequencing lab (University of Alabama at Birmingham, Birmingham, AL) using an ABI automated sequencer.

Cell Lines

Vero E6 cells and HeLa cells were cultured in advanced modified eagles medium (A-MEM, GIBCO™, Grand Island, NY) supplemented with 10% fetal bovine serum (FBS), 1% penicillin-streptomycin and 1% L-glutamine.

Transfections and Infections

Vero E6 cells were seeded in Lab-Tek II 2-well chamber slides (Nalge Nunc International, Naperville, IL) and transfected with 1 μg of plasmid DNA at a 90% confluence (2 days post-seeding) using Lipofectamine 2000 (Invitrogen, Carlsbad, CA). After 1 h of incubation, complete A-MEM was added to the wells and allowed to incubate in CO_2 incubator at 37 ºC. At 24 h post-transfection, slides were acetone fixed for 10 min. For virus infections, Vero E6 cells were seeded in Lab-Tek II 2-well chamber slides and after 2 days, cells were infected with HTNV (strain 76-118) diluted to an MOI of 1.0 or 0.1 with MEM. At 1, 3, 5 and 7 days post-infection cells were acetone fixed for 10 min.

Immunofluorescence

The slides were washed three times with phosphate buffered saline (PBS). The N protein of HTNV was detected by incubation for 1 h at RT with either a monoclonal antibody (D3-27) to the HTNV N protein at a dilution of 1:250 or polyclonal antibody (#143) at a dilution of 1:15,000, washed 3 times in PBS followed by a 30 min incubation with anti-mouse antibodies conjugated to Alexa 488 or Alexa 594 (Molecular Probes, Eugene, OR) at a dilution of 1:250. To visualize the nucleus, the slides were washed three times with PBS and stained with Hoechst DAPI (Molecular Probes, Eugene, OR) for 5 min at a dilution of 1:20,000.

Golgi membranes were stained with wheat germ agglutinin (WGA) Alexa 594 conjugate (Molecular Probes, Eugene, OR) for 1 h. The endoplasmic reticulum (ER) was detected with a monoclonal antibody against protein disulfide isomerase (PDI) (Abcam Inc, MA) by incubation for 1 h at RT at a dilution of 1:150. Slides were washed three

times with PBS and incubated at RT with anti-mouse antibodies conjugated to Alexa 488 or Alexa 594 (Molecular Probes, Eugene, OR) for 30 min with a dilution of 1:250. Filamentous actin was visualized by staining with phalloidin conjugated to Alexa 594 (Molecular Probes, Eugene, OR) for 30 min at RT. All slides were mounted with Fluoromount-G (Southern Biotechnology Associated, Inc., Birmingham, AL) and coverslips (VWR Scientific, West Chester, PA). Slides were examined and analyzed using a Zeiss Axiovert 200 microscope and AxioVision 4.0 system software (Zeiss, Germany).

Confocal microscopy

For all microscopy studies, Vero E6 cells were seeded in Lab-Tek II 2-well chamber slides (Nalge Nunc International). For infection studies, Vero E6 cells at 60% confluence were infected with HTNV at a multiplicity of infection (MOI) of 0.1 or as noted for 1 h at 37°C with 5% CO2 as previously described (40), or they were transfected with 1 μg of plasmid DNA using Lipofectamine 2000 in OptiMEM (Invitrogen) according to manufacturer's instructions. After 1 h of incubation, complete DMEM was added to the wells, and the mixtures were incubated at 37°C in a 5% CO2 chamber. At different time points, Vero E6 cells were fixed either in acetone for 15 min or with 3.5% paraformaldehyde for 30 min at room temperature, followed by permeabilization with 0.1% Triton X-100 for 5 min. Slides were washed three times with phosphate-buffered saline (PBS). The HTNV N was detected by incubating the cells with either HTNV N MAb E-314 at a 1:200 dilution or rabbit polyclonal antibody no. 143 at a dilution of 1:10,000 for 1 h at room temperature. Golgi compartments were stained with TRITC-

conjugated Alexa 594 or with polyclonal anti-Mann II antibody at a dilution of 1:75. PDI, EEA1, ERGIC-53, actin, ß-tubulin, and vimentin were detected with the respective MAbs listed above at a dilution of 1:100 for 1 h at room temperature. Slides were washed three times with PBS and were incubated with secondary goat anti-mouse or anti-rabbit antibodies conjugated to Alexa 488 or Alexa 594 for 30 min at room temperature at a dilution of 1:400. F-actin was visualized by being stained with phalloidin conjugated to Alexa 594 for 30 min at room temperature. Slides were mounted with Fluoromount-G (Southern Biotechnology Associates), and confocal imaging was performed with a Leica DMIRBE inverted epifluorescence microscope outfitted with Leica TCS NT SP1 laser confocal optics at the High Resolution Imaging Facility at the University of Alabama—Birmingham. Epifluorescence imaging was also performed with a Zeiss Axiovert 200 microscope outfitted with an ApoTome for deconvolution purposes. The ApoTome uses the grid projection or structured illumination principle to obtain images with an improved signal-to-noise ratio, and it approximately doubles the resolution in the axial (*z*) direction. Final images were obtained by averaging four independent scans of the fields using _40, x63, or x100 magnification, corrected for oil immersion. Quantification of N in slides was calculated by measuring the area of the cell occupied by indirect labeling of N versus the total area of the cell using Image J image analysis software (National Institutes of Health).

Membrane fractionation

Vero E6 cells cultured in 6-well slides were grown to 90% confluence and transfected with plasmid DNA. The cells were washed three times with PBS and

harvested with 300 µl homogenization buffer (200 mM HEPES-KOH pH 7.2, 1M KCl, 20mM $MgCl_2$, 20 mM EDTA) with proteinase inhibitors at 24 hrs post-transfection. The cells were disrupted by passage through a 27 gauge needle 20-25 times. The homogenate was centrifuged at 3000 rpm for 15 min at 4º C to remove nuclei and cell debris. The supernatant was collected and transferred to a 500 µl centrifuge tube. A 60 µl sample representing the post-nuclear supernatant (PNS) was taken and stored at -80º C. The remaining sample was ultra-centrifuged using a Beckman Optima TLX Ultracentrifuge (Beckman Coulter, Fullerton, CA) at 45,000 rpm for in 1 hr at 4º C using a TLA 100.2 rotor (Beckman Coulter, Fullerton, CA). The supernatant was collected and measured, which represents the cytosolic fraction, while the pellet (membrane fraction) was washed in 100 µl homogenization buffer and ultra-centrifuged a second time using the above parameters. The supernatant was discarded and the membrane fraction was resuspended in RIPA buffer (150 mM NaCl, 1% nonidet P-40, 0.5% deoxycholate sodium, 0.1% SDS, 50 mM Tris-HCl, ph 8.0) using a volume equal to the volume of the cytosolic fraction. Fractions were analyzed by western blot.

Acknowledgements

We thank Dr. Anita McElroy and Dr. Connie Schmaljohn, USAMRIID, for plasmids and rabbit antibody to the ANDV N protein. We wish to acknowledge partial support of this research through funds from the Emil Hess Endowment at the Southern Research Institute as well as by internal funds provided by Southern Research Institute. This work also was supported by a grant from the Department of Defense, Contract No. W81XWH-04-C-0055, to C.B.J.

References

1. **Andersson, I., L. Bladh, M. Mousavi-Jazi, K. E. Magnusson, A. Lundkvist, O. Haller, and A. Mirazimi.** 2004. Human MxA protein inhibits the replication of Crimean-Congo hemorrhagic fever virus. J Virol **78:**4323-9.

2. **Andersson, I., M. Simon, A. Lundkvist, M. Nilsson, A. Holmstrom, F. Elgh, and A. Mirazimi.** 2004. Role of actin filaments in targeting of Crimean Congo hemorrhagic fever virus nucleocapsid protein to perinuclear regions of mammalian cells. J Med Virol **72:**83-93.

3. **Antic, D., K. E. Wright, and C. Y. Kang.** 1992. Maturation of Hantaan virus glycoproteins G1 and G2. Virology **189:**324-8.

4. **Appenzeller-Herzog, C., and H. P. Hauri.** 2006. The ER-Golgi intermediate compartment (ERGIC): in search of its identity and function. J Cell Sci **119:**2173-83.

5. **Bannykh, S. I., T. Rowe, and W. E. Balch.** 1996. The organization of endoplasmic reticulum export complexes. J Cell Biol **135:**19-35.

6. **da Costa, S. R., C. T. Okamoto, and S. F. Hamm-Alvarez.** 2003. Actin microfilaments et al.--the many components, effectors and regulators of epithelial cell endocytosis. Adv Drug Deliv Rev **55:**1359-83.

7. **Gahmberg, N., E. Kuismanen, S. Keranen, and R. F. Pettersson.** 1986. Uukuniemi virus glycoproteins accumulate in and cause morphological changes of the Golgi complex in the absence of virus maturation. J Virol **57:**899-906.

8. **Gavrilovskaya, I. N., E. J. Brown, M. H. Ginsberg, and E. R. Mackow.** 1999. Cellular entry of hantaviruses which cause hemorrhagic fever with renal syndrome is mediated by beta3 integrins. J Virol **73:**3951-9.

9. **Gavrilovskaya, I. N., M. Shepley, R. Shaw, M. H. Ginsberg, and E. R. Mackow.** 1998. beta3 Integrins mediate the cellular entry of hantaviruses that cause respiratory failure. Proc Natl Acad Sci U S A **95:**7074-9.

10. **Goldsmith, C. S., L. H. Elliott, C. J. Peters, and S. R. Zaki.** 1995. Ultrastructural characteristics of Sin Nombre virus, causative agent of hantavirus pulmonary syndrome. Arch Virol **140:**2107-22.

11. **Hiscox, J. A., T. Wurm, L. Wilson, P. Britton, D. Cavanagh, and G. Brooks.** 2001. The coronavirus infectious bronchitis virus nucleoprotein localizes to the nucleolus. J Virol **75:**506-12.

12. **Hutchinson, K. L., C. J. Peters, and S. T. Nichol.** 1996. Sin Nombre virus mRNA synthesis. Virology **224:**139-49.

13. **Jantti, J., P. Hilden, H. Ronka, V. Makiranta, S. Keranen, and E. Kuismanen.** 1997. Immunocytochemical analysis of Uukuniemi virus budding compartments: role of the intermediate compartment and the Golgi stack in virus maturation. J Virol **71:**1162-72.

14. **Jayakar, H. R., E. Jeetendra, and M. A. Whitt.** 2004. Rhabdovirus assembly and budding. Virus Res **106:**117-32.

15. **Jin, M., J. Park, S. Lee, B. Park, J. Shin, K. J. Song, T. I. Ahn, S. Y. Hwang, B. Y. Ahn, and K. Ahn.** 2002. Hantaan virus enters cells by clathrin-dependent receptor-mediated endocytosis. Virology **294:**60-9.

16. **Jonsson, C. a. S., CS.** 2001. Replication of Hantaviruses. Curr Top Microbiol Immunol **256:**15-32.

17. **Klumperman, J., A. Schweizer, H. Clausen, B. L. Tang, W. Hong, V. Oorschot, and H. P. Hauri.** 1998. The recycling pathway of protein ERGIC-53 and dynamics of the ER-Golgi intermediate compartment. J Cell Sci **111 (Pt 22):**3411-25.

18. **Kolesnikova, L., E. Muhlberger, E. Ryabchikova, and S. Becker.** 2000. Ultrastructural organization of recombinant Marburg virus nucleoprotein: comparison with Marburg virus inclusions. J Virol **74:**3899-904.

19. **Kuismanen, E., K. Hedman, J. Saraste, and R. F. Pettersson.** 1982. Uukuniemi virus maturation: accumulation of virus particles and viral antigens in the Golgi complex. Mol Cell Biol **2:**1444-58.

20. **Kukkonen, S. K., A. Vaheri, and A. Plyusnin.** 2004. Tula hantavirus L protein is a 250 kDa perinuclear membrane-associated protein. J Gen Virol **85:**1181-9.

21. **Lamb, R. A., and R. M. Krug.** 2001. *Orthomyxoviridae*: The viruses and their replication, p. 1487-1531. *In* K. D. Fields BN, Howley PM. (ed.), Virology, 4 ed, vol. 1. Lippincott-Raven, Philadelphia.

22. **Lober, C., B. Anheier, S. Lindow, H. D. Klenk, and H. Feldmann.** 2001. The Hantaan virus glycoprotein precursor is cleaved at the conserved pentapeptide WAASA. Virology **289:**224-9.

23. **Mackenzie, J. M., M. K. Jones, and E. G. Westaway.** 1999. Markers for trans-Golgi membranes and the intermediate compartment localize to induced

membranes with distinct replication functions in flavivirus-infected cells. J Virol **73:**9555-67.

24. **Nichol, S. T.** 2001. Bunyaviruses, p. 1603-1633. *In* K. D. Fields BN, Howley PM. (ed.), Virology, 4 ed, vol. 2. Lippincott-Raven, Philadelphia.

25. **Pettersson, R. F., and L. Melin.** 1996. Synthesis, assembly and intracellular transport of *Bunyaviridae* membrane proteins, p. 159-188. *In* E. R.M. (ed.), The *Bunyaviridae*. Plenum Press, New York.

26. **Ravkov, E. V., and R. W. Compans.** 2001. Hantavirus nucleocapsid protein is expressed as a membrane-associated protein in the perinuclear region. J Virol **75:**1808-15.

27. **Ravkov, E. V., S. T. Nichol, and R. W. Compans.** 1997. Polarized entry and release in epithelial cells of Black Creek Canal virus, a New World hantavirus. J Virol **71:**1147-54.

28. **Ravkov, E. V., S. T. Nichol, C. J. Peters, and R. W. Compans.** 1998. Role of actin microfilaments in Black Creek Canal virus morphogenesis. J Virol **72:**2865-70.

29. **Ridley, A. J.** 2001. Rho proteins: linking signaling with membrane trafficking. Traffic **2:**303-10.

30. **Risco, C., J. R. Rodriguez, C. Lopez-Iglesias, J. L. Carrascosa, M. Esteban, and D. Rodriguez.** 2002. Endoplasmic reticulum-Golgi intermediate compartment membranes and vimentin filaments participate in vaccinia virus assembly. J Virol **76:**1839-55.

31. **Rodriguez, J. R., C. Risco, J. L. Carrascosa, M. Esteban, and D. Rodriguez.** 1997. Characterization of early stages in vaccinia virus membrane biogenesis: implications of the 21-kilodalton protein and a newly identified 15-kilodalton envelope protein. J Virol **71:**1821-33.

32. **Roghi, C., and V. J. Allan.** 1999. Dynamic association of cytoplasmic dynein heavy chain 1a with the Golgi apparatus and intermediate compartment. J Cell Sci **112 (Pt 24):**4673-85.

33. **Ruusala, A., R. Persson, C. S. Schmaljohn, and R. F. Pettersson.** 1992. Coexpression of the membrane glycoproteins G1 and G2 of Hantaan virus is required for targeting to the Golgi complex. Virology **186:**53-64.

34. **Salanueva, I. J., J. L. Carrascosa, and C. Risco.** 1999. Structural maturation of the transmissible gastroenteritis coronavirus. J Virol **73:**7952-64.

35. **Salanueva, I. J., R. R. Novoa, P. Cabezas, C. Lopez-Iglesias, J. L. Carrascosa, R. M. Elliott, and C. Risco.** 2003. Polymorphism and structural maturation of bunyamwera virus in Golgi and post-Golgi compartments. J Virol **77:**1368-81.

36. **Salmons, T., A. Kuhn, F. Wylie, S. Schleich, J. R. Rodriguez, D. Rodriguez, M. Esteban, G. Griffiths, and J. K. Locker.** 1997. Vaccinia virus membrane proteins p8 and p16 are cotranslationally inserted into the rough endoplasmic reticulum and retained in the intermediate compartment. J Virol **71:**7404-20.

37. **Schmaljohn, C.** 1996. Molecular Biology of Hantaviruses, p. 63-90. *In* R. Elliot (ed.), *The Bunyaviridae.* Plenum Press, New York.

38. **Schmaljohn, C. S., and J. W. Hooper.** 2001. *Bunyaviridae*: The viruses and their replication., p. 1581-1602. *In* K. D. Fields BN, Howley PM. (ed.), Virology, 4 ed, vol. 2. Lippincott-Raven, Philadelphia.

39. **Sesso, A., F. P. de Faria, E. S. Iwamura, and H. Correa.** 1994. A three-dimensional reconstruction study of the rough ER-Golgi interface in serial thin sections of the pancreatic acinar cell of the rat. J Cell Sci **107 (Pt 3):**517-28.

40. **Severson, W. E., C. S. Schmaljohn, A. Javadian, and C. B. Jonsson.** 2003. Ribavirin causes error catastrophe during Hantaan virus replication. J Virol **77:**481-8.

41. **Sodeik, B., R. W. Doms, M. Ericsson, G. Hiller, C. E. Machamer, W. van 't Hof, G. van Meer, B. Moss, and G. Griffiths.** 1993. Assembly of vaccinia virus: role of the intermediate compartment between the endoplasmic reticulum and the Golgi stacks. J Cell Biol **121:**521-41.

42. **Spiropoulou, C. F.** 2001. Hantavirus maturation. Curr Top Microbiol Immunol **256:**33-46.

43. **Spiropoulou, C. F., C. S. Goldsmith, T. R. Shoemaker, C. J. Peters, and R. W. Compans.** 2003. Sin Nombre virus glycoprotein trafficking. Virology **308:**48-63.

44. **Takimoto, T., and A. Portner.** 2004. Molecular mechanism of paramyxovirus budding. Virus Res **106:**133-45.

45. **van Vliet, C., E. C. Thomas, A. Merino-Trigo, R. D. Teasdale, and P. A. Gleeson.** 2003. Intracellular sorting and transport of proteins. Prog Biophys Mol Biol **83:**1-45.

46. **Vapalahti, O., H. Kallio-Kokko, A. Narvanen, I. Julkunen, A. Lundkvist, A. Plyusnin, H. Lehvaslaiho, M. Brummer-Korvenkontio, A. Vaheri, and H. Lankinen.** 1995. Human B-cell epitopes of Puumala virus nucleocapsid protein, the major antigen in early serological response. J Med Virol **46:**293-303.

47. **Whittaker, G., M. Bui, and A. Helenius.** 1996. Nuclear trafficking of influenza virus ribonuleoproteins in heterokaryons. J Virol **70:**2743-56.

48. **Whittaker, G., M. Bui, and A. Helenius.** 1996. The role of nuclear import and export in influenza virus infection. Trends Cell Biol **6:**67-71.

49. **Wurm, T., H. Chen, T. Hodgson, P. Britton, G. Brooks, and J. A. Hiscox.** 2001. Localization to the nucleolus is a common feature of coronavirus nucleoproteins, and the protein may disrupt host cell division. J Virol **75:**9345-56.

HANTAAN VIRUS NUCLEOCAPSID PROTEIN FUNCTIONS TO MODULATE IMMUNE SIGNALING

STEVEN J. ONTIVEROS AND COLLEEN B. JONSSON

Submitted to [In preparation for] *Virology*

Format adapted for dissertation

CHAPTER 4

HANTAAN VIRUS NUCLEOCAPSID PROTEIN FUNCTIONS TO MODULATE IMMUNE SIGNALING

Abstract

Hantaviruses are known to cause two human diseases, such as hantavirus pulmonary syndrome and hemorrhagic fever with renal syndrome. Apoptosis has been previously reported *in vitro* for hantaviruses, however, the underlying molecular interactions between the virus and cell that drive these processes are unknown. Interestingly, lymphocyte apoptosis has also observed *in vivo* in hamsters infected with hantaviruses. Herein, we show for the first time a direct relationship between the hantaviral nucleocapsid (N) protein and modulation of apoptosis. We observed a caspase-7 and -8, but not -9 response in cells expressing mutants lacking amino acids 270-330 within the Hantaan (HTNV) virus N protein. Intriguingly, it is the removal of this region that leads to apoptosis suggesting that this region may interact with cellular proteins to down-regulate this response during the virus life cycle. We also observed that the HTNV virus N protein is capable of circumventing immune signaling within the tumor necrosis factor receptor (TNF-R) pathway by disrupting the nuclear import of nuclear factor kappa B (NF-κB). Other viruses have developed several strategies to evade activation of the inflammatory response, specifically targeting NF-κB. Herein, we show that NF-κB is sequestered to the cytoplasmic region after TNF-R stimulation in cells expressing HTNV N protein, which functions to inhibit caspases. Furthermore, we demonstrate that mutants lacking 270-330 region of the N protein are incapable of inhibiting nuclear import of NF-κB.

Introduction

Transmission of some strains of *Hantavirus*, family *Bunyaviridae,* from their rodent reservoirs to humans results in serious disease; Old World hantaviruses can cause hemorrhagic fever with renal syndrome, while New World hantaviruses can cause hantavirus pulmonary syndrome (53, 59, 60). Despite differences in clinical manifestations, Old World and New World hantaviruses share highly conserved genomes comprised of three, negative-sensed, single-stranded RNAs. The segments, S, M, and L, encode a nucleocapsid (N) protein, glycoprotein precursor complex (GPC) and L protein, respectively (60). The glycoproteins, G_n and G_c, mediate entry via β-integrin receptors (26, 27), while the L protein plays a dominant role in replication (23). The N protein preferentially binds genomic viral RNA to form a ribonucleoprotein (RNP) complex with each segment (48, 61, 62).

Over the past few years, research suggest a complex structure and function of N in trafficking, assembly and more recently in modulation of immune signaling (69). The N protein is known to oligomerize into trimers (2, 3), where trimeric forms preferentially bind the vRNA panhandle (double-stranded vRNA) (48), binding is genus-specific (46), and its conformation is altered upon binding (47). Additionally, the N protein shows specificity for ssRNA and preference for its own RNA (Severson). Furthermore, structural studies suggest that the amino-terminal region of N is a dimmer. Taken together, these studies underscore the complexity of N proteins structure and function during the life cycle suggesting that different conformations and specificity of N may modulate the various stages of the life cycle. We have been particularly interested in trafficking of the N protein following infection to gain insight into the virus life cycle

(Rama and Rama, cite both). In relation to these studies, we probed the Hantaan virus (HTNV) N protein determinants for trafficking to the perinuclear region and we noted cell death in cells expressing several deletion mutants of N protein. We hypothesized that the N protein truncation may be activating apoptosis.

Virus modulation of apoptosis has been demonstrated for several enveloped RNA viruses such as influenza A, respiratory syncytial, and vesicular stomatitis viruses (13, 25, 49, 66, 78). The respiratory syncytial virus NS protein suppresses apoptosis early in infection (13). The ability of viruses to regulate this host response early in infection may be critical to viral survival. Further, viruses may use apoptosis or cell-death to promote release of virus from cells as noted for numerous non-enveloped viruses (11, 52, 77, 80). In the case of avian influenza A (H5N1), apoptosis may play a role in lung pathogenesis as suggested from limited autopsy specimens from patients who died from infection with the virus (71).

The presence of apoptotic cells following hantaviral infection has been reported for HTNV, Andes (ANDV), Seoul (SEOV), and Prospect Hill (PHV) viruses *in vitro* (31, 39, 43), and in one study of Puumala (PUUV) virus-infected patients (34). Lymphocyte apoptosis was observed in hamsters infected with ANDV (72). Infection of Vero E6 cells with HTNV or Tula viruses shows DNA fragmentation and caspase-8 activation, respectively (31, 39). Finally, two-hybrid experiments revealed a direct interaction between PUU N protein and Daxx, a Fas-mediated apoptosis enhancer (40). The HTNV and SEOV (35, 42) and Tula (32) N proteins have been shown to interact with small ubiquitin-like modifier (SUMO-1) and ubiquitin conjugating enzyme 9 (Ubc9). In light of these findings, Hardestam et al. have effectively argued that hantaviruses are very poor

inducers of apoptosis (29). In light of these arguments and the reports in the literature, cell phenotype, and perhaps culture and infection conditions, may modulate hantaviral-induced CPE and apoptosis.

Most of the events that lead to cell death are executed by a group of cystein-dependent aspartate-directed proteases termed caspases that cleave a variety of intracellular polypeptides (21). Caspase activation ultimately leads to cell infrastructure damage and cell death. Depending on their function and point of entry into the apoptotic pathway, caspases are classified as initiators or executioners. As mentioned above, we noted that expression of truncations of the N protein caused cell death. We hypothesized that the N protein mutant may be activating apoptosis, or alternatively, had lost its ability to down-regulate apoptosis. To address this hypothesis, we measured caspase activity with each of the N- and C-terminal N protein deletion constructs. Elevated caspase-7 activity was measured in Vero E6 cells expressing a C-terminal fragment. We also examined factors involved in the caspase pathways to gain insight into the interactions of N protein with these pathways. Our studies suggest that the N protein suppresses apoptosis through its interaction with nuclear factor-kB (NF-κB).

Results

Construction, localization and discovery of cell death in HTNV N protein deletion mutants

Using amino acid sequence alignments as a guide (30, 76), we constructed a series of constructs that removed the N- and/or C-terminus of the HTNV N protein (Fig. 1A). N-terminal deletions of the HTNV N protein included NΔ270, NΔ300, NΔ330, and

NΔ360, which removed 270, 300, 330 and 360 amino acids from the N-terminus, respectively (Fig. 1). C-terminal deletions of the HTNV N protein included CΔ99, CΔ129, CΔ159, and CΔ189, which removed 99, 129, 159, and 189 amino acids from the C-terminus, respectively (Fig. 1). Deletion construct 271-300 contained both N- and C-terminal deletions, and comprised amino acids 271-300 of the HTNV N protein (Fig. 1). Each construct had an N-terminal GFP tag fusion to facilitate intracellular detection.

Plasmids containing full-length or truncated N open reading frames were transfected into Vero E6 cells. Cells expressing the full length N protein (GFP-HTNS) showed punctuated perinuclear localization (Fig. 1B), which has been previously reported (55). GFP-NΔ270, which has nearly two-thirds of the N protein removed from the N-terminus, retained perinuclear localization (Fig. 1B). We also observed that Vero E6 cells expressing GFP-CΔ99, which lacked 99 amino acids of the C-terminus, resulted in perinuclear localization patterns similar to wild type N protein (Fig. 1B). Perinuclear localization was abrogated when 300 amino acids were removed from the N-terminus (Fig. 1B, GFP-NΔ300) or 99 amino acids from the C-terminus (Fig. 1B GFP-CΔ99.This suggested that the region between 271 and 300 may contain a signal for targeting of N protein to the perinuclear region. Surprisingly, however, when the region from 271-300 was expressed, it was uniformly found throughout the cell (Fig. 1B). These data suggest that amino acids 271-300 play a role in the intracellular localization of the HTNV N protein, however, this domain is insufficient by itself.

Intriguingly, localization of N protein was indeterminate (I) in cells transfected with N protein mutants lacking more than 300 amino acids from the N-terminus or 99 amino acids from the C-terminus (Fig. 1, data not shown). Visual examination of cells

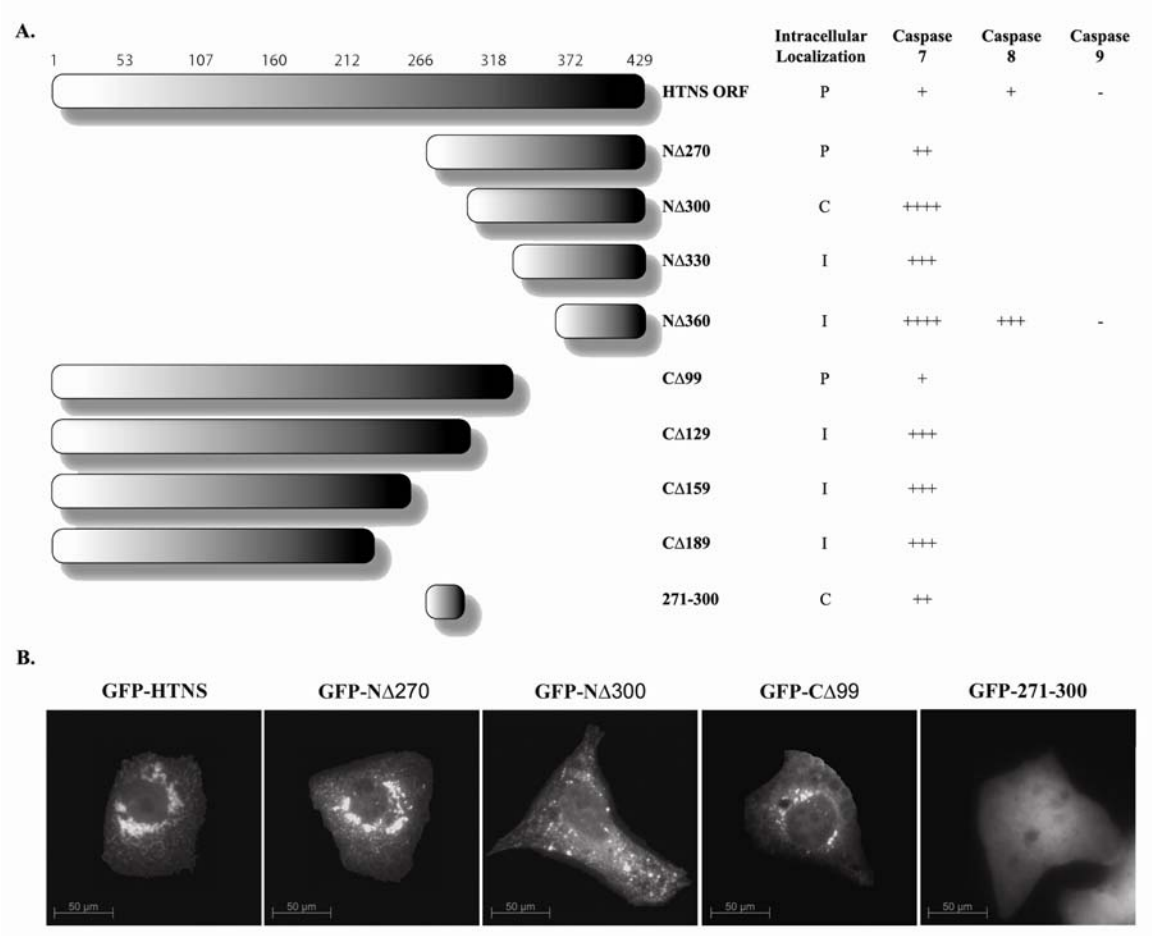

Figure 1: Illustration of HTNV N protein deletion mutants and summary of their localization and caspase activities. (A) N-terminal deletion mutants of the HTNV N protein included NΔ270, NΔ300, NΔ330, and NΔ360, which were lacking 270, 300, 330 and 360 amino acids from the N-terminus respectively. C-terminally deleted HTNV N protein mutants included CΔ99, CΔ129, CΔ159, and CΔ189, lacking 99, 129, 159, and 189 amino acids from the C-terminus, respectively. Deletion mutant 271-300 contained both N- and C-terminal deletions. Intracellular localization was determined and noted as perinuclear (P), cytoplasmic (C), or indeterminate (I) (see panel B, data not shown for all constructs). We summarize caspase activities for each construct from experiments presented in Figures 3 and 4. Caspase activation was scored with increasing activity correlating with increasing number of plus-signs; ++++ (high) and + (low). Data for these results are shown in subsequent figures. (B) Vero E6 cells were transfected with plasmid DNA expressing the fusion proteins indicated at the top of each panel. After incubation at 37 °C, 5% CO_2 for 24 h, N protein expression was detected by fluorescence generated by GFP. Slides were acetone fixed and processed, and examined for fluorescence at excitation and emission spectra of 470 and 509 nm, respectively, using a Zeiss Axiovert 200 microscope. Scale bar, 50 µm, with 40X objective at 1.6 optovar/tubelens (Zeiss Axiovert 200).

expressing these proteins revealed cell death, and hence, we focused our efforts to probe the nature of these unexpected findings.

Deletion of amino acids 270 to 330 in the HTNV N protein triggers caspase-7 activity in HeLa cells

We hypothesized that the cell death noted in Vero E6 cells expressing certain N protein truncations were undergoing apoptosis. To address this, we performed a caspase-like activity assay as an intracellular marker of apoptosis following the expression of the various plasmids for 24 h post-transfection. The activity of caspase-3/7 was measured using a caspase substrate, which cannot discriminate between caspase-3 and -7.

Substantial levels of caspase-3/7 activity were observed with specific N- or C-terminal deletion mutants in Vero E6 cells (Fig. 2A). N-terminal deletions of the N protein elicited a slightly higher caspase-3/7 response than C-terminal deletions (Fig. 2A). The greatest caspase-3/7 activity was noted in cells expressing GFP-NΔ360, GFP-NΔ300, GFP-CΔ159 and GFP-CΔ189 (Fig. 2A). In comparison, GFP-CΔ99, which comprises amino acids 1-330, and GFP-NΔ270, which comprises amino acids 271-429, showed levels similar to the full-length N protein (Fig. 2A). The finding that cells expressing GFP-NΔ270 and GFP-CΔ99 have diminished caspase-3/7 activity, while cells expressing GFP-NΔ360 and GFP-CΔ159 had higher caspase-3/7 activation suggested that removal of amino acids 270-330 of the HTNV N protein enhanced caspase-3/7 levels (Fig. 2A).

GFP-NΔ360 increases caspase-3/7 and -8 activity but not caspase-9

Initiator caspases, such as caspase-8 or -10, are directly capable of activating executioner caspases, such as caspase-3 or -7 with sufficient magnitude to indicate direct processing of apoptosis *in vivo (64)*. Caspases-3 and -7 exist in the cytosol as inactive dimers or pro-caspases and function to initiate the characteristics of apoptosis (14, 64). To further explore the possible apoptotic pathways employed, we analyzed the activation of caspase-8 and -9. For these studies, we compared GFP-NΔ360 against the full-length GFP-HTNS since GFP-NΔ360 showed the greatest activity of caspase-3/7.

As expected from our observations (Fig. 2A), GFP-NΔ360 showed higher caspase-3/7 activity than GFP-HTNS (Fig. 2B). Although caspase-8 was slightly elevated in cells expressing GFP-HTNS and GFP-NΔ360 compared to cell control, there was no significant difference between GFP-HTNS or GFP-NΔ360 (Fig. 2B). We noted no significant difference in caspase-9 activity among any of the groups (Fig. 2B). Staurosporine (STR), a known activator of caspases, was employed as a positive control (Fig. 2B) (79). Since caspase-8 is a known activator of effector caspases (64), these data suggest that activation of caspase-3/7 is mediated by either the Fas receptor (Fas-R) or tumor necrosis factor receptor 1 (TNFR-1) pathways through the use of caspase-8.

NΔ360 elicits caspase-7 and -8 activity, while HTNV N protein plays apoptotic inhibitory roles in HeLa cells

Since our previous assays were unable to discriminate between caspase-3 and -7, we performed western blots of cell extracts for the presence of active caspase-3, -7 and -8 in HeLa cells (Fig 2C). We employed HeLa cells for these studies given the lack of antibody reagents available for Vero E6 cells. HeLa cells were transfected with plasmids

expressing full-length HTNV N protein, NΔ360, or mock (Fig. 2C). Cells treated with 1 μM STR served as a positive control (Fig. 2C). Interestingly, caspase-3 was not detected in cells expressing N protein or NΔ360 (Fig. 2C). A small amount of caspase-3 was observed in STR treated cells (Fig. 2C). In contrast, significant levels of caspase-7 were observed in cells transfected with NΔ360 (Fig. 2C). Minor amounts of caspase-7 were observed in cells expressing full-length N protein (Fig 2C). This experiment suggested that the cell death we observed (data not shown) and the caspase activity (Fig 2A and B) were predominantly through the effects of caspase-7.

Since both the Fas-R and TNFR-1 pathways are known to activate initiator caspases, we asked which pathway was affected. We assayed for Fas-R and TNFR-1 protein levels in cells expressing N protein or NΔ360. We observed no difference in the relative amounts of Fas-R in cells expressing N protein, NΔ360, STR, or mock (Fig 2C), which suggested no involvement. In contrast, reduced levels of TNFR-1 were observed in NΔ360 and STR (Fig 2C). This was a surprising finding, because we expected higher expression levels of TNF-R1 in cells expressing NΔ360. We expected cell death to be mediated through this receptor since there was no increase in Fas-R in cells expressing NΔ360. Although TNFR-1 does play roles in the activation of caspases, it is known to play multiple roles, including the activation of NF-κB.

To confirm our findings, we chose a second hantavirus to examine caspase activity through western blot. We generated an identical construct for ANDV based on the HTNV N protein mutant NΔ360. HeLa cells were transfected with plasmids expressing full-length ANDV N protein, NΔ360, or mock (Fig. 2D). One μM STR served as a positive control (Fig 2D). Similar to HTNV, the ANDV N protein did not activate a

caspase-3 response in HeLa cells expressed full-length ANDV N protein or NΔ360 (Fig. 2D). A significant amount of caspase-7 was observed in cells transfected with NΔ360 as compared to full-length ANDV N protein (Fig. 2D). The levels of caspase-7 in cells expressing NΔ360 were comparable to the levels of STR-treated cells (Fig. 2D). Similar to the results obtained from cells expressing HTNV N protein (Fig. 2C), we observed only a minor amount caspase-8 activity in cells expressing ANDV NΔ360 mutant and no activity in cells expressing full-length ANDV N protein (Fig. 2D). These data suggest that the functionality of the N protein in terms of apoptosis does not differ significantly between Old and New World hantaviruses.

To further substantiate that cell death was occurring in cells expressing HTNV NΔ360, we probed for nuclear enzyme poly(ADP-ribose) polymerase (PARP) cleavage using western blot using antibodies against cleaved PARP (Fig. 2E) and by IFA (Fig 2F). Caspases-3 and -7 are capable of cleaving at specific tetrapeptide substrates, such as PARP, that contain amino acids DEVD. Although PARP enzyme plays important roles in genomic stability and DNA repair (18, 19), PARP cleavage is a major hallmark of apoptosis (15). HeLa cells were transfected with plasmids expressing GFP-tagged HTNV N protein (GFP-HTNS), GFP-NΔ360, or treated with STR (Fig. 2E). As expected, 3 hrs after STR treatment, cells showed significant signs of PARP cleavage (Fig. 2F). This was further validated by western blots that showed significant levels of cleaved PARP (Fig. 2E). Cells expressing GFP-NΔ360 also showed PARP cleavage (Fig. 2F) showing similar levels as STR-treated cells when measured by western blot (Fig. 2E). Importantly, cells expressing HTNV N protein had significantly lower levels of cleaved PARP when measured by western blot as compared to untreated cells (Fig. 2E). A small amount of

naturally occurring PARP cleavage was observable by IFA and by western blot in cells expressing HTNV N protein or mock cells. In summary, these data suggest that the apoptosis that is occurring in cells expressing GFP-NΔ360 functions through initiator caspase-8, which activates caspase-7, resulting in the cleavage of PARP, and thus apoptosis. An interesting observation is that although there was a slight activation of caspase-7 in cells expressing HTNV N protein (Fig. 2C), there were lower levels of cleaved PARP present as compared to mock cells (Fig. 2E), which suggested that the HTNV N protein may play caspase inhibitory roles in HeLa cells.

Since we observed no involvement of the Fas-R, we wanted to determine possible downstream mediators of the TNF-R1 pathway that may be affected by NΔ360 such as NF-κB. There were no differences in cellular levels of NF-κB in cells expressing HTNV N protein, NΔ360, and mock treated cells (Fig. 2E). However, we noted a significant reduction in phosphorylated NF-κB (p-NF-κB) in cells expressing HTNV N protein as compared to mock cells (Fig. 2E). This suggests HTNV N protein may inhibit or delay the nuclear import of NF-κB. The HTNV N protein has been shown to interact with nuclear import proteins, which can inhibit translocation of NF-κB into the nucleus (69). Overall, these data suggested that the full-length HTNV N protein may function to modulate apoptosis and an immune response as evident through the reduction of PARP cleavage and through the inhibition of nuclear import of NF-κB, respectively.

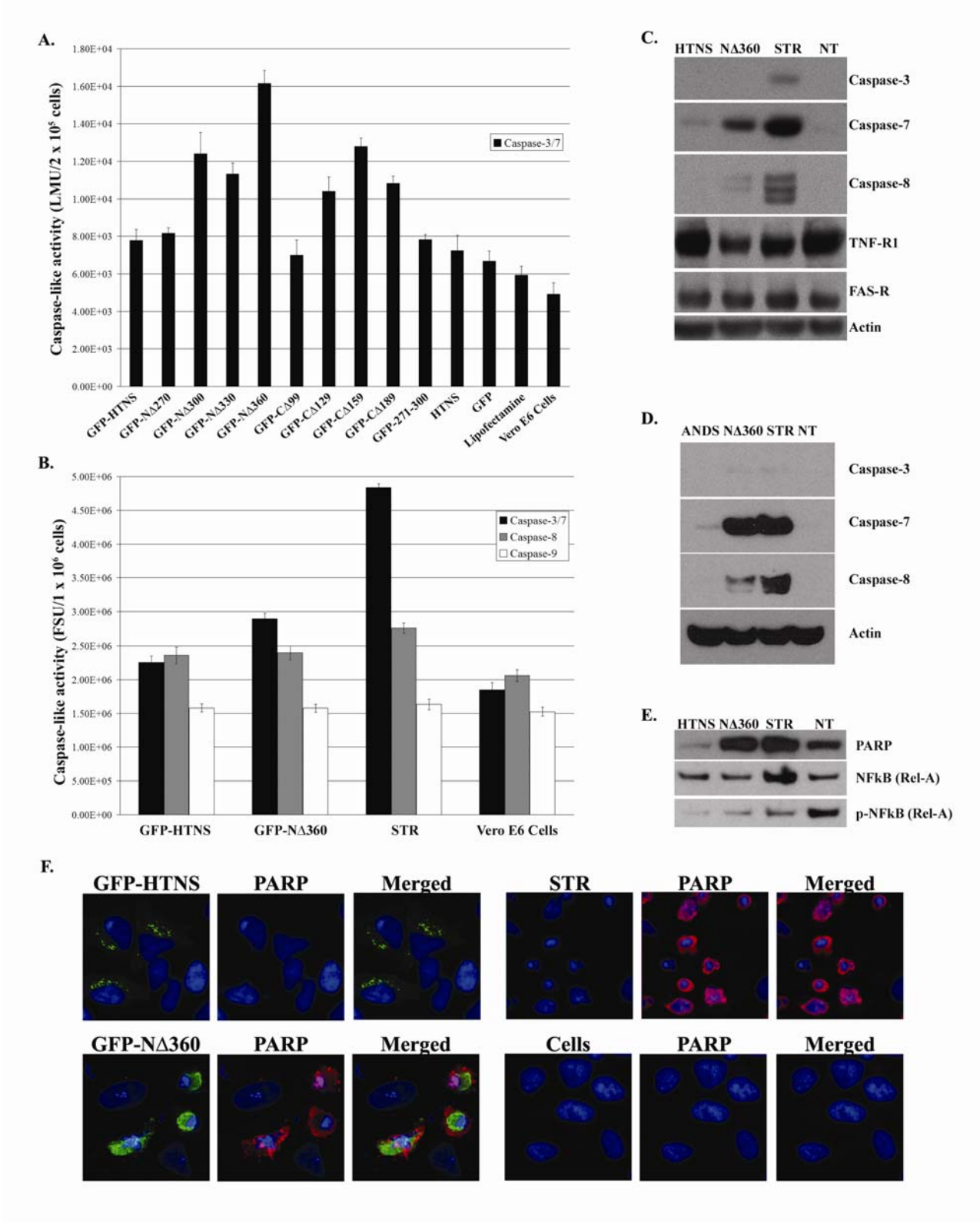

Figure 2: Deletion of amino acids 270 to 330 results in the activation of caspase-7 and -8, but not caspase-9 in HeLa cells. (A) Quantification of caspase-3/7-like activity, expressed as luminescence unit (LMU) in 2 x 10^5 cells, using Caspase-Glo® 3/7 Assay in Vero E6

cells after transfection with 0.8 µg plasmid DNA at 24 h in 24 well plates. (B) Caspase-3/7, -8, and -9-like activity in Vero E6 cells after transfection with 5 µg plasmid DNA at 24 h in 6 well plates as measured by Ac-DEVD-AMC, Ac-IETD-AMC, or Ac-LEHD-AMC cleavage, respectively, expressed as the fluorescence unit (FSU) in 1 x 10^6 cells, after transfection with plasmid DNA for 24 h. For A and B, each value is the mean of three different samples, and the vertical bars represent the standard deviation. (C) Examination of caspase-3, -7, and -8, TNRF-1, and Fas-R levels in HTNV N protein or NΔ360 expressing cells. (D) Examination of caspase-3, -7, and -8 levels in ANDV N protein or NΔ360 expressing cells. (E) Examination of PARP cleavage, NF-κB (Rel-A), and p-NF-κB (p-Rel-A) in HTNV N protein or NΔ360 expressing cells. For western blots, HeLa cells were transfected with 5 µg plasmid DNA expressing HTNV or ANDV N protein, HTNV or ANDV NΔ360, or mock, or treated with 1 µM staurosporine (STR). Proteins were transferred onto nitrocellulose membranes and probed with antibodies against caspase-3, -7, and -8, cleaved PARP, NF-κB (Rel-A), p-NF-κB (p-Rel-A), or actin (loading control). (E) HeLa cells were transfected with 0.8 µg of plasmid DNA expressing HTNV N protein, NΔ360, or mock, or treated with 1µM STR for 3 h. Slides were examined by indirect immunofluorescence for N protein or NΔ360 (Green) as GFP expression, or cleaved PARP (Red) with polyclonal antibodies as described in materials and methods with 63x objectives using a Leica confocal microscope.

HTNV N protein does not affect downstream mediators of Fas-R signaling during inhibition of apoptosis

Although we showed no difference in the levels of Fas-R in cells expressing HTNV N protein versus mock cells (Fig. 2C), this did not rule out downstream mediators. Herein, we focused our efforts on Fas-associated protein with death domain (FADD), which is an adapter molecule that is the basic bridge or mediator between the Fas-R and caspase-8.

HeLa cells were transfected with the HTNV S-segment in the presence or absence of anti-Fas antibodies. FADD was detected with rabbit polyclonal antibodies followed by a secondary alexa-594 antibody. FADD localized predominantly to the nucleus in cells that were mock-treated (Fig. 3). To explore this pathway, we used anti-Fas antibodies to induce Fas-R mediated cell death. We observed a larger amount of cytoplasmic FADD following Fas stimulation, in cells that were mock-treated or expressing HTNV N protein as compared to unstimulated mock cells (Fig. 3). Since FADD was capable of being recruited to the cytoplasm in the presence of HTNV N protein, this suggested that the N protein does not play any inhibitory roles within this pathway. This finding was further validated when cells expressing HTNV N protein underwent apoptosis after treatment with anti-Fas antibodies (data not shown).

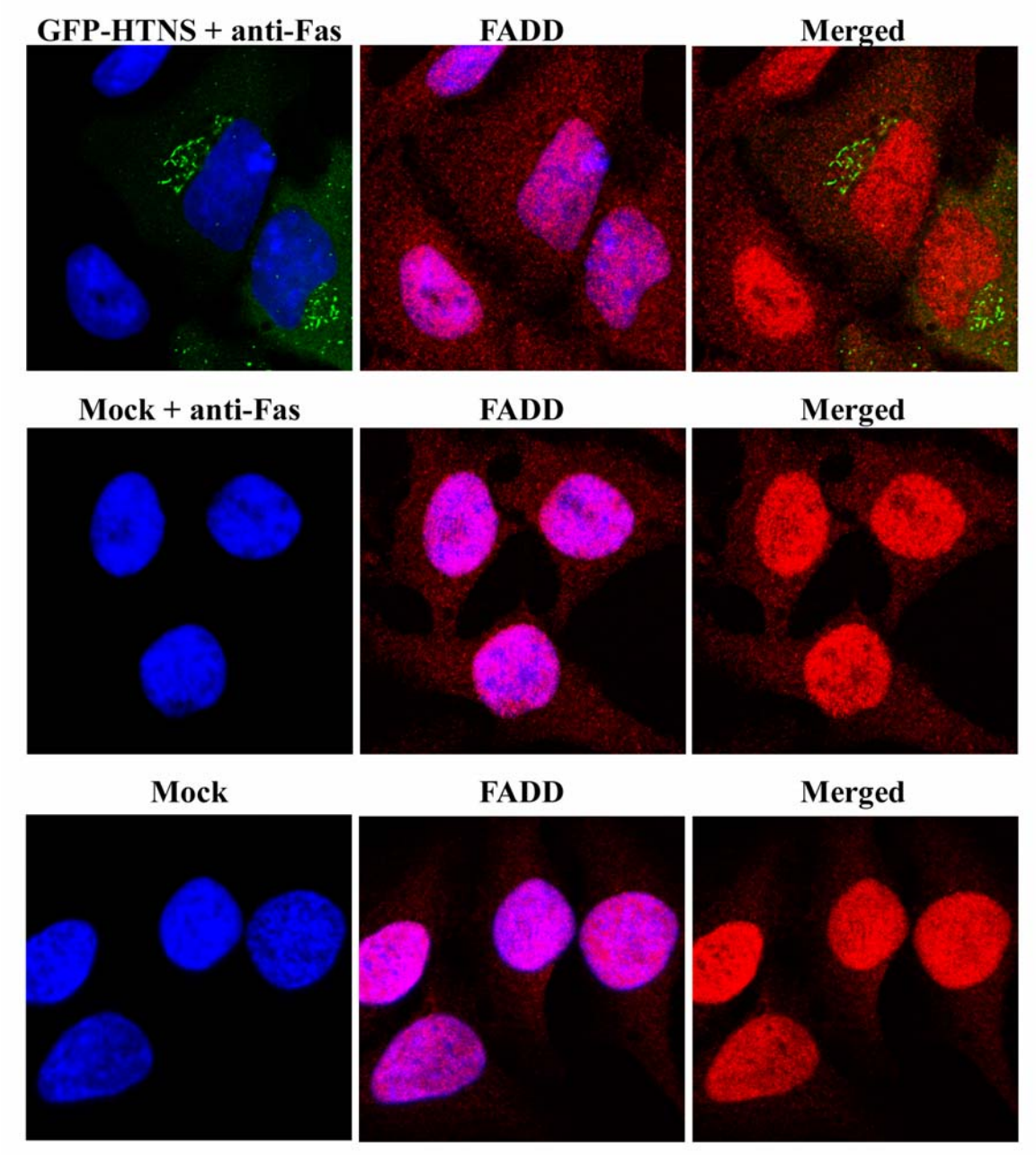

Figure 3: Fas-R pathway is not affected by HTNV N protein. HeLa cells were transfected with 0.8 µg of plasmid DNA expressing HTNV N protein, NΔ360, or mock, or treated with 1µM STR for 3 h. Slides were examined by indirect immunofluorescence for N protein or NΔ360 (Green) as GFP expression, or FADD (Red) with polyclonal antibodies as described in materials and methods with 63x objectives using a Leica confocal microscope.

HTNV N protein delays nuclear translocation of NF-κB and promotes the degradation of IκB

We next focused our efforts on the TNF-R1 receptor pathway, since we observed no interaction between Fas-R signaling cascade and inhibition by HTNV N protein. The TNFR-1 pathway is capable of activating downstream mediators such as NF-κB (33, 37, 45), which plays crucial roles in facilitating immune and inflammatory responses through gene regulation of pro-inflammatory cytokines and chemokines within innate and adaptive immunity (24).

HeLa cells were transfected with the HTNS or mock for 24 hrs in the presence or absence of TNF-α. Whole cell extracts were made and levels of TNFR-associated via death domain (TRADD), TNFR-associated factor (TRAF)-2, and protein A20 were probed by western blot. We observed no difference in the relative amounts of TRADD or TRAF-2 among cells treated with TNF-α or mock, but did see a minor decrease in cells expressing HTNV N protein alone (Fig. 4A). These data suggest that the HTNV N protein indeed can affect the signaling of TNFR-1 pathway, which is why possibly why we observed an overall decrease of nuclear p-NF-κB (Fig. 2E).

Since protein A20 (TNFAIP3) is known to play roles in the inhibiting both NF-κB activity and TNF-mediated cell death (12, 36), we wanted to determine if elevated levels of protein A20 were involved in the caspase inhibitory roles that we observed in cells expressing HTNV N protein. We observed a minor decrease in the levels of protein A20 in cells expressing HTNV N protein as compared to vector cells in the presence or absence of TNF-α (Fig. 4A). This suggests that the HTNV N protein does not function

through protein A20 in mediation of its inhibition of caspase activity, which resulted in the reduction of PARP cleavage (Fig. 2C).

The ability of the HTNV N protein to act on upstream mediators of the TNFR-1 pathway suggests downstream effects. We asked whether the HTNV N protein or mutants are capable acting on IκB or NF-κB, since we observed an overall decrease in nuclear p-NF-κB in cells expressing full-length HTNV N protein (Fig 2E) and a decrease in TRADD and TRAF-2 (Fig. 4A). To explore further, we expressed HTNV N protein, various mutants, such as NΔ270, NΔ360, CΔ99, and CΔ159, or empty vector and co-treated with or without TNF-α (Fig. 4B). Irrespective of whether the cells were expressing full-length HTNV N protein or the truncated N proteins, or whether they were treated with or without TNF-α, there were relatively no differences in the levels of cellular NF-κB expression (Fig. 4B). In contrast, we noticed a dramatic decrease in the amount of IκB in cells that were treated with TNF-α as compared to untreated cells (Fig. 4B). Although the levels of IκB in cells expressing NΔ360 or CΔ99 were significantly lower than cells with vector alone, we noted that after treatment with TNF-α the decrease was more profound in cells expressing HTNV N protein or NΔ270 (Fig. 4B). Similar findings were observed in the levels of p-IκB (Fig. 4B). Although we observed reduced levels of TRADD and TRAF-2 in cells expressing HTNV N protein (Fig. 4A), this reduction was not enough to protect IκB from degradation (Fig. 4B). This data suggests that the HTNV N protein is capable of facilitating the degradation of IκB, and that it might be directed by a central region within the HTNV N protein since both NΔ270 and CΔ99 were capable of promoting degradation. This region could be within amino acids 270-330, which also falls within the possible localization signal. Although we did

observe a decrease in the total levels of IκB in cells that were expressing NΔ360, our data suggest that the decrease we observed could be due to apoptosis rather than IκB inhibition.

Degradation of IκB leads to an assumption that the HTNV N protein could promote the liberation and nuclear import of NF-κB, but our earlier findings would suggest otherwise (Fig. 2E). To probe further, HeLa cells were transfected with full-length HTNS, NΔ270, NΔ360, CΔ99, CΔ159, or empty vector, and treated in the absence (Fig. 4C) or presence (Fig. 4D) of TNF-α followed by separation of the cytoplasmic and nuclear fractions. Specifically, we asked whether the reduction in p-NF-κB (Fig. 2E) was due to decreased nuclear import of NF-κB. We observed no difference in NF-κB levels in the cytoplasm in cells expressing the HTNV N protein or mutants (Fig. 4C). This was an expected result, because in whole cell extracts we observed no difference in the levels of NF-κB in unstimulated cells (Fig. 4B). In contrast, we observed a dramatic decrease in the levels of NF-κB in the nucleus in cells that were expressing full-length N protein versus cells expressing mutants or vector alone (Fig. 4C). No difference in nuclear NF-κB was observed between mutants and vector (Fig. 4C). Interestingly, a different cytoplasmic profile of NF-κB was observed in TNF-α treated cells (Fig. 4D). A small amount of NF-κB was present in the cytoplasm in cells transfected with vector alone, however, most was found in the nucleus (Fig. 4D). In contrast, the majority of NF-κB remained in the cytoplasm in cells expressing full-length HTNV N protein (Fig. 4D). There were similar levels of cytoplasmic NF-κB in cells expressing NΔ270 and CΔ99, but high levels of NF-κB was detected in the nucleus (Fig. 4D). Interestingly in cells expressing NΔ360, NF-κB was only detected in the nucleus (Fig. 4D). These data imply

that the HTNV N protein effectively inhibited the nuclear import of NF-κB, while NΔ360 lost this function. Although we did find similar levels of cytoplasmic NF-κB in cells transfected with NΔ270 and CΔ99, as compared to cells expressing full-length N protein, no differences were in the amount of nuclear NF-κB were observed with vector alone (Fig. 4D). This suggests that the complete abrogation of NF-κB transport into the nucleus may require full-length, or possibly higher-ordered, multimeric forms of HTNV N protein.

We asked whether the inhibition of NF-κB observed could be visually detected by direct microscopy. HeLa cells expressing HTNS or vector were examined with or without TNF-α, and analyzed by IFA (Fig. 4E). As expected, similar findings were observed between cells expressing GFP-HTNS and vector with no TNF-α treatment (Fig. 4E). Nuclear import of NF-κB was abrogated in cells expressing HTNV N protein after TNF-α treatment (Fig. 4E). Interestingly, a significant difference was observed in the total amount of nuclear NF-κB (as shown by arrows) between cells that are actively expressing HTNV N protein, versus cells that are not (Fig. 4E). This data demonstrates the inhibition of nuclear import of NF-κB by HTNV N protein.

HTNV N protein binds to NF-κB, facilitating its cytoplasmic retention, indirectly regulating caspases

The above data suggested that the HTNV N protein is capable of sequestering NF-κB to the cytoplasm, and is capable of promoting IκB degradation. To examine the possibility that the HTNV N protein directly binds to NF-KB, TRADD or TRAF-2 mediators of the TNFR-1 pathway, we performed co-immunoprecipitation experiments in

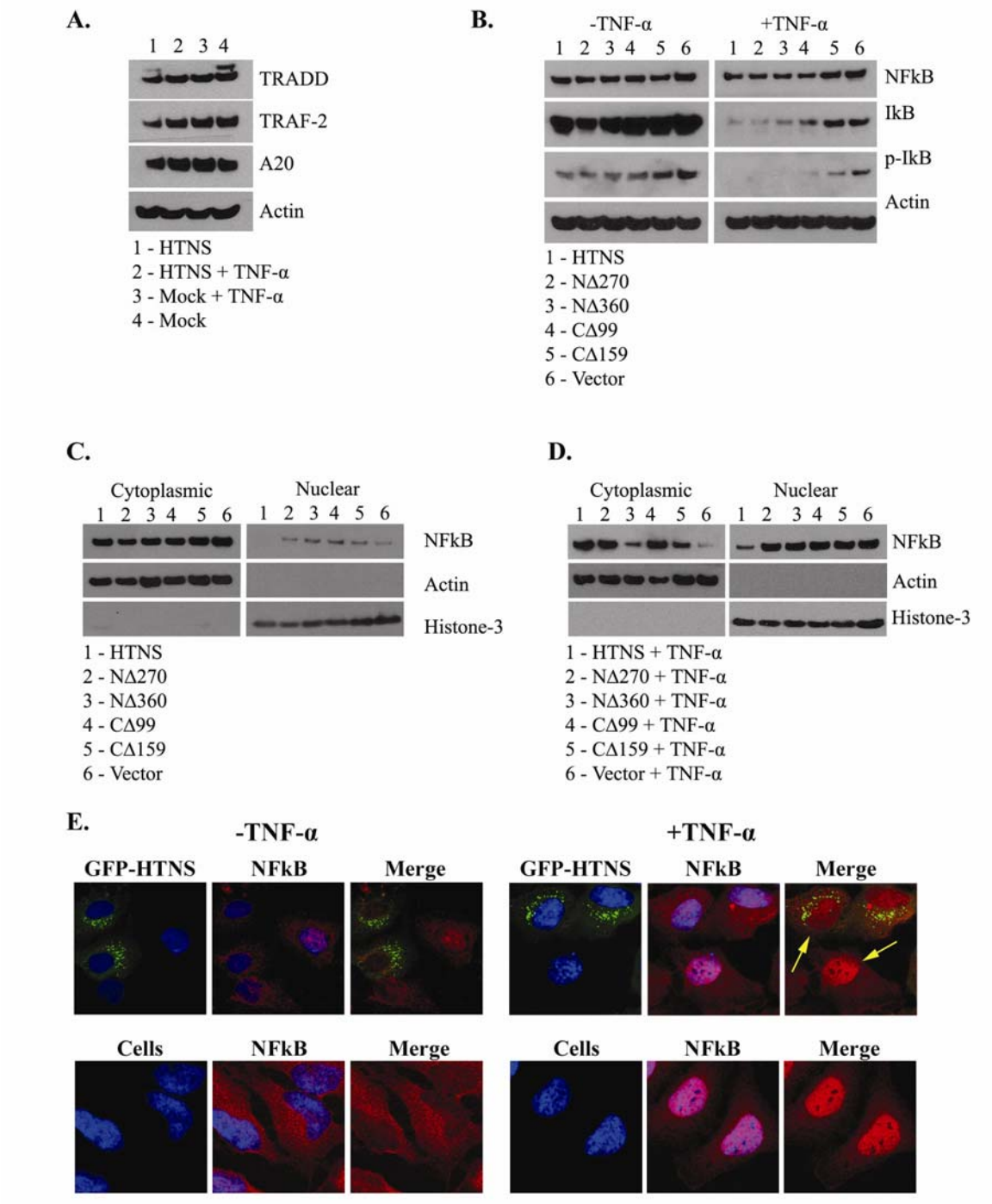

Figure 4: HTNV N protein affects the TNFR-1 signaling pathway, promotes the degradation of IκB, and inhibits nuclear translocation of NF-κB. Cell lysates were made of HeLa cells and the levels of various cellular proteins were measured. Cells were transfected with 5 μg plasmid DNA expressing HTNV N protein, or mock, untreated or treated with 20 ng/ml of TNF-α for 20 min (A), HTNV N protein, NΔ270, NΔ360, CΔ99, CΔ159, or vector untreated or treated with 20 ng/ml of TNF-α for 20 min (B). Cell lysates were separated into cytoplasmic and nuclear fractions of cells treated (C) or

untreated with 20 ng/ml of TNF-α for 20 min (D). Proteins were transferred onto nitrocellulose membranes and probed with antibodies against TRADD, TRAF-2, protein A20, or actin (A), NF-κB (Rel-A), p-NF-κB (p-Rel-A), IκB, p-IκB or actin (B), NF-κB (Rel-A), actin, or histone-3 (C and D). Actin and histone-3 served as loading controls for cytoplasmic or nuclear fractions, respectively.

HeLa cells expressing myc-tagged HTNV N protein. HeLa cells were transfected with myc-tagged HTNS or myc-tag vector and allowed to incubate for 24 hrs. Our results revealed that NF-KB, but not TRADD or TRAF-2 co-immunoprecipitated with HTNV N protein, albeit weakly (Fig. 5A). Furthermore, we did not observe IκB to co-immunoprecipitate with HTNV N protein (Fig. 5A). This result was somewhat surprising since our data suggested that the HTNV N protein may facilitate the degradation of IκB. Comparable levels of HTNV N protein were observed between cell extract and immunoprecipitated samples (Fig. 5A). These data suggest the N protein is capable of directly interacting with NF-κB, and we hypothesize that this interaction could facilitate liberation and degradation of IκB.

Since we were able to find that the HTNV N protein is capable of having inhibitory effects on the TNFR-1 pathway, and can directly bind to NF-κB, we wanted to examine whether the extra molar concentration of cytoplasmic NF-κB could play roles in inhibiting caspases, since NF-κB subunits can serve as a substrate for caspases (56). HeLa cells were transfected with the HTNS or empty vector and were allowed to incubate for 24 hrs. The cells were then co-treated with TNF-α for 20 min. An additional set of cells with no TNF-α were processed. The cytoplasmic fraction of these cells was harvested and the proteins were concentrated. In another set of cells, whole cell extract were made of cells that were treated or untreated with STR. The concentrated proteins were added to the whole cell extracts, and then the activity of caspase-7 was measured using a caspase-3/7 substrate. HeLa cells that were treated with STR had higher caspase-7 activity than that of untreated cells (Fig 5B). This activity was blocked with the addition of caspase inhibitors to the extract (Fig. 5B). We next wanted to determine if the

cytoplasmic fraction of cells expressing HTNV N protein had any effect on caspase-7 activity. The cytosolic extract of cells that were not transfected or treated with TNF-α had no effect on caspase-7 activity within extracts of STR treated cells (Fig. 5B). Interestingly, cells that were transfected with HTNS and treated with TNF-α had a small reduction in caspase-7 activity in the extracts of STR treated cells (Fig. 5B). This finding suggests that the retention of cytosolic NF-κB by HTNV N protein plays a role in the inhibition of caspase-7 activity, and hence, a general reduction of total cleaved PARP in cells expressing N protein versus mock cells (Fig. 2C).

Discussion

Viruses have developed many strategies and elaborate schemes to try and evade immune responses. One key player in generating an immune response is NF-κB (5, 10), which is rapidly activated by cytokines, such as TNF-α, through the TNF receptor family (33, 37). Upon its activation, NF-κB translocates to the nucleus, utilizing nuclear import molecules, and serves as a transcription factor to trigger both the innate and adaptive immune responses. In normal signaling NF-κB is sequestered in the cytoplasm by IκB by masking a nuclear localization signal that is nested within one of the NF-κB subunits. As also reported by Taylor et al, our studies suggest that the HTNV N protein can block trafficking of NF-κB into the nucleus. We also show a direct, albeit weak, interaction between NF-κB and HTNV N protein. We demonstrated that the N protein is capable of promoting the degradation of IκB, which we hypothesize is through the direct inhibition of Ubc9 (42). This finding supports a link between SUMO-1 and Ubc9 interactions and the nuclear import inhibition of NF-κB in HeLa cells. We hypothesize that the retention

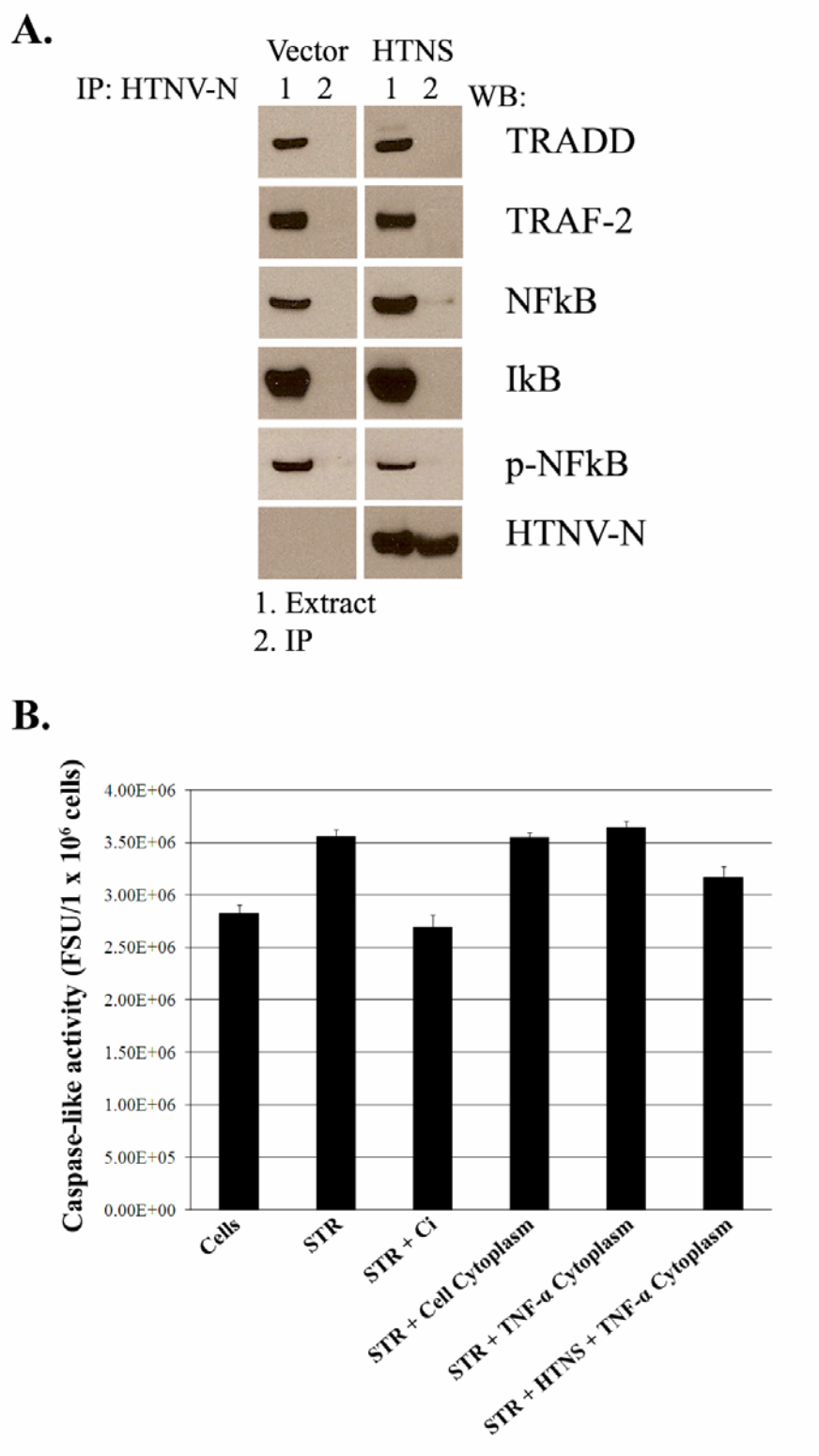

Figure 5: Analysis of HTNV N protein interaction with NF-κB, and the examination the cytoplasmic fraction from cells expressing HTNV N protein has on caspase activity. (A) HeLa cells were transfected with 75 µg of plasmid expressing Myc-tagged HTNV N

protein or empty vector. Immunoprecipitations (IP) were performed with anti-myc antibody bound to magnetic Dynabeads. Immunoprecipitations and whole cell extracts were analyzed by western blot for the levels of HTNV N protein, TRADD, TRAF-2, NF-κB (Rel-A), p-NF-κB (p-Rel-A), or IκB. (B) HeLa cells were transfected with 5 μg or 10 μg of plasmid DNA in 6-well plates or T-25 flasks, respectively. Whole cell extracts were made from cells lysed with caspase extract buffer in 6-well plates that were untreated or treated with 5 μM STR and the caspase-3/7 activity was measured. Caspase activity was also measured in the presence of caspase inhibitor (Ci) Z-D(OMe)E(OMe)VD(OMe)–FMK. The cytoplasmic fraction of cells expressing HTNV N protein or mock, untreated or treated with 20 ng/ml of TNF-α for 20 min was extracted and concentrated from cells in T-25 flasks. Caspase activity in cells treated with STR (6-well plates) was measured that were supplemented with 15 μl of cytoplasmic extracts from T-25 flasks. Each value is the mean of three different samples, and the vertical bars represent the standard deviation.

of NF-κB in the cytoplasm facilitates the reduction of caspase activity, and apoptosis. It is understandable that the HTNV N protein could manipulate these mechanisms to facilitate its evasion from the hosts cellular and immune responses to enhance propagation.

Here in, we addressed the hypothesis that the HTNV N protein can function to regulate apoptosis. Although, apoptosis has been observed in HEK293 (embryonic kidney) cells infected with HTNV, SEOV, or ANDV as early as 3-4 days post-infection (43), it was not apparent whether infected cells or bystander cells became apoptotic. Furthermore, no apoptosis or CPE was induced in fully confluent Vero E6 cells inoculated with HTNV, PUUV, Dobrava hantavirus, or Saarema hantavirus up to 12 days post-infection (29). Interestingly, apoptosis has been observed in lymphocytes (1, 72). Within our studies, we observed significant elevated levels of caspase-7 in cells transfected with certain deletion mutants, such as NΔ360 as compared to cells expressing full-length HTNV N protein. Despite having slightly increased levels of active caspase-7 as compared to mock cells, cells expressing full-length N protein had reduced levels of PARP cleavage, directly suggesting that the N protein may function to suppress caspase activity. This would also suggest that cellular detection of N protein results in the activation of an apoptotic response, but full-length functions to counter these effects. Furthermore, we observed nuclear and total cell shrinkage in cells expressing constructs GFP-NΔ360 or GFP-CΔ159, but not in neighboring cells, indicating that there is no bystander effect. These data suggest that constructs missing amino acids 270-330 resulted in the highest caspase activity. Another interesting observation is that the deletion mutants lacking the full N-terminus resulted in the highest activation of caspases.

Caspases are activated by a variety of receptors including a superfamily of known death receptors such as Fas (CD95 or APO-1) and TNFR (65). Both receptors are known to facilitate the recruitment of procaspase-8 monomers, leading to the dimerization and activation of caspase-8 (4, 14, 20). Stimulation of Fas-R induces an interaction between the cytosolic death domain of Fas with the adapter molecule FADD (50, 51). Utilizing the death effector domain of FADD, pro-caspase-8 is recruited in the formation of the death-inducing signaling complex (DISC), is activated and released into the cytosol (44, 58). TNFR is capable of transducing an apoptotic signal by activating caspase-8 similar to Fas-R, but utilizes TRADD as a mediator (28, 37, 63).

TNF-α is known to elicit a wide range of biological responses such as cell proliferation, inflammation, differentiation, and apoptosis through the TNFR. There are two known receptors types of TNFR that are capable of transducing distinct cellular responses: type 1 (TNF-R1; CD120a) and type 2 (TNF-R2; CD120b) (67). TRADD can also associate with TRAF-2, and receptor interacting protein to activate NF-κB (33, 37), which induces the activation of inflammatory genes to mediate the innate and adaptive immune responses (45).

Although NF-κB can initiate an immune and inflammatory response, it can also act to inhibit apoptosis (6, 8, 41). NF-κB plays most of its major functions as an inhibitor of apoptosis by induction of survival genes, such as TRAF1, TRAF2, c-IAP1, c-IAP2, and Bcl-2 (74, 75). Although NF-κB functions mostly as an inhibitor of apoptosis, studies have demonstrated that it does contain some pro-apoptotic functions. NF-κB, along with AP-1, can induce the expression of Fas-R ligand (73).

Our findings suggest a model in which N protein sequesters NF-κB to the cytoplasm, which inhibits the activation of the immune response, and can function to directly inhibit caspase activity (Fig. 6). Although the anti-apoptotic properties of NF-κB function mostly through the activation of pro-life genes, NF-κB can directly serve as a caspase substrate (7, 56). The increased molar ratio of cytoplasmic NF-κB in cells expressing HTNV N protein can serve as a substrate for caspases, inhibiting or delaying apoptosis, which is possibly why we observed a reduction of caspase activity in STR cell extracts that were supplemented with the cytoplasmic fraction of cells treated with TNF-α that were expressing HTNV N protein. This is in-part the reason for N protein liberating NF-κB from IκB. Furthermore, IκB degradation is known to be facilitated by Ubc9, which has been observed to directly interact with HTNV N protein (42). Overexpression of a catalytically inactive Ubc9 delayed both IκB-α degradation and NF-κB activation following TNF-α induction (68). Interactions observed between HTNV N protein and Ubc9 could help facilitate the degradation of IκB, and thus provide a direct substrate (NF-κB) for caspases.

Although we show the HTNV N protein may function to directly inhibit NF-κB, we believe that other mechanisms of inhibition may also be involved since we observed a weak interaction. Taylor et al., showed no interaction between N protein and NF-κB, but they indicated that this could be due to condition within their assays (69). These other factors include Caspase-induced truncation of IκBα which can function as a stable inhibitor of NF-κB during apoptosis (9, 57). Caspase-mediated cleavage of IκB occurs immediately 5' of Ser-32 (9). This could be a reason why we were unable to detect

cellular levels of p-IκB in cells expressing N protein, which would suggest IκB playing partial inhibitory roles of NF-κB.

The characteristics of hantavirus pathogenesis, such as vascular dysfunction and leakage have been characterized primarily in autopsies of human cases (16, 17, 53, 54), but the underlying mechanisms of HFRS and HPS remains. Immunopathogenesis has been regarded as a major contributor of hantavirus pathogenesis. Capillary leakage has been accredited to endothelial cell lysis by armed cytotoxic T lymphocytes (CTL) (70). CTLs isolated from patients infected with SNV recognized a specific epitope of the N protein (22). Furthermore, CTLs increased permeability and caused cell lysis of endothelial cell monolayers infected with SNV (70). Apoptosis of epithelial cells due to the loss of membrane integrity was observed in PUUV-infected patients (34). It is therefore tempting to hypothesize that the HTNV N protein plays role in pathogenesis in the regulation of apoptosis through the direct use of NF-κB. Activation of cellular caspases is evident in cells expressing HTNV N protein, but the N protein functions to circumvent these actions. Overall, the N protein is capable of playing a bi-functional mode to inhibit apoptosis and the immune response. The pathways that result in the activation or deactivation of the immune system or caspases is so vast, it is possible that many regions within these pathways have yet to be explored. Although our studies clearly show a direct relationship between the HTNV N protein and apoptosis, direct caspase inhibition by HTNV N protein cannot be completely ruled out. Further studies are needed to fully determine the involvement of N protein and caspase inhibition.

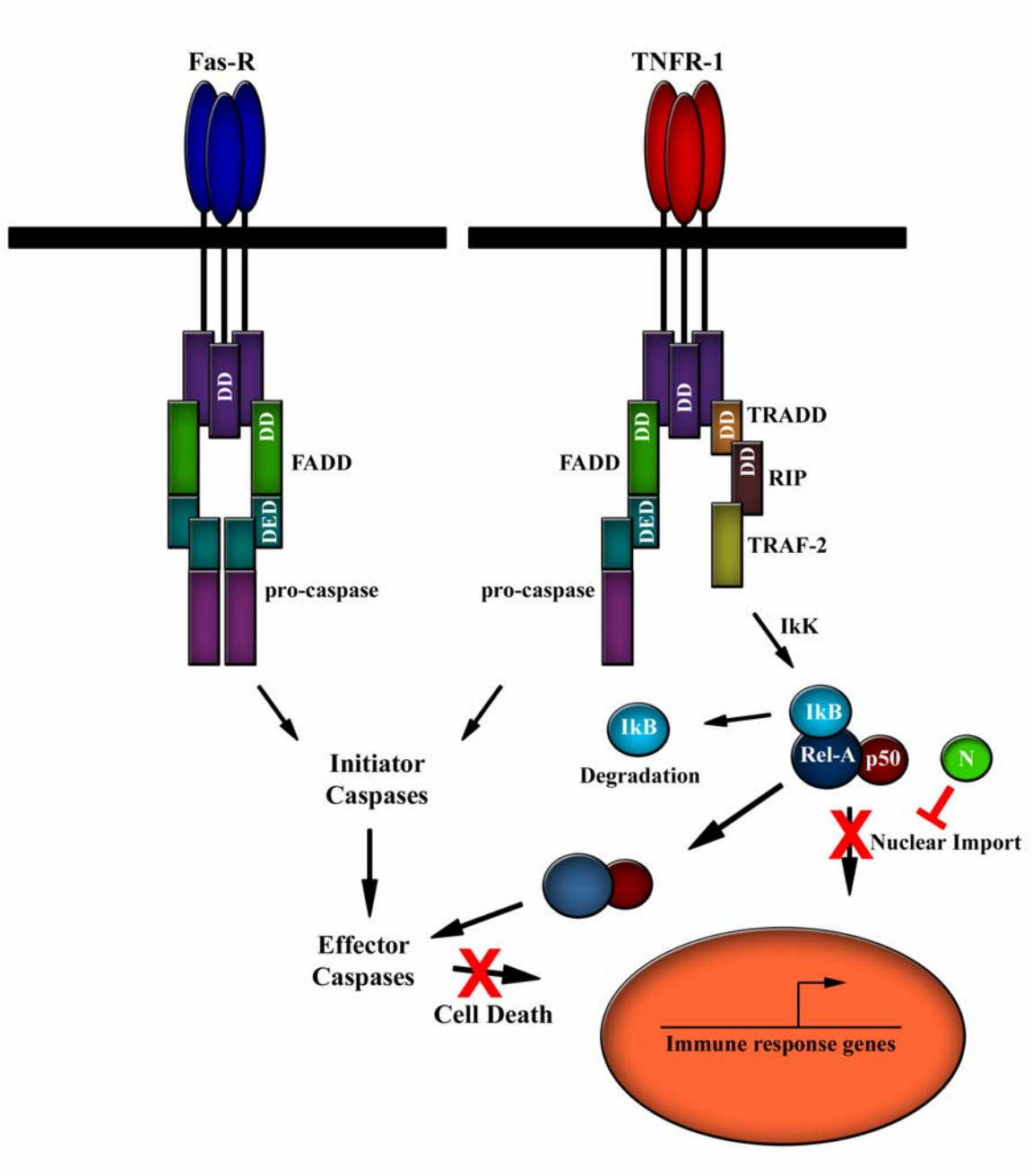

Figure 6: Schematic illustration of the HTNV N protein in the modulation of immune signaling and inhibition of apoptosis.

Materials and Methods

Cell culture

Vero E6 or HeLa cells from American Tissue Culture Collection (ATCC, Manassas, VA) were cultured in advanced modified eagles medium (A-MEM, GIBCO™, Grand Island, NY) supplemented with 10% fetal bovine serum (FBS), 1% penicillin-streptomycin and 1% L-glutamine.

Construction of plasmids

The plasmid pcHTNS was generated by ligating the coding region of the S-segment from HTNV 76-118 into pcDNA4/TO (Invitrogen™, Carlsbad, CA). The coding region was PCR-amplified from the vector pGEM1-HTNVS (gift of Connie Schmaljohn, Virology Division, USAMRIID, GenBank #M14626) with oligonucleotides synthesized by Integrated DNA Technologies (IDT, Coralville, Iowa). The forward primer (5'-GCG*GAATTC*ACTATG…3') incorporated an EcoRI site (shown in italics), while the reverse primer (5'-GCG*CTCGAG*TTAGAGTTTCAAAGGCTCTTGG-3') incorporated an *XhoI* site (shown in italics). The coding region of the GFP was PCR-amplified with oligonucleotides synthesized by IDT and fused to the *EcoRI* site located in N-terminus of the HTNV N protein.

For deletion constructs, primers were designed to reamplify the entire plasmid with HiFi Taq DNA polymerase yet delete the region of interest in the HTNV S-segment. The plasmid pcGFP-HTNS was used as target DNA for amplification. N-terminal deletion mutants of the HTNV N protein included NΔ270, NΔ300, NΔ330, and NΔ360,

which had N-terminal deletions of 270, 300, 330 and 360 amino acids respectively. They were created in the N-terminus by using a universal reverse primer (5'-AAGGAAAAAA*GCGGCCGC*AGAATTCGAGAGT GATCCCGG-3') and different forward primers that incorporated a *NotI* site (shown in italics) to facilitate recircularization and the removal of the sequences in the 5' end of the S-segment ORF. The PCR products were recircularized with Quick Ligase (New England Biolabs, Ipswich, MA) and transformed into JM109 *E. coli* competent cells (Promega, Madison, WI). The forward primers used were as follows: NΔ270 (5'-AAGGAAAAAA*GCGGCCGC*ACGATGGTGGCATTAGGCAATATGAG-3'), NΔ300 (5'-AAGGAAAAAA*GCGGCCGC*AGCATGTCACCATCATCAATATGGG-3'), NΔ330 (5'-AAGGAAAAAA*GCGGCCGC*ACGATGTTTTTTTCCATCCTGCAGGAC-3'), and NΔ360 (5'-AAGGAAAAAA*GCGGCCGC*ACGATGTTTTATCAGTCCTACCTCAGAAG-3').

C-terminal deleted HTNV N protein mutants included CΔ99, CΔ129, CΔ159, and CΔ189, with deletions of 99, 129, 159, and 189 amino acids from the C-terminus respectively. They were created in the C-terminus by using a universal forward primer (5'-AAGGAAAAAA*GCGGCCGC*ACTCGAGTCTAGAGGGCCCG-3'). The reverse primers used were as follows: CΔ99 (5'-AAGGAAAAAA*GCGGCCGC*TTATGCCCCAAGCTCAGCAATAC-3'), CΔ129 (5'-AAGGAAAAAA*GCGGCCGC*TTACTCAATATCTTCAATCATGCTAC-3'), CΔ159 (5'-AAGGAAAAAA*GCGGCCGC*TTATTGCCGCTGCCGTAAGTAG-3'), and CΔ189 (5'-AAGGAAAAAA*GCGGCCGC*TTATAACCATTGTTCGATACGATCAC-3').

The synthesis of the 271-300 construct with N- and C-terminal deletions was made by using NΔ270 mutant as the target DNA and used the universal forward primer and the CΔ129 reverse primer for PCR amplification. The Myc tagged HTNV N protein was constructed by PCR amplification of the pcHTNS plasmid using a specific forward primer (5'-GATGGAACAAAAACTCATCTCAGAAAGAGGATCTGATGGCACTATGGAGGAATTACAGAG-3'), that contained the Myc sequence (EQKLISEEDLN) and reverse primer (5'-CCGGAATTCGGATCCAGCTTAAGTTTAAACGCTAGCCAGCTTGGGTCT-3').

To obtain the ORF from ANDV S-segment, total ANDV RNA was reverse transcribed and amplified using Enhanced Avian RT-PCR kit (Sigma®, St. Louis, MO). The gene specific forward and reverse primers were designed based Genbank # AF291702.1 sequence with *Bam*HI and *Xho*I restriction sites (sense, 5′-GCGCGCGGATCCGGGATGGGCACCCTCCAAG-3′, antisense, 5′-GCGCGCCTCGAGTTACAACTTGAGTGGCTC-3′). The PCR products were gel purified using QIAquick Spin Gel Extraction kit (Qiagen, MD), digested with *Bam*HI and *Xho*I and ligated to pcDNA4/TO (Invitrogen, Carlsbad, CA). To generate the ANDV NΔ360, the region of interest was PCR amplified with the forward (5′–CGGAATTCACCATGTACCAATCATACCTAAGAAGGAC-3′) and reverse (5′–CGCTCGAGCTACAACTTAAGTGGCTCTTGG-3′) primers with 5′ EcoRI and 3′ XhoI restriction sites, then cloned into pcDNA4/TO. The nucleotide sequences of each construct was confirmed in our lab by bidirectional sequencing using the pcDNA4/TO

CMV forward (5'-CGCAAATGGGCGGTAGGCGTG-3') and BGH reverse (5′-TAGAAGGCACAGTCGAGG-3') sites using an ABI automated sequencer.

Transfections

In preparation of cell extract, Vero E6 or HeLa cells were seeded in 6-well plates (Nalge Nunc International, Naperville, IL) and transfected with 5 µg of plasmid DNA at 60% confluence using Lipofectamine 2000 (Invitrogen™, Carlsbad, CA) or TransIT-LT1 (Mirus, Houston, TX), respectively. For Vero cells, after 1 h of incubation with DNA, complete A-MEM was added to the wells and allowed to incubate in CO_2 incubator at 37 ºC for an additional 23 h. At 24 h post-transfection cells were lysed and harvested.

For IFA analysis, Vero E6 or HeLa cells were seeded in Lab-Tek II 4-well slides (Nalge Nunc International, Naperville, IL) and transfected with 0.8 µg of plasmid DNA at 60% confluence using Lipofectamine 2000 or TransIT-LT1, respectively. For Vero E6 cells, after 1 h of incubation with DNA, complete A-MEM was added to the wells and allowed to incubate in CO_2 incubator at 37 ºC for an additional 23 h. At 24 h post-transfection, slides were fixed and mounted.

Immunofluorescence microscopy

Slides were washed three times with phosphate buffered saline (PBS). Slides were fixed with 2% paraformaldehyde for 15 min then permeabilized with cold methanol for 15 min at -20 °C. Slides were blocked with blocking buffer (PBS pH 7.4, 3% BSA, 0.3% Triton-X100) for 30 min. The HTNV N protein and mutants were detected by GFP

expression. NF-κB, FADD, PARP cleavage, caspase-7 and -8, were detected with polyclonal antibodies (Cell Signaling Technologies, Danvers, MA) by overnight incubation at 4 °C. Antibodies were diluted in antibody dilution buffer (PBS pH 7.4, 1% BSA, 0.3% Triton-X100) at a dilution of 1:100, 1:150, 1:200, 1:100, and 1:100 for NF-κB, FADD, PARP cleavage, caspase-7 and -8, respectively. Slides were washed three times with PBS and incubated at room temperature with anti-rabbit antibody conjugated to Alexa 594 (Molecular Probes, Eugene, OR) for 30 min with a dilution of 1:450. To visualize the nucleus, the slides were washed three times with PBS and stained with Hoechst DAPI (Molecular Probes, Eugene, OR) for 5 min at a dilution of 1:5,000. Slides were mounted with Fluoromount-G (Southern Biotechnology Associates, Birmingham, AL) then analyzed using Zeiss Axiovert 200 microscope and AxioVison 4.5 system software (Zeiss, Thornwood, NY) or by confocal imaging analysis, which was performed with a Leica DMIRBE inverted epifluorescence microscope outfitted with Leica TCS NT SP1 laser confocal optics at the High Resolution Imaging Facility at the University of Alabama – Birmingham.

Caspase-3/7 Glo activity assay

The activity of caspase-3/7 was measured using a Caspase-Glo 3/7 Assay (Promega, Madison, WI). Vero E6 cells were transfected at 80% confluence with 0.8 μg of plasmid DNA in 24-well plates and grown for 24 h. Samples were read 30 min after exposure to substrate using an Envison 2101 microplate reader (Perkin Elmer, Waltham, MA) at an excitation at 360 nm and emission of 465 nm.

Caspase-3/7, 8, and 9 activity assay

Vero E6 or HeLa cells were transfected with 5 µg of plasmid DNA in 6-well plates. Cells were harvested by trypsin and were pelleted in a 15 ml centrifuge tube (per well) at 150 x g using a Sorvall H1000B rotor for 5 min. The supernatant was removed and the cells were washed in 1 ml of ice cold PBS. The cells were re-pelleted and washed for an additional 2x. The cells were resuspended in 115 µl per well with 0.2 µm filter sterile caspase extract buffer (10mM HEPES pH 7.5, 2mM EDTA, 0.1% CHAPS, 10mM DTT). Cells extracts were prepared as previously described (38), with some minor modifications. Fifty µm caspase-3/7, -8, and -9 substrates (Sigma, St. Louis, MO) containing fluorogenic tetrapeptide Ac-DEVD-AMC [acetyl-Asp-Glu-Val-Asp-7-(amido-4-methylcoumarin)], Ac-IETD-AMC [acetyl-Ile-Glu-Thr-Asp-7-(amido-4-methylcoumarin)], and Ac-LEHD [acetyl- Leu-Glu-His-Asp-7-(amido-4-trifluoromethylcoumarin)] respectively were used. Cleavage was followed fluorometrically, with excitation at 360 nm and emission at 465 nm. Microplates were read 45 min after exposure to substrate using the Envison 2101 microplate reader to detect activity as indicated by release of free amino-methyl-coumarin.

Western blots

For western blot analysis, HeLa cells were transfected with 5 µg of plasmid DNA in 6-well plates. Cells were harvested by trypsin and were pelleted in a 15 ml centrifuge tube (per well) at 150 g using a Sorvall H1000B rotor for 5 min. The supernatant was removed and the cells were washed in 1 ml of ice cold PBS. The cells were re-pelleted and washed for an additional 2x. The cells were resuspended in 100 µl per well with 0.2

μm filter sterile extract buffer (10mM HEPES ph 7.5, 0.1% CHAPS, 2mM EDTA, 10% Glycerol, 1% NP40). Cells were mechanically lysed by passaging through a 27 gauge needle 15-20x. The cell lysate was centrifuged at 600 x g for 12 min at 4 °C. The supernatant was removed and saved, then analyzed by SDS-PAGE analysis. Proteins were separated on a 4 to 12% gradient polyacrylamide gel and transferred to nitrocellulose. Blots were blocked with 5% nonfat milk in Tris-buffered saline with 0.5% tween-20 (TBST) for 1 hr, and probed overnight at 4 °C with antibodies directed against caspase-3, caspase-7, caspase-8, TNF-R1, Fas-R, PARP, NF-κB (Rel-A), p-NF-κB (p-Rel-A), IκB, TRADD, TRAF-2, A20, actin, and histone-3 (Cell Signaling Technologies, Danvers, MA) each at a dilution of 1:1000. Blots were washed 3x with TBST for 5 min and probed with anti-rabbit HRP-conjugated secondary antibody for 30 min. Blots were developed with SuperSignal West Pico chemiluminescent substrates (Pierce, Thermo Fisher Scientific, Rockford, IL).

NF-κB Translocation assay

HeLa cells were transfected with 5 μg or 0.8 μg of plasmid DNA in 6-well plates or 4-well slides, respectively, and were allowed to express for 24 hrs. Post-transfection, cells were treated or untreated with 20 ng/ml of TNF-α for 20 min. For the cells in 6-well plates, the cytoplasmic and nuclear extracts were isolated using ProteoExtract™ Subcellular Proteome Extraction Kit (Calbiochem, San Diego, CA). Extracts were analyzed by western blot analysis. For the cells in 4-well slides, slides were prepared and probed for NF-κB as described above then analyzed by confocal microscopy.

Coimmunoprecipitations

HeLa cells were transfected with 75 µg of myc-tagged HTNV N protein plasmid DNA in T-150 flask. Cells were harvested by trypsin and were pelleted in a 50 ml centrifuge tube at 150 g using a Sorvall H1000B rotor for 5 min. The supernatant was removed and the cells were washed in 6 ml of ice cold PBS. The cells were re-pelleted and washed for an additional 2x. Cells were resuspended in 300 µl of immunoprecipitation buffer (20 mM Tris-HCl (pH 7.5), 150 mM NaCl, 1 mM Na2EDTA, 1mM EGTA, 1% Triton, 2.5 mM Sodium Pyrophosphate, 1 mM beta-glycerophosphate, 1 mM Na3VO4, 1 ug/ml Leupeptin). Cells were mechanically lysed by passaging through a 27 gauge needle 15-20x. Extracts were centrifuged at 600 x g for 12 min at 4 °C, and the supernatant was precleared with 25 µl of protein A Dynabeads (Invitrogen™, Carlsbad, CA) for 3 hrs. In another tube, protein A Dynabeads were washed with 200 µl ice-cold wash and bind buffer (0.1 M NaH2PO4, 0.01% Tween-20). Anti-myc antibody was added to the washed Dynabeads, then crosslinked with 5mM BS3 for 30 min at room temperature using rotation. The crosslinking was quenched by adding 1M Tris-HCL (ph7.5) for 15 min at room temperature. The Dynabead-antibody complex was washed 5x with wash and bind buffer. After removal of wash and bind buffer from Dynabeads, 300 µl of precleared lysate was added and incubated overnight using rotation at 4 °C. The immune complex (Dynabeads-antibody-antigen) was carefully washed 3x with 200 µl ice-cold PBS, using a new tube for each wash. On the last wash, the sample was mixed end-over-end using rotation at 4 °C for 30 min. The HTNV N protein was eluted from the immune complex by adding 30 µl of SDS buffer. Samples were heated at 70 °C for 10 min and were analyzed by western blot analysis.

HTNV N functional assay

HeLa cells were transfected with 5 µg or 10 µg of plasmid DNA in 6-well plates or T-25 flasks, respectively, and were allowed to incubate for 24 hrs. Within the 6-well plates, cells were prepared and lysed in 115 µl caspase extract buffer for caspase activity as explained above in caspase-3/7, 8, and 9 activity assay. To the T-25 flasks, cells were untreated or treated with 20 ng/ml of TNF-α for 20 min, followed by isolation of the cytoplasmic fraction using 1.0 ml of ProteoExtract™ Subcellular Proteome Extraction Kit. Half of the cytoplasmic fraction (500 µl) was concentrated to 15 µl using the ProteoExtract™ Protein Precipitation Kit (Calbiochem, San Diego, CA). Using caspase-3/7 substrate, the caspase activity was measured as described above with some minor modifications. Samples prepared were from untreated or STR treated cells for negative and positive controls, respectively. In one sample, the caspase extract of STR treated cells (6-well plate) were supplemented with 15 µl of 100 µM caspase inhibitor Z-D(OMe)E(OMe)VD(OMe)–FMK [Z-Asp(OMe)-Glu(OMe)-Val-Asp(OMe)-FMK] (Imgenex, San Diego, CA) to determine the effect of inhibitors on caspase extract activity. For three other samples, caspase extracts of STR treated cells from 6-well plates were supplemented with 15 µl of concentrated cytoplasmic extract (T-25 flask) from cells untransfected or transfected with HTNV S-segment, and untreated or treated with 20 ng/ml of TNF-α. Caspase activity was measured as explained above by the release of free amino-methyl-coumarin.

References

1. **Akhmatova, N. K., R. S. Yusupova, S. F. Khaiboullina, and S. V. Sibiryak.** 2003. Lymphocyte Apoptosis during Hemorragic Fever with Renal Syndrome. Russ J Immunol **8:**37-46.

2. **Alfadhli, A., Z. Love, B. Arvidson, J. Seeds, J. Willey, and E. Barklis.** 2001. Hantavirus nucleocapsid protein oligomerization. J Virol **75:**2019-23.

3. **Alfadhli, A., E. Steel, L. Finlay, H. P. Bachinger, and E. Barklis.** 2002. Hantavirus nucleocapsid protein coiled-coil domains. J Biol Chem **277:**27103-8.

4. **Ashkenazi, A., and V. M. Dixit.** 1998. Death receptors: signaling and modulation. Science **281:**1305-8.

5. **Baeuerle, P. A., and T. Henkel.** 1994. Function and activation of NF-kappa B in the immune system. Annu Rev Immunol **12:**141-79.

6. **Baichwal, V. R., and P. A. Baeuerle.** 1997. Activate NF-kappa B or die? Curr Biol **7:**R94-6.

7. **Barkett, M., J. E. Dooher, L. Lemonnier, L. Simmons, J. N. Scarpati, Y. Wang, and T. D. Gilmore.** 2001. Three mutations in v-Rel render it resistant to cleavage by cell-death protease caspase-3. Biochim Biophys Acta **1526:**25-36.

8. **Barkett, M., and T. D. Gilmore.** 1999. Control of apoptosis by Rel/NF-kappaB transcription factors. Oncogene **18:**6910-24.

9. **Barkett, M., D. Xue, H. R. Horvitz, and T. D. Gilmore.** 1997. Phosphorylation of IkappaB-alpha inhibits its cleavage by caspase CPP32 in vitro. J Biol Chem **272:**29419-22.

10. **Barnes, P. J., and M. Karin.** 1997. Nuclear factor-kappaB: a pivotal transcription factor in chronic inflammatory diseases. N Engl J Med **336:**1066-71.

11. **Bauder, B., A. Suchy, C. Gabler, and H. Weissenbock.** 2000. Apoptosis in feline panleukopenia and canine parvovirus enteritis. J Vet Med B Infect Dis Vet Public Health **47:**775-84.

12. **Beyaert, R., K. Heyninck, and S. Van Huffel.** 2000. A20 and A20-binding proteins as cellular inhibitors of nuclear factor-kappa B-dependent gene expression and apoptosis. Biochem Pharmacol **60:**1143-51.

13. **Bitko, V., O. Shulyayeva, B. Mazumder, A. Musiyenko, M. Ramaswamy, D. C. Look, and S. Barik.** 2007. Nonstructural proteins of respiratory syncytial virus suppress premature apoptosis by an NF-kappaB-dependent, interferon-independent mechanism and facilitate virus growth. J Virol **81:**1786-95.

14. **Boatright, K. M., and G. S. Salvesen.** 2003. Mechanisms of caspase activation. Curr Opin Cell Biol **15:**725-31.

15. **Boulares, A. H., A. G. Yakovlev, V. Ivanova, B. A. Stoica, G. Wang, S. Iyer, and M. Smulson.** 1999. Role of poly(ADP-ribose) polymerase (PARP) cleavage in apoptosis. Caspase 3-resistant PARP mutant increases rates of apoptosis in transfected cells. J Biol Chem **274:**22932-40.

16. **Cosgriff, T. M.** 1989. Hemorrhagic fever with renal syndrome: four decades of research. Ann Intern Med **110:**313-6.

17. **Cosgriff, T. M., and R. M. Lewis.** 1991. Mechanisms of disease in hemorrhagic fever with renal syndrome. Kidney Int Suppl **35:**S72-9.

18. **Ding, R., Y. Pommier, V. H. Kang, and M. Smulson.** 1992. Depletion of poly(ADP-ribose) polymerase by antisense RNA expression results in a delay in DNA strand break rejoining. J Biol Chem **267:**12804-12.

19. **Ding, R., and M. Smulson.** 1994. Depletion of nuclear poly(ADP-ribose) polymerase by antisense RNA expression: influences on genomic stability, chromatin organization, and carcinogen cytotoxicity. Cancer Res **54:**4627-34.

20. **Donepudi, M., A. Mac Sweeney, C. Briand, and M. G. Grutter.** 2003. Insights into the regulatory mechanism for caspase-8 activation. Mol Cell **11:**543-9.

21. **Earnshaw, W. C., L. M. Martins, and S. H. Kaufmann.** 1999. Mammalian caspases: structure, activation, substrates, and functions during apoptosis. Annu Rev Biochem **68:**383-424.

22. **Ennis, F. A., J. Cruz, C. F. Spiropoulou, D. Waite, C. J. Peters, S. T. Nichol, H. Kariwa, and F. T. Koster.** 1997. Hantavirus pulmonary syndrome: CD8+ and CD4+ cytotoxic T lymphocytes to epitopes on Sin Nombre virus nucleocapsid protein isolated during acute illness. Virology **238:**380-90.

23. **Flick, K., J. W. Hooper, C. S. Schmaljohn, R. F. Pettersson, H. Feldmann, and R. Flick.** 2003. Rescue of Hantaan virus minigenomes. Virology **306:**219-24.

24. **Franzoso, G., L. Carlson, L. Poljak, E. W. Shores, S. Epstein, A. Leonardi, A. Grinberg, T. Tran, T. Scharton-Kersten, M. Anver, P. Love, K. Brown, and U. Siebenlist.** 1998. Mice deficient in nuclear factor (NF)-kappa B/p52 present with defects in humoral responses, germinal center reactions, and splenic microarchitecture. J Exp Med **187:**147-59.

25. **Gaddy, D. F., and D. S. Lyles.** 2007. Oncolytic vesicular stomatitis virus induces apoptosis via signaling through PKR, Fas, and Daxx. J Virol **81:**2792-804.

26. **Gavrilovskaya, I. N., E. J. Brown, M. H. Ginsberg, and E. R. Mackow.** 1999. Cellular entry of hantaviruses which cause hemorrhagic fever with renal syndrome is mediated by beta3 integrins. J Virol **73:**3951-9.

27. **Gavrilovskaya, I. N., M. Shepley, R. Shaw, M. H. Ginsberg, and E. R. Mackow.** 1998. beta3 Integrins mediate the cellular entry of hantaviruses that cause respiratory failure. Proc Natl Acad Sci U S A **95:**7074-9.

28. **Grimm, S., B. Z. Stanger, and P. Leder.** 1996. RIP and FADD: two "death domain"-containing proteins can induce apoptosis by convergent, but dissociable, pathways. Proc Natl Acad Sci U S A **93:**10923-7.

29. **Hardestam, J., J. Klingstrom, K. Mattsson, and A. Lundkvist.** 2005. HFRS causing hantaviruses do not induce apoptosis in confluent Vero E6 and A-549 cells. J Med Virol **76:**234-40.

30. **Jonsson, C. a. S., CS.** 2001. Replication of Hantaviruses. Curr Top Microbiol Immunol **256:**15-32.

31. **Kang, J. I., S. H. Park, P. W. Lee, and B. Y. Ahn.** 1999. Apoptosis is induced by hantaviruses in cultured cells. Virology **264:**99-105.

32. **Kaukinen, P., A. Vaheri, and A. Plyusnin.** 2003. Non-covalent interaction between nucleocapsid protein of Tula hantavirus and small ubiquitin-related modifier-1, SUMO-1. Virus Res **92:**37-45.

33. **Kelliher, M. A., S. Grimm, Y. Ishida, F. Kuo, B. Z. Stanger, and P. Leder.** 1998. The death domain kinase RIP mediates the TNF-induced NF-kappaB signal. Immunity **8:**297-303.

34. **Klingstrom, J., J. Hardestam, M. Stoltz, B. Zuber, A. Lundkvist, S. Linder, and C. Ahlm.** 2006. Loss of cell membrane integrity in puumala hantavirus-infected patients correlates with levels of epithelial cell apoptosis and perforin. J Virol **80:**8279-82.

35. **Lee, B. H., K. Yoshimatsu, A. Maeda, K. Ochiai, M. Morimatsu, K. Araki, M. Ogino, S. Morikawa, and J. Arikawa.** 2003. Association of the nucleocapsid protein of the Seoul and Hantaan hantaviruses with small ubiquitin-like modifier-1-related molecules. Virus Res **98:**83-91.

36. **Lee, E. G., D. L. Boone, S. Chai, S. L. Libby, M. Chien, J. P. Lodolce, and A. Ma.** 2000. Failure to regulate TNF-induced NF-kappaB and cell death responses in A20-deficient mice. Science **289:**2350-4.

37. **Lee, T. H., Q. Huang, S. Oikemus, J. Shank, J. J. Ventura, N. Cusson, R. R. Vaillancourt, B. Su, R. J. Davis, and M. A. Kelliher.** 2003. The death domain kinase RIP1 is essential for tumor necrosis factor alpha signaling to p38 mitogen-activated protein kinase. Mol Cell Biol **23:**8377-85.

38. **Li, Q., H. Li, B. J. Blitvich, and J. Zhang.** 2007. The Aedes albopictus inhibitor of apoptosis 1 gene protects vertebrate cells from bluetongue virus-induced apoptosis. Insect Mol Biol **16:**93-105.

39. **Li, X. D., S. Kukkonen, O. Vapalahti, A. Plyusnin, H. Lankinen, and A. Vaheri.** 2004. Tula hantavirus infection of Vero E6 cells induces apoptosis involving caspase 8 activation. J Gen Virol **85:**3261-8.

40. **Li, X. D., T. P. Makela, D. Guo, R. Soliymani, V. Koistinen, O. Vapalahti, A. Vaheri, and H. Lankinen.** 2002. Hantavirus nucleocapsid protein interacts with the Fas-mediated apoptosis enhancer Daxx. J Gen Virol **83:**759-66.

41. **Li, Z. W., W. Chu, Y. Hu, M. Delhase, T. Deerinck, M. Ellisman, R. Johnson, and M. Karin.** 1999. The IKKbeta subunit of IkappaB kinase (IKK) is essential for nuclear factor kappaB activation and prevention of apoptosis. J Exp Med **189:**1839-45.

42. **Maeda, A., B. H. Lee, K. Yoshimatsu, M. Saijo, I. Kurane, J. Arikawa, and S. Morikawa.** 2003. The intracellular association of the nucleocapsid protein (NP) of hantaan virus (HTNV) with small ubiquitin-like modifier-1 (SUMO-1) conjugating enzyme 9 (Ubc9). Virology **305:**288-97.

43. **Markotic, A., L. Hensley, T. Geisbert, K. Spik, and C. Schmaljohn.** 2003. Hantaviruses induce cytopathic effects and apoptosis in continuous human embryonic kidney cells. J Gen Virol **84:**2197-202.

44. **Medema, J. P., C. Scaffidi, F. C. Kischkel, A. Shevchenko, M. Mann, P. H. Krammer, and M. E. Peter.** 1997. FLICE is activated by association with the CD95 death-inducing signaling complex (DISC). Embo J **16:**2794-804.

45. **Micheau, O., and J. Tschopp.** 2003. Induction of TNF receptor I-mediated apoptosis via two sequential signaling complexes. Cell **114:**181-90.

46. **Mir, M. A., B. Brown, B. Hjelle, W. A. Duran, and A. T. Panganiban.** 2006. Hantavirus N protein exhibits genus-specific recognition of the viral RNA panhandle. J Virol **80:**11283-92.

47. **Mir, M. A., and A. T. Panganiban.** 2005. The hantavirus nucleocapsid protein recognizes specific features of the viral RNA panhandle and is altered in conformation upon RNA binding. J Virol **79:**1824-35.

48. **Mir, M. A., and A. T. Panganiban.** 2004. Trimeric hantavirus nucleocapsid protein binds specifically to the viral RNA panhandle. J Virol **78:**8281-8.

49. **Mohsin, M. A., S. J. Morris, H. Smith, and C. Sweet.** 2002. Correlation between levels of apoptosis, levels of infection and haemagglutinin receptor binding interaction of various subtypes of influenza virus: does the viral neuraminidase have a role in these associations. Virus Res **85:**123-31.

50. **Muzio, M., A. M. Chinnaiyan, F. C. Kischkel, K. O'Rourke, A. Shevchenko, J. Ni, C. Scaffidi, J. D. Bretz, M. Zhang, R. Gentz, M. Mann, P. H. Krammer, M. E. Peter, and V. M. Dixit.** 1996. FLICE, a novel FADD-homologous ICE/CED-3-like protease, is recruited to the CD95 (Fas/APO-1) death--inducing signaling complex. Cell **85:**817-27.

51. **Muzio, M., G. S. Salvesen, and V. M. Dixit.** 1997. FLICE induced apoptosis in a cell-free system. Cleavage of caspase zymogens. J Biol Chem **272:**2952-6.

52. **Parish, J. L., A. Kowalczyk, H. T. Chen, G. E. Roeder, R. Sessions, M. Buckle, and K. Gaston.** 2006. E2 proteins from high- and low-risk human papillomavirus types differ in their ability to bind p53 and induce apoptotic cell death. J Virol **80:**4580-90.

53. **Peters, C. J., and A. S. Khan.** 2002. Hantavirus pulmonary syndrome: the new American hemorrhagic fever. Clin Infect Dis **34:**1224-31.

54. **Peters, C. J., G. L. Simpson, and H. Levy.** 1999. Spectrum of hantavirus infection: hemorrhagic fever with renal syndrome and hantavirus pulmonary syndrome. Annu Rev Med **50:**531-45.

55. **Ramanathan, H. N., D. H. Chung, S. J. Plane, E. Sztul, Y. K. Chu, M. C. Guttieri, M. McDowell, G. Ali, and C. B. Jonsson.** 2007. Dynein-dependent transport of the hantaan virus nucleocapsid protein to the endoplasmic reticulum-Golgi intermediate compartment. J Virol **81:**8634-47.

56. **Ravi, R., A. Bedi, and E. J. Fuchs.** 1998. CD95 (Fas)-induced caspase-mediated proteolysis of NF-kappaB. Cancer Res **58:**882-6.

57. **Reuther, J. Y., and A. S. Baldwin, Jr.** 1999. Apoptosis promotes a caspase-induced amino-terminal truncation of IkappaBalpha that functions as a stable inhibitor of NF-kappaB. J Biol Chem **274:**20664-70.

58. **Scaffidi, C., J. P. Medema, P. H. Krammer, and M. E. Peter.** 1997. FLICE is predominantly expressed as two functionally active isoforms, caspase-8/a and caspase-8/b. J Biol Chem **272:**26953-8.

59. **Schmaljohn, C., and B. Hjelle.** 1997. Hantaviruses: a global disease problem. Emerg Infect Dis **3:**95-104.

60. **Schmaljohn, C. S., and S. T. Nichol.** 2006. *Bunyaviridae*, p. 1741-1789. *In* D. Knipe (ed.), Virology, vol. 2. Lippincott-Raven, Philadelphia.

61. **Severson, W., L. Partin, C. S. Schmaljohn, and C. B. Jonsson.** 1999. Characterization of the Hantaan nucleocapsid protein-ribonucleic acid interaction. J Biol Chem **274:**33732-9.

62. **Severson, W. E., X. Xu, and C. B. Jonsson.** 2001. cis-Acting signals in encapsidation of Hantaan virus S-segment viral genomic RNA by its N protein. J Virol **75:**2646-52.

63. **Stanger, B. Z., P. Leder, T. H. Lee, E. Kim, and B. Seed.** 1995. RIP: a novel protein containing a death domain that interacts with Fas/APO-1 (CD95) in yeast and causes cell death. Cell **81:**513-23.

64. **Stennicke, H. R., J. M. Jurgensmeier, H. Shin, Q. Deveraux, B. B. Wolf, X. Yang, Q. Zhou, H. M. Ellerby, L. M. Ellerby, D. Bredesen, D. R. Green, J. C. Reed, C. J. Froelich, and G. S. Salvesen.** 1998. Pro-caspase-3 is a major physiologic target of caspase-8. J Biol Chem **273:**27084-90.

65. **Strasser, A., L. O'Connor, and V. M. Dixit.** 2000. Apoptosis signaling. Annu Rev Biochem **69:**217-45.

66. **Sumikoshi, M., K. Hashimoto, Y. Kawasaki, H. Sakuma, T. Suzutani, H. Suzuki, and M. Hosoya.** 2008. Human influenza virus infection and apoptosis induction in human vascular endothelial cells. J Med Virol **80:**1072-8.

67. **Tartaglia, L. A., R. F. Weber, I. S. Figari, C. Reynolds, M. A. Palladino, Jr., and D. V. Goeddel.** 1991. The two different receptors for tumor necrosis factor mediate distinct cellular responses. Proc Natl Acad Sci U S A **88:**9292-6.

68. **Tashiro, K., M. P. Pando, Y. Kanegae, P. M. Wamsley, S. Inoue, and I. M. Verma.** 1997. Direct involvement of the ubiquitin-conjugating enzyme

Ubc9/Hus5 in the degradation of IkappaBalpha. Proc Natl Acad Sci U S A **94:**7862-7.

69. **Taylor, S. L., N. Frias-Staheli, A. Garcia-Sastre, and C. S. Schmaljohn.** 2009. Hantaan virus nucleocapsid protein binds to importin alpha proteins and inhibits tumor necrosis factor alpha-induced activation of nuclear factor kappa B. J Virol **83:**1271-9.

70. **Terajima, M., D. Hayasaka, K. Maeda, and F. A. Ennis.** 2007. Immunopathogenesis of hantavirus pulmonary syndrome and hemorrhagic fever with renal syndrome: Do CD8+ T cells trigger capillary leakage in viral hemorrhagic fevers? Immunol Lett **113:**117-20.

71. **Uiprasertkul, M., R. Kitphati, P. Puthavathana, R. Kriwong, A. Kongchanagul, K. Ungchusak, S. Angkasekwinai, K. Chokephaibulkit, K. Srisook, N. Vanprapar, and P. Auewarakul.** 2007. Apoptosis and pathogenesis of avian influenza A (H5N1) virus in humans. Emerg Infect Dis **13:**708-12.

72. **Wahl-Jensen, V., J. Chapman, L. Asher, R. Fisher, M. Zimmerman, T. Larsen, and J. W. Hooper.** 2007. Temporal analysis of Andes virus and Sin Nombre virus infections of Syrian hamsters. J Virol **81:**7449-62.

73. **Wallach, D., E. E. Varfolomeev, N. L. Malinin, Y. V. Goltsev, A. V. Kovalenko, and M. P. Boldin.** 1999. Tumor necrosis factor receptor and Fas signaling mechanisms. Annu Rev Immunol **17:**331-67.

74. **Wang, C. Y., M. W. Mayo, R. G. Korneluk, D. V. Goeddel, and A. S. Baldwin, Jr.** 1998. NF-kappaB antiapoptosis: induction of TRAF1 and TRAF2 and c-IAP1 and c-IAP2 to suppress caspase-8 activation. Science **281:**1680-3.

75. **Wang, M., B. Wang, and X. Wang.** 2001. [A novel antiapoptosis gene, survivin, bcl-2, p53 expression in cervical carcinomas]. Zhonghua Fu Chan Ke Za Zhi **36:**546-8.

76. **Xu, X., W. Severson, N. Villegas, C. S. Schmaljohn, and C. B. Jonsson.** 2002. The RNA binding domain of the hantaan virus N protein maps to a central, conserved region. J Virol **76:**3301-8.

77. **Yun, C. O., E. Kim, T. Koo, H. Kim, Y. S. Lee, and J. H. Kim.** 2005. ADP-overexpressing adenovirus elicits enhanced cytopathic effect by induction of apoptosis. Cancer Gene Ther **12:**61-71.

78. **Zamarin, D., A. Garcia-Sastre, X. Xiao, R. Wang, and P. Palese.** 2005. Influenza virus PB1-F2 protein induces cell death through mitochondrial ANT3 and VDAC1. PLoS Pathog **1:**e4.

79. **Zhang, X. D., S. K. Gillespie, and P. Hersey.** 2004. Staurosporine induces apoptosis of melanoma by both caspase-dependent and -independent apoptotic pathways. Mol Cancer Ther **3:**187-97.

80. **Zou, A., I. Atencio, W. M. Huang, M. Horn, and M. Ramachandra.** 2004. Overexpression of adenovirus E3-11.6K protein induces cell killing by both caspase-dependent and caspase-independent mechanisms. Virology **326:**240-9.

CHAPTER 5

CONCLUDING REMARKS AND FUTURE PROSPECTS

Conclusion

This study helps to demonstrate the multi-functionality of the N protein and the many faces or roles it plays in the HTN virus life cycle, specifically in helping to evade the immune response. Very little information is known as to how the virus interacts with the host at the cellular level. There is more information in terms of intracellular trafficking, localization, and studies demonstrating the interactions of N protein with vRNA, or the formation of N protein multimeric structures. As multifunctional the N protein may be, there are still many roles it may be playing that are yet to be found.

There are many studies that have been done on the N protein of hantaviruses and other family members of the *Bunyaviridae* that show interactions with other viral components, but there are still many areas of uncertainty especially in terms of the N protein interaction with the RdRp or the GPs. The N protein is known to interact with vRNA (8, 55, 130, 185, 188, 222), but there are still conflicting results as to whether the N protein binds vRNA as a single molecule or as a multimer. Although it is known that the N protein is capable of interacting with itself in the formation of N-N multimeric, higher-order N protein structures, it is still speculative to say that it interacts with other viral components. The N protein is capable of oligomerizing into higher-ordered

multimers that helps to stabilize the N protein (3, 4, 8, 80, 108). The carboxy-terminal amino acids 393 to 398 have been shown to be crucial for multimerization, while the amino-terminal facilitates these interactions (79).

It is generally believed that the N protein interacts with the two GPs and possibly the RdRp, but these studies have come by means of IFA by determining the localization of N protein and finding that it is found in similar cellular compartments as other viral proteins. Furthermore, hantaviruses do not have matrix proteins to help connect the N protein and the GPs, so it is highly assumed that within each virion particle the N protein is capable of physically associating with the cytoplasmic tails of either Gn or Gc, which may also facilitate packaging and maturation. To date, models or mechanisms that explain intracellular packaging of virion particles have not been fully studied. The mechanisms that have been discussed are by far only through speculation.

The N protein has also been found to associate with a wide variety of intracellular proteins, such as SUMO-1 or Ubc9 (81, 98, 118), Daxx (110), MxA proteins (1, 58, 84, 167), cytoskeletal proteins (159, 164) and α-importin molecules (209). Although these studies are significant in showing the multi-functionality of the N protein, there are possibly many more intracellular partners that which the N protein may interact. Understanding with what intracellular proteins the N proteins interacts with is imperative to help elucidate how the virus is capable of evading the immune response during early time-frames of infection. Only the studies showing that the N protein is capable of interacting with MxA proteins or with α-importin molecules has given a glimpse into some of its mechanistic roles as to how it might facilitate viral evasion of the immune

system. This project initially began with the premise that the N protein is the viral component that helps with the evasion.

Within some of our initial results, we demonstrated that when a region within the HTN virus N protein was removed, activation of caspases was initiated resulting in apoptosis. Although we did observe some caspase activation with cells transfected with full-length HTN virus N protein, we observed no cell death. This finding was further corroborated once we probed for cleaved PARP, an intracellular marker of apoptosis. Although we observed that cells expressing full-length HTN virus N protein were capable of activating a signaling cascade that resulted in the activation of caspase-7, we observed less overall cleaved PARP (a substrate for caspase-7) than in cells that were mock transfected. Furthermore, cells expressing deletion mutants lacking amino acids 270-330 had a significantly higher caspase response (Fig. 1 and Table 1). This finding lead to the hypothesis that the HTN virus N protein is capable of modulating caspase activity, thus apoptosis, and that the region of 270-330 is necessary to facilitate regulation (Fig 1). This could be one mechanism that the virus utilizes to help evade intracellular detection.

Based on our results, we propose a model of N protein mediated inhibition of apoptosis. As previously explained, in response to stimulus, caspases are able to be activated through the Fas-R and TNFR-1 mediated pathways (Fig. 14, chapter 1). Both utilize their DD which are known to recruit FADD, a mediator that facilitates in activating initiator caspases, such as caspase-8 or -10. Once the pro-caspase is activated, it then targets and activates effector caspases, such as caspase-3 or -7, by proteolytic cleavage. These caspases then function as mediators of cell death by proteolytic cleavage of intracellular proteins which results in apoptosis (Fig. 14, chapter 1). In addition to

caspase activation, the TNFR-1 pathway is capable of activating NF-κB through an adapter mediator known as TRAF-2 (Fig. 14, chapter 1). TRAF-2 is capable of signaling the inhibition and proteosome degradation of IκB, which releases the two NF-κB subunits. IκB is capable of inhibiting the nuclear import of NF-κB by sheltering the nuclear localization signal. When inhibited, NF-κB remains in the cytoplasm. Upon stimulation of TRAF-2, IκB is inhibited, thus allowing the nuclear import of NF-κB by the use of importin molecules.

We also hypothesize that the HTN virus N protein is capable of inhibiting the nuclear import of NF-κB by direct and indirect methods. It has been previously demonstrated that the HTN virus N protein is capable of serving as a decoy protein for importin molecules, which results in inhibiting the nuclear import of NF-κB (209). Although our studies show that the HTN virus N protein is capable of directly binding to NF-κB, the interaction was minor, which suggests that the N protein may directly inhibit the nuclear import of NF-κB, but other means, such as binding to importin molecules, might play more significant roles.

In addition, since our studies demonstrated less amount of IκB present in cells expressing HTNV N protein, the binding observed between N protein and NF-κB could serve to inhibit IκB and promote its degradation (Fig. 6, chapter 4). The inhibition of IκB is a very important key in establishing NF-κB as caspase substrate, because only the two subunits of NF-κB are capable of being cleaved by caspases. Through the inhibition by N protein, active NF-κB remains in the cytoplasm and is unable to translocate to the nucleus and serve as a transcription factor (Fig. 6, chapter 4). NF-κB translocation to the nucleus results in the expression of genes that inhibits this pathway and activates the

immune response. Since this pathway no longer receives feedback inhibition, the molar ratio of cytoplasmic NF-κB significantly increases. The increased concentration of cytoplasmic NF-κB serves as a quenching substrate for effector caspases, which results in the inhibition of caspase-mediated apoptosis (Fig. 6, chapter 4). Our studies have demonstrated that the cytoplasmic extract of cells expressing HTN virus N protein, that have been co-treated with TNF-α, is capable of reducing the effector caspase activity of cells treated with apoptotic inducing agents such as STR. Although we see inhibition of effector caspases, such as caspase-7, we do believe that the inhibition *in vivo* is only temporary. Overall, we hypothesize that the N protein serves a dual function within these pathways, as an inhibitor of caspases through the use of the region 270-330 (Fig. 1) and the innate and adaptive immune response (Fig. 6, chapter 4).

Future Directions

It will be interesting to know what region(s) of the N protein are capable of influencing the inhibition of NF-κB, whether it is through direct inhibition or through the use of importin molecules. The use of mutant or deletion constructs of N protein would help to distinguish the region that may be involved. This can easily be done through co-immunoprecipitation experiments or through IFA functional cellular assays. Cells can be transfected with N protein mutant or deletion constructs and co-treated with TNF-α. The location of NF-κB can be probed by microscopically by IFA or through western blot by the separation of cytoplasmic and nuclear fractions. Similar co-immunoprecipitation experiments can be done with importin molecules. Furthermore, to test the effectiveness

of the N protein serving as a decoy for importin molecules, it would be interesting to determine if the nuclear import of other intracellular proteins that utilize these molecules is also inhibited. This would definitely be the defining factor to determine the importance of direct or indirect inhibition of NF-κB nuclear import.

It is also quite possible that there is no specific region involved within the N protein that facilitates this nuclear import inhibition of NF-κB. It is a possibility that since the N protein is capable of localizing to the perinuclear region in significant quantity, it may serve as a wall or "molecular sponge" that serves as a non-specific inhibitor of the import. The building of this nuclear wall can most definitely serve as a major barrier, but not only for NF-κB, for all proteins that are being imported and/or exported. This could also be the basis observed behind the inhibition of caspases. The mutation and deletion analysis of the experiments above would shed some light as to how important the non-specific interactions are for the inhibition.

Additionally, it would be very interesting to determine mechanistically how the N protein is capable of promoting the degradation of IκB. One question to ask, are mutants that are incapable of binding to NF-κB still able to direct the degradation of IκB? The results of the co-immunoprecipitations along with western blot analysis of cell extracts that were transfected with mutants would help reveal if a specific region within the N protein is capable of promoting IκB degradation. Our future studies to elucidate the mechanism behind our current findings are quite endearing and will help to answer the mechanistic roles of the HTN virus N protein in evading cellular detection.

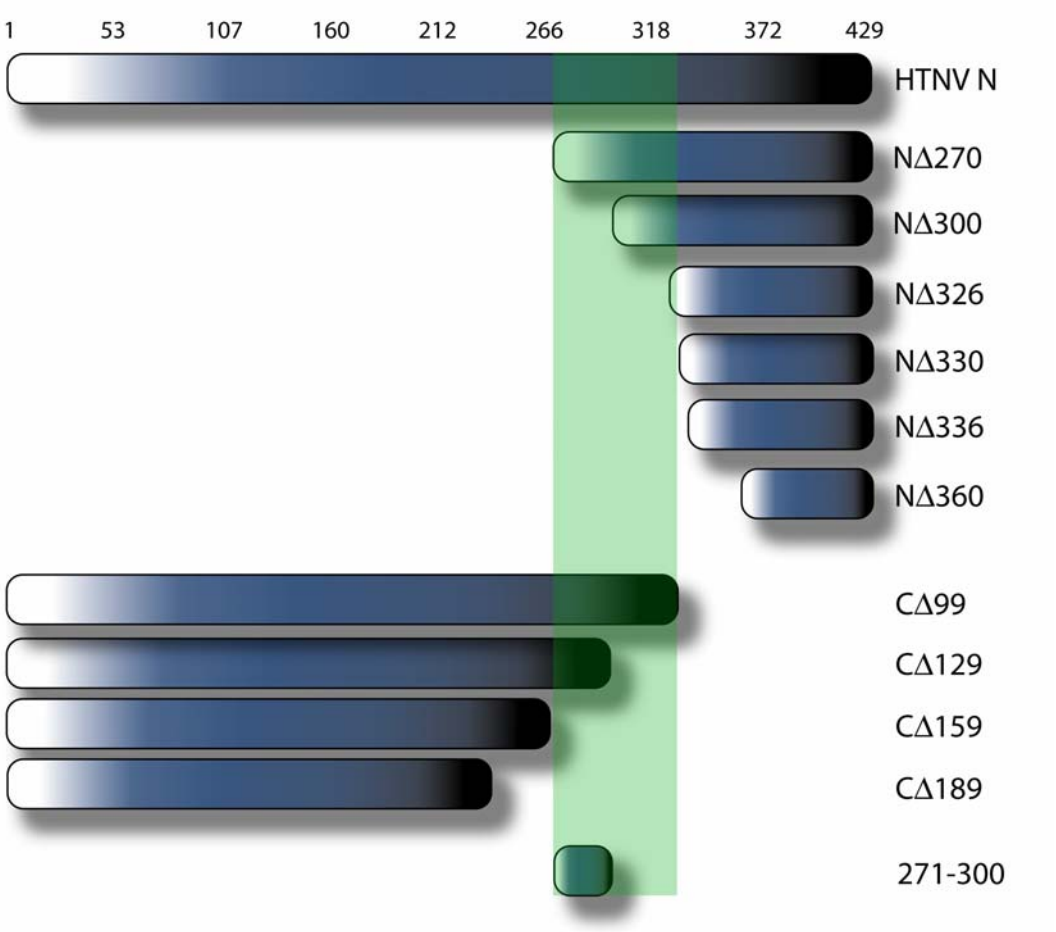

Figure 1: The region of 270-330 of the HTN virus N protein functions to inhibit caspases. N-terminal deletion mutants of the HTNV N protein included NΔ270, NΔ300, NΔ330, and NΔ360, which were lacking 270, 300, 330 and 360 amino acids from the N-terminus respectively. C-terminally deleted HTNV N protein mutants included CΔ99, CΔ129, CΔ159, and CΔ189, lacking 99, 129, 159, and 189 amino acids from the C-terminus, respectively. Deletion mutant 271-300 contained both N- and C-terminal deletions. The region of 270-330 (highlighted in green) was observed to be necessary to inhibit caspase activity.

Table 1: Caspase activation of cells expressing HTN virus N protein or mutants.

Construct	Amino acids	Caspase-3	Caspase-7	Caspase-8	Caspase-9
HTNV N Protein	1-429	-	+	+	-
NΔ270	271-429	-	+	nt	-
NΔ300	301-429	-	+++	nt	-
NΔ330	331-429	-	+++	nt	-
NΔ360	361-429	-	++++	+++	-
CΔ99	1-330	-	+	nt	-
CΔ129	1-300	-	+++	nt	-
CΔ159	1-270	-	+++	nt	-
CΔ189	1-240	-	+++	nt	-
271-300	271-300	-	+	nt	-

N-terminal and C-terminal deletion mutants of the HTNV N protein. Caspase activity was summarized for each construct from experiments presented in chapter 4. Caspase activation was scored with increasing activity correlating with increasing number of plus-signs; ++++ (high) and + (low). *nt – not tested

GENERAL LIST OF REFERENCES

1. **Accola, M. A., B. Huang, A. Al Masri, and M. A. McNiven.** 2002. The antiviral dynamin family member, MxA, tubulates lipids and localizes to the smooth endoplasmic reticulum. J Biol Chem **277:**21829-35.

2. **Akhmatova, N. K., R. S. Yusupova, S. F. Khaiboullina, and S. V. Sibiryak.** 2003. Lymphocyte Apoptosis during Hemorragic Fever with Renal Syndrome. Russ J Immunol **8:**37-46.

3. **Alfadhli, A., Z. Love, B. Arvidson, J. Seeds, J. Willey, and E. Barklis.** 2001. Hantavirus nucleocapsid protein oligomerization. J Virol **75:**2019-23.

4. **Alfadhli, A., E. Steel, L. Finlay, H. P. Bachinger, and E. Barklis.** 2002. Hantavirus nucleocapsid protein coiled-coil domains. J Biol Chem **277:**27103-8.

5. **Algeciras-Schimnich, A., L. Shen, B. C. Barnhart, A. E. Murmann, J. K. Burkhardt, and M. E. Peter.** 2002. Molecular ordering of the initial signaling events of CD95. Mol Cell Biol **22:**207-20.

6. **Anderson, G. W., Jr., and J. F. Smith.** 1987. Immunoelectron microscopy of Rift Valley fever viral morphogenesis in primary rat hepatocytes. Virology **161:**91-100.

7. **Andersson, A. M., and R. F. Pettersson.** 1998. Targeting of a short peptide derived from the cytoplasmic tail of the G1 membrane glycoprotein of Uukuniemi virus (Bunyaviridae) to the Golgi complex. J Virol **72:**9585-96.

8. **Andersson, I., L. Bladh, M. Mousavi-Jazi, K. E. Magnusson, A. Lundkvist, O. Haller, and A. Mirazimi.** 2004. Human MxA protein inhibits the replication of Crimean-Congo hemorrhagic fever virus. J Virol **78:**4323-9.

9. **Antic, D., K. E. Wright, and C. Y. Kang.** 1992. Maturation of Hantaan virus glycoproteins G1 and G2. Virology **189:**324-8.

10. **Arikawa, J., A. L. Schmaljohn, J. M. Dalrymple, and C. S. Schmaljohn.** 1989. Characterization of Hantaan virus envelope glycoprotein antigenic determinants defined by monoclonal antibodies. J Gen Virol **70 (Pt 3):**615-24.

11. **Ashkenazi, A., and V. M. Dixit.** 1998. Death receptors: signaling and modulation. Science **281:**1305-8.

12. **Barkett, M., J. E. Dooher, L. Lemonnier, L. Simmons, J. N. Scarpati, Y. Wang, and T. D. Gilmore.** 2001. Three mutations in v-Rel render it resistant to cleavage by cell-death protease caspase-3. Biochim Biophys Acta **1526:**25-36.

13. **Barr, F. A., and B. Short.** 2003. Golgins in the structure and dynamics of the Golgi apparatus. Curr Opin Cell Biol **15:**405-13.

14. **Bertolotti-Ciarlet, A., J. Smith, K. Strecker, J. Paragas, L. A. Altamura, J. M. McFalls, N. Frias-Staheli, A. Garcia-Sastre, C. S. Schmaljohn, and R. W. Doms.** 2005. Cellular localization and antigenic characterization of crimean-congo hemorrhagic fever virus glycoproteins. J Virol **79:**6152-61.

15. **Betenbaugh, M., M. Yu, K. Kuehl, J. White, D. Pennock, K. Spik, and C. Schmaljohn.** 1995. Nucleocapsid- and virus-like particles assemble in cells infected with recombinant baculoviruses or vaccinia viruses expressing the M and the S segments of Hantaan virus. Virus Res **38:**111-24.

16. **Bishop, D. H., C. H. Calisher, J. Casals, M. P. Chumakov, S. Y. Gaidamovich, C. Hannoun, D. K. Lvov, I. D. Marshall, N. Oker-Blom, R. F.**

Pettersson, J. S. Porterfield, P. K. Russell, R. E. Shope, and E. G. Westaway. 1980. Bunyaviridae. Intervirology **14:**125-43.

17. **Boatright, K. M., M. Renatus, F. L. Scott, S. Sperandio, H. Shin, I. M. Pedersen, J. E. Ricci, W. A. Edris, D. P. Sutherlin, D. R. Green, and G. S. Salvesen.** 2003. A unified model for apical caspase activation. Mol Cell **11:**529-41.

18. **Boudko, S. P., R. J. Kuhn, and M. G. Rossmann.** 2007. The coiled-coil domain structure of the Sin Nombre virus nucleocapsid protein. J Mol Biol **366:**1538-44.

19. **Boulares, A. H., A. G. Yakovlev, V. Ivanova, B. A. Stoica, G. Wang, S. Iyer, and M. Smulson.** 1999. Role of poly(ADP-ribose) polymerase (PARP) cleavage in apoptosis. Caspase 3-resistant PARP mutant increases rates of apoptosis in transfected cells. J Biol Chem **274:**22932-40.

20. **Bouloy, M., and C. Hannoun.** 1976. Studies on lumbo virus replication. I. RNA-dependent RNA polymerase associated with virions. Virology **69:**258-64.

21. **Casals, J., B. E. Henderson, H. Hoogstraal, K. M. Johnson, and A. Shelokov.** 1970. A review of Soviet viral hemorrhagic fevers, 1969. J Infect Dis **122:**437-53.

22. **Chang, D. W., Z. Xing, V. L. Capacio, M. E. Peter, and X. Yang.** 2003. Interdimer processing mechanism of procaspase-8 activation. Embo J **22:**4132-42.

23. **Chen, H. X., and F. X. Qiu.** 1993. Epidemiologic surveillance on the hemorrhagic fever with renal syndrome in China. Chin Med J (Engl) **106:**857-63.

24. **Chen, H. X., F. X. Qiu, B. J. Dong, S. Z. Ji, Y. T. Li, Y. Wang, H. M. Wang, G. F. Zuo, X. X. Tao, and S. Y. Gao.** 1986. Epidemiological studies on hemorrhagic fever with renal syndrome in China. J Infect Dis **154:**394-8.

25. **Chen, S. Y., and R. W. Compans.** 1991. Oligomerization, transport, and Golgi retention of Punta Toro virus glycoproteins. J Virol **65:**5902-9.

26. **Chernukha, Y. G., O. A. Evdokimova, and A. V. Cheechovich.** 1986. Results of karyologic and immunobiological studies of the striped field mouse (Apodemus agrarius) from different areas of its range. Zool J **65:**471-475.

27. **Chu, Y. K., C. Rossi, J. W. Leduc, H. W. Lee, C. S. Schmaljohn, and J. M. Dalrymple.** 1994. Serological relationships among viruses in the Hantavirus genus, family Bunyaviridae. Virology **198:**196-204.

28. **Clement, J., P. Colson, and P. McKenna.** 1994. Hantavirus pulmonary syndrome in New England and Europe. N Engl J Med **331:**545-6; author reply 547-8.

29. **Cohen, G. M.** 1997. Caspases: the executioners of apoptosis. Biochem J **326 (Pt 1):**1-16.

30. **Cory, S., and J. M. Adams.** 2002. The Bcl2 family: regulators of the cellular life-or-death switch. Nat Rev Cancer **2:**647-56.

31. **Dahlberg, J. E., J. F. Obijeski, and J. Korb.** 1977. Electron microscopy of the segmented RNA genome ofLa Crosse virus: absence of circular molecules. J Virol **22:**203-9.

32. **Danial, N. N.** 2007. BCL-2 family proteins: critical checkpoints of apoptotic cell death. Clin Cancer Res **13:**7254-63.

33. **Danial, N. N., and S. J. Korsmeyer.** 2004. Cell death: critical control points. Cell **116:**205-19.

34. **Dantas, J. R., Jr., Y. Okuno, O. Tanishita, Y. Takahashi, M. Takahashi, T. Kurata, H. W. Lee, and K. Yamanishi.** 1987. Viruses of hemorrhagic fever with renal syndrome (HFRS) grouped by immunoprecipitation and hemagglutination inhibition. Intervirology **27:**161-5.

35. **Deveraux, Q. L., and J. C. Reed.** 1999. IAP family proteins--suppressors of apoptosis. Genes Dev **13:**239-52.

36. **Deveraux, Q. L., R. Takahashi, G. S. Salvesen, and J. C. Reed.** 1997. X-linked IAP is a direct inhibitor of cell-death proteases. Nature **388:**300-4.

37. **Ding, R., Y. Pommier, V. H. Kang, and M. Smulson.** 1992. Depletion of poly(ADP-ribose) polymerase by antisense RNA expression results in a delay in DNA strand break rejoining. J Biol Chem **267:**12804-12.

38. **Ding, R., and M. Smulson.** 1994. Depletion of nuclear poly(ADP-ribose) polymerase by antisense RNA expression: influences on genomic stability, chromatin organization, and carcinogen cytotoxicity. Cancer Res **54:**4627-34.

39. **Domingo, E., and J. J. Holland.** 1994. Mutation rates and rapid evolution of viruses, The Evolutionary Biology of Viruses, Morse, S. S. ed. Raven Press, New York.

40. **Donepudi, M., A. Mac Sweeney, C. Briand, and M. G. Grutter.** 2003. Insights into the regulatory mechanism for caspase-8 activation. Mol Cell **11:**543-9.

41. **Donets, M. A., M. P. Chumakov, M. B. Korolev, and S. G. Rubin.** 1977. Physicochemical characteristics, morphology and morphogenesis of virions of the causative agent of Crimean hemorrhagic fever. Intervirology **8:**294-308.

42. **Duchin, J. S., F. T. Koster, C. J. Peters, G. L. Simpson, B. Tempest, S. R. Zaki, T. G. Ksiazek, P. E. Rollin, S. Nichol, E. T. Umland, and et al.** 1994. Hantavirus pulmonary syndrome: a clinical description of 17 patients with a newly recognized disease. The Hantavirus Study Group. N Engl J Med **330:**949-55.

43. **Earnshaw, W. C., L. M. Martins, and S. H. Kaufmann.** 1999. Mammalian caspases: structure, activation, substrates, and functions during apoptosis. Annu Rev Biochem **68:**383-424.

44. **Elliott, R. M.** 1989. Nucleotide sequence analysis of the large (L) genomic RNA segment of Bunyamwera virus, the prototype of the family Bunyaviridae. Virology **173:**426-36.

45. **Ellis, D. S., P. V. Shirodaria, E. Fleming, and D. I. Simpson.** 1988. Morphology and development of Rift Valley fever virus in Vero cell cultures. J Med Virol **24:**161-74.

46. **Fazakerley, J. K., F. Gonzalez-Scarano, J. Strickler, B. Dietzschold, F. Karush, and N. Nathanson.** 1988. Organization of the middle RNA segment of snowshoe hare Bunyavirus. Virology **167:**422-32.

47. **Fazakerley, J. K., and A. M. Ross.** 1989. Computer analysis suggests a role for signal sequences in processing polyproteins of enveloped RNA viruses and as a mechanism of viral fusion. Virus Genes **2:**223-39.

48. **Fenner, F.** 1975. The classification and nomenclature of viruses. Summary of results of meetings of the International Committee on Taxonomy of Viruses in Madrid, September 1975. Intervirology **6:**1-12.

49. **Garcin, D., M. Lezzi, M. Dobbs, R. M. Elliott, C. Schmaljohn, C. Y. Kang, and D. Kolakofsky.** 1995. The 5' ends of Hantaan virus (Bunyaviridae) RNAs suggest a prime-and-realign mechanism for the initiation of RNA synthesis. J Virol **69:**5754-62.

50. **Gavrilovskaya, I. N., E. J. Brown, M. H. Ginsberg, and E. R. Mackow.** 1999. Cellular entry of hantaviruses which cause hemorrhagic fever with renal syndrome is mediated by beta3 integrins. J Virol **73:**3951-9.

51. **Gavrilovskaya, I. N., M. Shepley, R. Shaw, M. H. Ginsberg, and E. R. Mackow.** 1998. beta3 Integrins mediate the cellular entry of hantaviruses that cause respiratory failure. Proc Natl Acad Sci U S A **95:**7074-9.

52. **Ghayur, T., S. Banerjee, M. Hugunin, D. Butler, L. Herzog, A. Carter, L. Quintal, L. Sekut, R. Talanian, M. Paskind, W. Wong, R. Kamen, D. Tracey, and H. Allen.** 1997. Caspase-1 processes IFN-gamma-inducing factor and regulates LPS-induced IFN-gamma production. Nature **386:**619-23.

53. **Glass, G. E., W. Livingstone, J. N. Mills, W. G. Hlady, J. B. Fine, W. Biggler, T. Coke, D. Frazier, S. Atherley, P. E. Rollin, T. G. Ksiazek, C. J. Peters, and J. E. Childs.** 1998. Black Creek Canal Virus infection in Sigmodon hispidus in southern Florida. Am J Trop Med Hyg **59:**699-703.

54. **Goldsmith, C. S., L. H. Elliott, C. J. Peters, and S. R. Zaki.** 1995. Ultrastructural characteristics of Sin Nombre virus, causative agent of hantavirus pulmonary syndrome. Arch Virol **140:**2107-22.

55. **Gott, P., R. Stohwasser, P. Schnitzler, G. Darai, and E. K. Bautz.** 1993. RNA binding of recombinant nucleocapsid proteins of hantaviruses. Virology **194:**332-7.

56. **Grimm, S., B. Z. Stanger, and P. Leder.** 1996. RIP and FADD: two "death domain"-containing proteins can induce apoptosis by convergent, but dissociable, pathways. Proc Natl Acad Sci U S A **93:**10923-7.

57. **Hacker, J. K., and J. L. Hardy.** 1997. Adsorptive endocytosis of California encephalitis virus into mosquito and mammalian cells: a role for G1. Virology **235:**40-7.

58. **Haller, O., and G. Kochs.** 2002. Interferon-induced mx proteins: dynamin-like GTPases with antiviral activity. Traffic **3:**710-7.

59. **Hansen, J. L., A. M. Long, and S. C. Schultz.** 1997. Structure of the RNA-dependent RNA polymerase of poliovirus. Structure **5:**1109-22.

60. **Hardestam, J., J. Klingstrom, K. Mattsson, and A. Lundkvist.** 2005. HFRS causing hantaviruses do not induce apoptosis in confluent Vero E6 and A-549 cells. J Med Virol **76:**234-40.

61. **Hewlett, M. J., R. F. Pettersson, and D. Baltimore.** 1977. Circular forms of Uukuniemi virion RNA: an electron microscopic study. J Virol **21:**1085-93.

62. **Hiscox, J. A.** 2003. The interaction of animal cytoplasmic RNA viruses with the nucleus to facilitate replication. Virus Res **95:**13-22.

63. **Hjelle, B., N. Torrez-Martinez, and F. T. Koster.** 1996. Hantavirus pulmonary syndrome-related virus from Bolivia. Lancet **347:**57.

64. **Honda, A., K. Ueda, K. Nagata, and A. Ishihama.** 1988. RNA polymerase of influenza virus: role of NP in RNA chain elongation. J Biochem (Tokyo) **104:**1021-6.

65. **Hung, T., Z. Y. Chou, T. X. Zhao, S. M. Xia, and C. S. Hang.** 1985. Morphology and morphogenesis of viruses of hemorrhagic fever with renal syndrome (HFRS). I. Some peculiar aspects of the morphogenesis of various strains of HFRS virus. Intervirology **23:**97-108.

66. **Hutchinson, K. L., C. J. Peters, and S. T. Nichol.** 1996. Sin Nombre virus mRNA synthesis. Virology **224:**139-49.

67. **Hutchinson, K. L., P. E. Rollin, W. J. Shieh, S. Zaki, P. W. Greer, and C. J. Peters.** 2000. Transmission of Black Creek Canal virus between cotton rats. J Med Virol **60:**70-6.

68. **Inaba, Y., H. Kurogi, and T. Omori.** 1975. Letter: Akabane disease: epizootic abortion, premature birth, stillbirth and congenital arthrogryposis-hydranencephaly in cattle, sheep and goats caused by Akabane virus. Aust Vet J **51:**584-5.

69. **Jantti, J., P. Hilden, H. Ronka, V. Makiranta, S. Keranen, and E. Kuismanen.** 1997. Immunocytochemical analysis of Uukuniemi virus budding compartments: role of the intermediate compartment and the Golgi stack in virus maturation. J Virol **71:**1162-72.

70. **Jin, H., and R. M. Elliott.** 1993. Characterization of Bunyamwera virus S RNA that is transcribed and replicated by the L protein expressed from recombinant vaccinia virus. J Virol **67:**1396-404.

71. **Jin, M., J. Park, S. Lee, B. Park, J. Shin, K. J. Song, T. I. Ahn, S. Y. Hwang, B. Y. Ahn, and K. Ahn.** 2002. Hantaan virus enters cells by clathrin-dependent receptor-mediated endocytosis. Virology **294:**60-9.

72. **Jonsson, C. a. S., CS.** 2001. Replication of Hantaviruses. Curr Top Microbiol Immunol **256:**15-32.

73. **Jonsson, C. B., J. Hooper, and G. Mertz.** 2008. Treatment of hantavirus pulmonary syndrome. Antiviral Res **78:**162-9.

74. **Kainz, M., P. Hilson, L. Sweeney, E. Derose, and T. L. German.** 2004. Interaction Between Tomato spotted wilt virus N Protein Monomers Involves Nonelectrostatic Forces Governed by Multiple Distinct Regions in the Primary Structure. Phytopathology **94:**759-65.

75. **Kanerva, M., J. Mustonen, and A. Vaheri.** 1998. Pathogenesis of puumala and other hantavirus infections. Rev Med Virol **8:**67-86.

76. **Kang, J. I., S. H. Park, P. W. Lee, and B. Y. Ahn.** 1999. Apoptosis is induced by hantaviruses in cultured cells. Virology **264:**99-105.

77. **Kaplan, H. M., N. R. Brewer, and W. H. Blair.** 1982. Physiology, p. 260-292, The Mouse in Biomedical Research, Foster, H. L., Small, J. D., Fox, J. G. ed, vol. III. Academic Press, New York.

78. **Kariwa, H., H. Tanabe, T. Mizutani, Y. Kon, K. Lokugamage, N. Lokugamage, M. A. Iwasa, T. Hagiya, K. Araki, K. Yoshimatsu, J. Arikawa, and I. Takashima.** 2003. Synthesis of Seoul virus RNA and structural proteins in cultured cells. Arch Virol **148:**1671-85.

79. **Kaukinen, P., V. Koistinen, O. Vapalahti, A. Vaheri, and A. Plyusnin.** 2001. Interaction between molecules of hantavirus nucleocapsid protein. J Gen Virol **82:**1845-53.

80. **Kaukinen, P., V. Kumar, K. Tulimaki, P. Engelhardt, A. Vaheri, and A. Plyusnin.** 2004. Oligomerization of Hantavirus N protein: C-terminal alpha-helices interact to form a shared hydrophobic space. J Virol **78:**13669-77.

81. **Kaukinen, P., A. Vaheri, and A. Plyusnin.** 2003. Non-covalent interaction between nucleocapsid protein of Tula hantavirus and small ubiquitin-related modifier-1, SUMO-1. Virus Res **92:**37-45.

82. **Keegan, K., and M. S. Collett.** 1986. Use of bacterial expression cloning to define the amino acid sequences of antigenic determinants on the G2 glycoprotein of Rift Valley fever virus. J Virol **58:**263-70.

83. **Kelliher, M. A., S. Grimm, Y. Ishida, F. Kuo, B. Z. Stanger, and P. Leder.** 1998. The death domain kinase RIP mediates the TNF-induced NF-kappaB signal. Immunity **8:**297-303.

84. **Khaiboullina, S. F., A. A. Rizvanov, V. M. Deyde, and S. C. St Jeor.** 2005. Andes virus stimulates interferon-inducible MxA protein expression in endothelial cells. J Med Virol **75:**267-75.

85. **Khaiboullina, S. F., A. A. Rizvanov, E. Otteson, A. Miyazato, J. Maciejewski, and S. St Jeor.** 2004. Regulation of cellular gene expression in endothelial cells by sin nombre and prospect hill viruses. Viral Immunol **17:**234-51.

86. **Khan, A. S., M. Gaviria, P. E. Rollin, W. G. Hlady, T. G. Ksiazek, L. R. Armstrong, R. Greenman, E. Ravkov, M. Kolber, H. Anapol, E. D.**

Sfakianaki, S. T. Nichol, C. J. Peters, and R. F. Khabbaz. 1996. Hantavirus pulmonary syndrome in Florida: association with the newly identified Black Creek Canal virus. Am J Med **100:**46-8.

87. **Khan, A. S., R. F. Khabbaz, L. R. Armstrong, R. C. Holman, S. P. Bauer, J. Graber, T. Strine, G. Miller, S. Reef, J. Tappero, P. E. Rollin, S. T. Nichol, S. R. Zaki, R. T. Bryan, L. E. Chapman, C. J. Peters, and T. G. Ksiazek.** 1996. Hantavirus pulmonary syndrome: the first 100 US cases. J Infect Dis **173:**1297-303.

88. **Kikkert, M., J. Van Lent, M. Storms, P. Bodegom, R. Kormelink, and R. Goldbach.** 1999. Tomato spotted wilt virus particle morphogenesis in plant cells. J Virol **73:**2288-97.

89. **Kischkel, F. C., D. A. Lawrence, A. Tinel, H. LeBlanc, A. Virmani, P. Schow, A. Gazdar, J. Blenis, D. Arnott, and A. Ashkenazi.** 2001. Death receptor recruitment of endogenous caspase-10 and apoptosis initiation in the absence of caspase-8. J Biol Chem **276:**46639-46.

90. **Klingstrom, J., J. Hardestam, M. Stoltz, B. Zuber, A. Lundkvist, S. Linder, and C. Ahlm.** 2006. Loss of cell membrane integrity in puumala hantavirus-infected patients correlates with levels of epithelial cell apoptosis and perforin. J Virol **80:**8279-82.

91. **Kormelink, R., P. de Haan, D. Peters, and R. Goldbach.** 1992. Viral RNA synthesis in tomato spotted wilt virus-infected Nicotiana rustica plants. J Gen Virol **73 (Pt 3):**687-93.

92. **Kuida, K., J. A. Lippke, G. Ku, M. W. Harding, D. J. Livingston, M. S. Su, and R. A. Flavell.** 1995. Altered cytokine export and apoptosis in mice deficient in interleukin-1 beta converting enzyme. Science **267:**2000-3.

93. **Kuismanen, E., K. Hedman, J. Saraste, and R. F. Pettersson.** 1982. Uukuniemi virus maturation: accumulation of virus particles and viral antigens in the Golgi complex. Mol Cell Biol **2:**1444-58.

94. **Kukkonen, S. K., A. Vaheri, and A. Plyusnin.** 2004. Tula hantavirus L protein is a 250 kDa perinuclear membrane-associated protein. J Gen Virol **85:**1181-9.

95. **Lazebnik, Y. A., S. H. Kaufmann, S. Desnoyers, G. G. Poirier, and W. C. Earnshaw.** 1994. Cleavage of poly(ADP-ribose) polymerase by a proteinase with properties like ICE. Nature **371:**346-7.

96. **Le May, N., N. Gauliard, A. Billecocq, and M. Bouloy.** 2005. The N terminus of Rift Valley fever virus nucleoprotein is essential for dimerization. J Virol **79:**11974-80.

97. **LeDuc, J. W.** 1987. Epidemiology of Hantaan and related viruses. Lab Anim Sci **37:**413-8.

98. **Lee, B. H., K. Yoshimatsu, A. Maeda, K. Ochiai, M. Morimatsu, K. Araki, M. Ogino, S. Morikawa, and J. Arikawa.** 2003. Association of the nucleocapsid protein of the Seoul and Hantaan hantaviruses with small ubiquitin-like modifier-1-related molecules. Virus Res **98:**83-91.

99. **Lee, H. W.** 1989. Clinical Manifestations of HFRS, p. 19-38, Manual of Hemorrhagic Fever with Renal Syndrome, Lee, H. W., Dalrymple, J. M. ed, Seoul.

100. **Lee, H. W.** 1989. Hemorrhagic fever with renal syndrome in Korea. Rev Infect Dis **11:**S864-S867.

101. **Lee, H. W.** 1982. Korean hemorrhagic fever. Prog Med Virol **28:**96-113.

102. **Lee, H. W., L. J. Baek, and K. M. Johnson.** 1982. Isolation of Hantaan virus, the etiologic agent of Korean hemorrhagic fever, from wild urban rats. J Infect Dis **146:**638-44.

103. **Lee, H. W., G. R. French, P. W. Lee, L. J. Baek, K. Tsuchiya, and R. S. Foulke.** 1981. Observations on natural and laboratory infection of rodents with the etiologic agent of Korean hemorrhagic fever. Am J Trop Med Hyg **30:**477-82.

104. **Lee, H. W., and K. M. Johnson.** 1976. Korean hemorrhagic fever: Demonstration of causative antigen and antibodies. Jorean J. Intern. Med **19:**371.

105. **Lee, H. W., P. W. Lee, and K. M. Johnson.** 1978. Isolation of the etiologic agent of Korean Hemorrhagic fever. J Infect Dis **137:**298-308.

106. **Lee, H. W., and G. van der Groen.** 1989. Hemorrhagic fever with renal syndrome. Prog. Med Virol **36:**62.

107. **Lee, M.** 1987. [Hemorrhagic fever with renal syndrome (Korean hemorrhagic fever)]. Rinsho Ketsueki **28:**496-504.

108. **Leonard, V. H., A. Kohl, J. C. Osborne, A. McLees, and R. M. Elliott.** 2005. Homotypic interaction of Bunyamwera virus nucleocapsid protein. J Virol **79:**13166-72.

109. **Li, P., D. Nijhawan, I. Budihardjo, S. M. Srinivasula, M. Ahmad, E. S. Alnemri, and X. Wang.** 1997. Cytochrome c and dATP-dependent formation of

Apaf-1/caspase-9 complex initiates an apoptotic protease cascade. Cell **91:**479-89.

110. **Li, X. D., T. P. Makela, D. Guo, R. Soliymani, V. Koistinen, O. Vapalahti, A. Vaheri, and H. Lankinen.** 2002. Hantavirus nucleocapsid protein interacts with the Fas-mediated apoptosis enhancer Daxx. J Gen Virol **83:**759-66.

111. **Liang, M., D. Li, S. Y. Xiao, C. Hang, C. A. Rossi, and C. S. Schmaljohn.** 1994. Antigenic and molecular characterization of hantavirus isolates from China. Virus Res **31:**219-33.

112. **Lippincott-Schwartz, J., J. G. Donaldson, A. Schweizer, E. G. Berger, H. P. Hauri, L. C. Yuan, and R. D. Klausner.** 1990. Microtubule-dependent retrograde transport of proteins into the ER in the presence of brefeldin A suggests an ER recycling pathway. Cell **60:**821-36.

113. **Lober, C., B. Anheier, S. Lindow, H. D. Klenk, and H. Feldmann.** 2001. The Hantaan virus glycoprotein precursor is cleaved at the conserved pentapeptide WAASA. Virology **289:**224-9.

114. **Lodish, H., A. Berk, P. Matsudaira, C. A. Kaiser, M. Krieger, M. P. Scott, L. Zipursky, and J. Darnell.** 2003. Molecular Cell Biology, 5th ed. W.H. Freeman and Company.

115. **Lopez, N., P. Padula, C. Rossi, M. E. Lazaro, and M. T. Franze-Fernandez.** 1996. Genetic identification of a new hantavirus causing severe pulmonary syndrome in Argentina. Virology **220:**223-6.

116. **Lukes, R. J.** 1954. The pathology of thirty-nine fatal cases of epidemic hemorrhagic fever. Am J Med **16:**639-50.

117. **Lundkvist, A., A. Fatouros, and B. Niklasson.** 1991. Antigenic variation of European haemorrhagic fever with renal syndrome virus strains characterized using bank vole monoclonal antibodies. J Gen Virol **72 (Pt 9):**2097-103.

118. **Maeda, A., B. H. Lee, K. Yoshimatsu, M. Saijo, I. Kurane, J. Arikawa, and S. Morikawa.** 2003. The intracellular association of the nucleocapsid protein (NP) of hantaan virus (HTNV) with small ubiquitin-like modifier-1 (SUMO-1) conjugating enzyme 9 (Ubc9). Virology **305:**288-97.

119. **Markotic, A., L. Hensley, T. Geisbert, K. Spik, and C. Schmaljohn.** 2003. Hantaviruses induce cytopathic effects and apoptosis in continuous human embryonic kidney cells. J Gen Virol **84:**2197-202.

120. **Marriott, A. C., and P. A. Nuttall.** 1992. Comparison of the S RNA segments and nucleoprotein sequences of Crimean-Congo hemorrhagic fever, Hazara, and Dugbe viruses. Virology **189:**795-9.

121. **Martin, M. L., H. Lindsey-Regnery, D. R. Sasso, J. B. McCormick, and E. Palmer.** 1985. Distinction between Bunyaviridae genera by surface structure and comparison with Hantaan virus using negative stain electron microscopy. Arch Virol **86:**17-28.

122. **Matsuoka, Y., S. Y. Chen, and R. W. Compans.** 1994. A signal for Golgi retention in the bunyavirus G1 glycoprotein. J Biol Chem **269:**22565-73.

123. **Matsuoka, Y., S. Y. Chen, C. E. Holland, and R. W. Compans.** 1996. Molecular determinants of Golgi retention in the Punta Toro virus G1 protein. Arch Biochem Biophys **336:**184-9.

124. **McCormick, J. B., D. R. Sasso, E. L. Palmer, and M. P. Kiley.** 1982. Morphological identification of the agent of Korean haemorrhagic fever (Hantaan virus)as a member of the Bunyaviridae. Lancet **1:**765-8.

125. **McJunkin, J. E., R. R. Khan, and T. F. Tsai.** 1998. California-La Crosse encephalitis. Infect Dis Clin North Am **12:**83-93.

126. **Medema, J. P., C. Scaffidi, F. C. Kischkel, A. Shevchenko, M. Mann, P. H. Krammer, and M. E. Peter.** 1997. FLICE is activated by association with the CD95 death-inducing signaling complex (DISC). Embo J **16:**2794-804.

127. **Micheau, O., and J. Tschopp.** 2003. Induction of TNF receptor I-mediated apoptosis via two sequential signaling complexes. Cell **114:**181-90.

128. **Mills, J. N., J. M. Johnson, T. G. Ksiazek, B. A. Ellis, P. E. Rollin, T. L. Yates, M. O. Mann, M. R. Johnson, M. L. Campbell, J. Miyashiro, M. Patrick, M. Zyzak, D. Lavender, M. G. Novak, K. Schmidt, C. J. Peters, and J. E. Childs.** 1998. A survey of hantavirus antibody in small-mammal populations in selected United States National Parks. Am J Trop Med Hyg **58:**525-32.

129. **Mir, M. A., and A. T. Panganiban.** 2006. The bunyavirus nucleocapsid protein is an RNA chaperone: possible roles in viral RNA panhandle formation and genome replication. Rna **12:**272-82.

130. **Mir, M. A., and A. T. Panganiban.** 2005. The hantavirus nucleocapsid protein recognizes specific features of the viral RNA panhandle and is altered in conformation upon RNA binding. J Virol **79:**1824-35.

131. **Monroe, M. C., S. P. Morzunov, A. M. Johnson, M. D. Bowen, H. Artsob, T. Yates, C. J. Peters, P. E. Rollin, T. G. Ksiazek, and S. T. Nichol.** 1999. Genetic diversity and distribution of Peromyscus-borne hantaviruses in North America. Emerg Infect Dis **5:**75-86.

132. **Muller, R., O. Poch, M. Delarue, D. H. Bishop, and M. Bouloy.** 1994. Rift Valley fever virus L segment: correction of the sequence and possible functional role of newly identified regions conserved in RNA-dependent polymerases. J Gen Virol **75 (Pt 6):**1345-52.

133. **Murphy, F. A., C. M. Fauquet, D. H. Bishop, S. A. Ghabrial, A. W. Jarvis, G. P. Martelli, M. A. Mayo, and M. D. Summers.** 1995. Classification and nomenclature of viruses, Virus Taxonomy. Springer-Verlag, Vienna.

134. **Murphy, F. A., A. K. Harrison, and S. G. Whitfield.** 1973. Bunyaviridae: morphologic and morphogenetic similarities of Bunyamwera serologic supergroup viruses and several other arthropod-borne viruses. Intervirology **1:**297-316.

135. **Muzio, M., A. M. Chinnaiyan, F. C. Kischkel, K. O'Rourke, A. Shevchenko, J. Ni, C. Scaffidi, J. D. Bretz, M. Zhang, R. Gentz, M. Mann, P. H. Krammer, M. E. Peter, and V. M. Dixit.** 1996. FLICE, a novel FADD-homologous ICE/CED-3-like protease, is recruited to the CD95 (Fas/APO-1) death--inducing signaling complex. Cell **85:**817-27.

136. **Muzio, M., G. S. Salvesen, and V. M. Dixit.** 1997. FLICE induced apoptosis in a cell-free system. Cleavage of caspase zymogens. J Biol Chem **272:**2952-6.

137. **Netski, D., B. H. Thran, and S. C. St Jeor.** 1999. Sin Nombre virus pathogenesis in Peromyscus maniculatus. J Virol **73:**585-91.

138. **Nichol, S. T., C. F. Spiropoulou, S. Morzunov, P. E. Rollin, T. G. Ksiazek, H. Feldmann, A. Sanchez, J. Childs, S. Zaki, and C. J. Peters.** 1993. Genetic identification of a hantavirus associated with an outbreak of acute respiratory illness. Science **262:**914-7.

139. **Nicoletti, L., P. Verani, S. Caciolli, M. G. Ciufolini, A. Renzi, D. Bartolozzi, P. Paci, F. Leoncini, P. Padovani, E. Traini, and et al.** 1991. Central nervous system involvement during infection by Phlebovirus toscana of residents in natural foci in central Italy (1977-1988). Am J Trop Med Hyg **45:**429-34.

140. **Niklasson, B., and J. W. LeDuc.** 1987. Epidemiology of nephropathia epidemica in Sweden. J Infect Dis **155:**269-76.

141. **Obijeski, J. F., D. H. Bishop, F. A. Murphy, and E. L. Palmer.** 1976. Structural proteins of La Crosse virus. J Virol **19:**985-97.

142. **Obijeski, J. F., D. H. Bishop, E. L. Palmer, and F. A. Murphy.** 1976. Segmented genome and nucleocapsid of La Crosse virus. J Virol **20:**664-75.

143. **Obijeski, J. F., and F. A. Murphy.** 1977. Bunyaviridae: recent biochemical developments. J Gen Virol **37:**1-14.

144. **O'Reilly, E. K., and C. C. Kao.** 1998. Analysis of RNA-dependent RNA polymerase structure and function as guided by known polymerase structures and computer predictions of secondary structure. Virology **252:**287-303.

145. **Osborne, J. C., and R. M. Elliott.** 2000. RNA binding properties of bunyamwera virus nucleocapsid protein and selective binding to an element in the 5' terminus of the negative-sense S segment. J Virol **74:**9946-52.

146. **Padula, P. J., A. Edelstein, S. D. Miguel, N. M. Lopez, C. M. Rossi, and R. D. Rabinovich.** 1998. Hantavirus pulmonary syndrome outbreak in Argentina: molecular evidence for person-to-person transmission of Andes virus. Virology **241:**323-30.

147. **Patton, J. T., N. L. Davis, and G. W. Wertz.** 1984. N protein alone satisfies the requirement for protein synthesis during RNA replication of vesicular stomatitis virus. J Virol **49:**303-9.

148. **Pekosz, A., J. Phillips, D. Pleasure, D. Merry, and F. Gonzalez-Scarano.** 1996. Induction of apoptosis by La Crosse virus infection and role of neuronal differentiation and human bcl-2 expression in its prevention. J Virol **70:**5329-35.

149. **Pensiero, M. N., and J. Hay.** 1992. The Hantaan virus M-segment glycoproteins G1 and G2 can be expressed independently. J Virol **66:**1907-14.

150. **Pensiero, M. N., J. B. Sharefkin, C. W. Dieffenbach, and J. Hay.** 1992. Hantaan virus infection of human endothelial cells. J Virol **66:**5929-36.

151. **Persson, R., and R. F. Pettersson.** 1991. Formation and intracellular transport of a heterodimeric viral spike protein complex. J Cell Biol **112:**257-66.

152. **Pesonen, M., E. Kuismanen, and R. F. Pettersson.** 1982. Monosaccharide sequence of protein-bound glycans of Uukuniemi virus. J Virol **41:**390-400.

153. **Pettersson, R. F., and L. Melin.** 1996. Synthesis, assembly and intracellular transport of *Bunyaviridae* membrane proteins, p. 159-188. *In* E. R.M. (ed.), The *Bunyaviridae*. Plenum Press, New York.

154. **Pilaski, J., H. Feldmann, S. Morzunov, P. E. Rollin, S. L. Ruo, B. Lauer, C. J. Peters, and S. T. Nichol.** 1994. Genetic identification of a new Puumala virus strain causing severe hemorrhagic fever with renal syndrome in Germany. J Infect Dis **170:**1456-62.

155. **Plyusnin, A., O. Vapalahti, and A. Vaheri.** 1996. Hantaviruses: genome structure, expression and evolution. J Gen Virol **77 (Pt 11):**2677-87.

156. **Poch, O., I. Sauvaget, M. Delarue, and N. Tordo.** 1989. Identification of four conserved motifs among the RNA-dependent polymerase encoding elements. Embo J **8:**3867-74.

157. **Powell, G. M.** 1954. Hemorrhagic fever: a study of 300 cases. Medicine (Baltimore) **33:**97-153.

158. **Raju, R., and D. Kolakofsky.** 1989. The ends of La Crosse virus genome and antigenome RNAs within nucleocapsids are base paired. J Virol **63:**122-8.

159. **Ramanathan, H. N., D. H. Chung, S. J. Plane, E. Sztul, Y. K. Chu, M. C. Guttieri, M. McDowell, G. Ali, and C. B. Jonsson.** 2007. Dynein-dependent transport of the hantaan virus nucleocapsid protein to the endoplasmic reticulum-Golgi intermediate compartment. J Virol **81:**8634-47.

160. **Ramanathan, H. N., and C. B. Jonsson.** 2008. New and Old World hantaviruses differentially utilize host cytoskeletal components during their life cycles. Virology **374:**138-50.

161. **Ravi, R., A. Bedi, and E. J. Fuchs.** 1998. CD95 (Fas)-induced caspase-mediated proteolysis of NF-kappaB. Cancer Res **58:**882-6.

162. **Ravkov, E. V., and R. W. Compans.** 2001. Hantavirus nucleocapsid protein is expressed as a membrane-associated protein in the perinuclear region. J Virol **75:**1808-15.

163. **Ravkov, E. V., S. T. Nichol, and R. W. Compans.** 1997. Polarized entry and release in epithelial cells of Black Creek Canal virus, a New World hantavirus. J Virol **71:**1147-54.

164. **Ravkov, E. V., S. T. Nichol, C. J. Peters, and R. W. Compans.** 1998. Role of actin microfilaments in Black Creek Canal virus morphogenesis. J Virol **72:**2865-70.

165. **Ravkov, E. V., P. E. Rollin, T. G. Ksiazek, C. J. Peters, and S. T. Nichol.** 1995. Genetic and serologic analysis of Black Creek Canal virus and its association with human disease and Sigmodon hispidus infection. Virology **210:**482-9.

166. **Regenmortel, V., C. M. Fauquet, and D. H. Bishop.** 2000. Virus Taxonomy. Springer-Verlag.

167. **Reichelt, M., S. Stertz, J. Krijnse-Locker, O. Haller, and G. Kochs.** 2004. Missorting of LaCrosse virus nucleocapsid protein by the interferon-induced MxA GTPase involves smooth ER membranes. Traffic **5:**772-84.

168. **Richmond, K. E., K. Chenault, J. L. Sherwood, and T. L. German.** 1998. Characterization of the nucleic acid binding properties of tomato spotted wilt virus nucleocapsid protein. Virology **248:**6-11.

169. **Ronka, H., P. Hilden, C. H. Von Bonsdorff, and E. Kuismanen.** 1995. Homodimeric association of the spike glycoproteins G1 and G2 of Uukuniemi virus. Virology **211:**241-50.

170. **Roy, N., Q. L. Deveraux, R. Takahashi, G. S. Salvesen, and J. C. Reed.** 1997. The c-IAP-1 and c-IAP-2 proteins are direct inhibitors of specific caspases. Embo J **16:**6914-25.

171. **Ruo, S. L., A. Sanchez, L. H. Elliott, L. S. Brammer, J. B. McCormick, and S. P. Fisher-Hoch.** 1991. Monoclonal antibodies to three strains of hantaviruses: Hantaan, R22, and Puumala. Arch Virol **119:**1-11.

172. **Ruusala, A., R. Persson, C. S. Schmaljohn, and R. F. Pettersson.** 1992. Coexpression of the membrane glycoproteins G1 and G2 of Hantaan virus is required for targeting to the Golgi complex. Virology **186:**53-64.

173. **Rwambo, P. M., M. K. Shaw, F. R. Rurangirwa, and J. C. DeMartini.** 1996. Ultrastructural studies on the replication and morphogenesis of Nairobi sheep disease virus, a Nairovirus. Arch Virol **141:**1479-92.

174. **Salanueva, I. J., R. R. Novoa, P. Cabezas, C. Lopez-Iglesias, J. L. Carrascosa, R. M. Elliott, and C. Risco.** 2003. Polymorphism and structural maturation of bunyamwera virus in Golgi and post-Golgi compartments. J Virol **77:**1368-81.

175. **Sankar, S., and A. G. Porter.** 1992. Point mutations which drastically affect the polymerization activity of encephalomyocarditis virus RNA-dependent RNA polymerase correspond to the active site of Escherichia coli DNA polymerase I. J Biol Chem **267:**10168-76.

176. **Schmaljohn, C.** 1996. Molecular Biology of Hantaviruses, p. 63-90. *In* R. Elliot (ed.), *The Bunyaviridae*. Plenum Press, New York.

177. **Schmaljohn, C., and B. Hjelle.** 1997. Hantaviruses: a global disease problem. Emerg Infect Dis **3:**95-104.

178. **Schmaljohn, C. S., and J. M. Dalrymple.** 1983. Analysis of Hantaan virus RNA: evidence for a new genus of bunyaviridae. Virology **131:**482-91.

179. **Schmaljohn, C. S., S. E. Hasty, S. A. Harrison, and J. M. Dalrymple.** 1983. Characterization of Hantaan virions, the prototype virus of hemorrhagic fever with renal syndrome. J Infect Dis **148:**1005-12.

180. **Schmaljohn, C. S., S. E. Hasty, L. Rasmussen, and J. M. Dalrymple.** 1986. Hantaan virus replication: effects of monensin, tunicamycin and endoglycosidases on the structural glycoproteins. J Gen Virol **67 (Pt 4):**707-17.

181. **Schmaljohn, C. S., and J. W. Hooper.** 2001. *Bunyaviridae*: The viruses and their replication., p. 1581-1602. *In* K. D. Fields BN, Howley PM. (ed.), Virology, 4 ed, vol. 2. Lippincott-Raven, Philadelphia.

182. **Schmaljohn, C. S., G. B. Jennings, J. Hay, and J. M. Dalrymple.** 1986. Coding strategy of the S genome segment of Hantaan virus. Virology **155:**633-43.

183. **Schmaljohn, C. S., and S. T. Nichol.** 2006. *Bunyaviridae*, p. 1741-1789. *In* D. Knipe (ed.), Virology, vol. 2. Lippincott-Raven, Philadelphia.

184. **Schmaljohn, C. S., A. L. Schmaljohn, and J. M. Dalrymple.** 1987. Hantaan virus M RNA: coding strategy, nucleotide sequence, and gene order. Virology **157:**31-9.

185. **Severson, W., L. Partin, C. S. Schmaljohn, and C. B. Jonsson.** 1999. Characterization of the Hantaan nucleocapsid protein-ribonucleic acid interaction. J Biol Chem **274:**33732-9.

186. **Severson, W., X. Xu, M. Kuhn, N. Senutovitch, M. Thokala, F. Ferron, S. Longhi, B. Canard, and C. B. Jonsson.** 2005. Essential amino acids of the hantaan virus N protein in its interaction with RNA. J Virol **79:**10032-9.

187. **Severson, W. E., C. S. Schmaljohn, A. Javadian, and C. B. Jonsson.** 2003. Ribavirin causes error catastrophe during Hantaan virus replication. J Virol **77:**481-8.

188. **Severson, W. E., X. Xu, and C. B. Jonsson.** 2001. cis-Acting signals in encapsidation of Hantaan virus S-segment viral genomic RNA by its N protein. J Virol **75:**2646-52.

189. **Shapiro, G. I., and R. M. Krug.** 1988. Influenza virus RNA replication in vitro: synthesis of viral template RNAs and virion RNAs in the absence of an added primer. J Virol **62:**2285-90.

190. **Sheedy, J. A., H. F. Froeb, H. A. Batson, C. C. Conley, J. P. Murphy, R. B. Hunter, D. W. Cugell, R. B. Giles, S. C. Bershadsky, J. W. Vester, and R. H. Yoe.** 1954. The clinical course of epidemic hemorrhagic fever. Am J Med **16:**619-28.

191. **Shi, X., and R. M. Elliott.** 2002. Golgi localization of Hantaan virus glycoproteins requires coexpression of G1 and G2. Virology **300:**31-8.

192. **Shi, X., D. F. Lappin, and R. M. Elliott.** 2004. Mapping the Golgi targeting and retention signal of Bunyamwera virus glycoproteins. J Virol **78:**10793-802.

193. **Simons, J. F., U. Hellman, and R. F. Pettersson.** 1990. Uukuniemi virus S RNA segment: ambisense coding strategy, packaging of complementary strands into virions, and homology to members of the genus Phlebovirus. J Virol **64:**247-55.

194. **Smadel, J. E.** 1950. Introduction, symposium on viral and rickettsial diseases. Bacteriol Rev **14:**193-7.

195. **Smithburn, K. C., A. J. Haddow, and A. F. Mahaffy.** 1946. A neurotropic virus isolated from Aedes mosquitos caught in the Semliki forest. Am J Trop Med Hyg **26:**189-208.

196. **Spiropoulou, C. F., C. S. Goldsmith, T. R. Shoemaker, C. J. Peters, and R. W. Compans.** 2003. Sin Nombre virus glycoprotein trafficking. Virology **308:**48-63.

197. **Spiropoulou, C. F., S. Morzunov, H. Feldmann, A. Sanchez, C. J. Peters, and S. T. Nichol.** 1994. Genome structure and variability of a virus causing hantavirus pulmonary syndrome. Virology **200:**715-23.

198. **Stanger, B. Z., P. Leder, T. H. Lee, E. Kim, and B. Seed.** 1995. RIP: a novel protein containing a death domain that interacts with Fas/APO-1 (CD95) in yeast and causes cell death. Cell **81:**513-23.

199. **Steinecke, P., C. Heinze, E. Oehmen, G. Adam, and P. H. Schreier.** 1998. Early events of tomato spotted wilt transcription and replication in protoplasts. New Microbiol **21:**263-8.

200. **Stennicke, H. R., J. M. Jurgensmeier, H. Shin, Q. Deveraux, B. B. Wolf, X. Yang, Q. Zhou, H. M. Ellerby, L. M. Ellerby, D. Bredesen, D. R. Green, J. C.**

Reed, C. J. Froelich, and G. S. Salvesen. 1998. Pro-caspase-3 is a major physiologic target of caspase-8. J Biol Chem **273:**27084-90.

201. **Stennicke, H. R., and G. S. Salvesen.** 1997. Biochemical characteristics of caspases-3, -6, -7, and -8. J Biol Chem **272:**25719-23.

202. **Storms, M. M., R. Kormelink, D. Peters, J. W. Van Lent, and R. W. Goldbach.** 1995. The nonstructural NSm protein of tomato spotted wilt virus induces tubular structures in plant and insect cells. Virology **214:**485-93.

203. **Strasser, A., L. O'Connor, and V. M. Dixit.** 2000. Apoptosis signaling. Annu Rev Biochem **69:**217-45.

204. **Sugiyama, K., S. Morikawa, Y. Matsuura, E. A. Tkachenko, C. Morita, T. Komatsu, Y. Akao, and T. Kitamura.** 1987. Four serotypes of haemorrhagic fever with renal syndrome viruses identified by polyclonal and monoclonal antibodies. J Gen Virol **68 (Pt 4):**979-87.

205. **Takahashi, A., and W. C. Earnshaw.** 1996. ICE-related proteases in apoptosis. Curr Opin Genet Dev **6:**50-5.

206. **Takahashi, A., P. J. Goldschmidt-Clermont, E. S. Alnemri, T. Fernandes-Alnemri, K. Yoshizawa-Kumagaya, K. Nakajima, M. Sasada, G. G. Poirier, and W. C. Earnshaw.** 1997. Inhibition of ICE-related proteases (caspases) and nuclear apoptosis by phenylarsine oxide. Exp Cell Res **231:**123-31.

207. **Talmon, Y., B. V. Prasad, J. P. Clerx, G. J. Wang, W. Chiu, and M. J. Hewlett.** 1987. Electron microscopy of vitrified-hydrated La Crosse virus. J Virol **61:**2319-21.

208. **Tartaglia, L. A., R. F. Weber, I. S. Figari, C. Reynolds, M. A. Palladino, Jr., and D. V. Goeddel.** 1991. The two different receptors for tumor necrosis factor mediate distinct cellular responses. Proc Natl Acad Sci U S A **88:**9292-6.

209. **Taylor, S. L., N. Frias-Staheli, A. Garcia-Sastre, and C. S. Schmaljohn.** 2009. Hantaan virus nucleocapsid protein binds to importin alpha proteins and inhibits tumor necrosis factor alpha-induced activation of nuclear factor kappa B. J Virol **83:**1271-9.

210. **Tschopp, J., F. Martinon, and K. Burns.** 2003. NALPs: a novel protein family involved in inflammation. Nat Rev Mol Cell Biol **4:**95-104.

211. **Uhrig, J. F., T. R. Soellick, C. J. Minke, C. Philipp, J. W. Kellmann, and P. H. Schreier.** 1999. Homotypic interaction and multimerization of nucleocapsid protein of tomato spotted wilt tospovirus: identification and characterization of two interacting domains. Proc Natl Acad Sci U S A **96:**55-60.

212. **Ulmanen, I., P. Seppala, and R. F. Pettersson.** 1981. In vitro translation of Uukuniemi virus-specific RNAs: identification of a nonstructural protein and a precursor to the membrane glycoproteins. J Virol **37:**72-79.

213. **van Knippenberg, I., R. Goldbach, and R. Kormelink.** 2002. Purified tomato spotted wilt virus particles support both genome replication and transcription in vitro. Virology **303:**278-86.

214. **van Poelwijk, F., K. Boye, R. Oosterling, D. Peters, and R. Goldbach.** 1993. Detection of the L protein of tomato spotted wilt virus. Virology **197:**468-70.

215. **van Vliet, C., E. C. Thomas, A. Merino-Trigo, R. D. Teasdale, and P. A. Gleeson.** 2003. Intracellular sorting and transport of proteins. Prog Biophys Mol Biol **83:**1-45.

216. **Vapalahti, O., H. Kallio-Kokko, A. Narvanen, I. Julkunen, A. Lundkvist, A. Plyusnin, H. Lehvaslaiho, M. Brummer-Korvenkontio, A. Vaheri, and H. Lankinen.** 1995. Human B-cell epitopes of Puumala virus nucleocapsid protein, the major antigen in early serological response. J Med Virol **46:**293-303.

217. **Wang, C. Y., M. W. Mayo, R. G. Korneluk, D. V. Goeddel, and A. S. Baldwin, Jr.** 1998. NF-kappaB antiapoptosis: induction of TRAF1 and TRAF2 and c-IAP1 and c-IAP2 to suppress caspase-8 activation. Science **281:**1680-3.

218. **Wang, Y., D. M. Boudreaux, D. F. Estrada, C. W. Egan, S. C. St Jeor, and R. N. De Guzman.** 2008. NMR structure of the N-terminal coiled coil domain of the Andes hantavirus nucleocapsid protein. J Biol Chem **283:**28297-304.

219. **Wells, R. M., S. Sosa Estani, Z. E. Yadon, D. Enria, P. Padula, N. Pini, J. N. Mills, C. J. Peters, and E. L. Segura.** 1997. An unusual hantavirus outbreak in southern Argentina: person-to-person transmission? Hantavirus Pulmonary Syndrome Study Group for Patagonia. Emerg Infect Dis **3:**171-4.

220. **White, J. D., F. G. Shirey, G. R. French, J. W. Huggins, O. M. Brand, and H. W. Lee.** 1982. Hantaan virus, aetiological agent of Korean haemorrhagic fever, has Bunyaviridae-like morphology. Lancet **1:**768-71.

221. **Xiao, S. Y., J. W. Leduc, Y. K. Chu, and C. S. Schmaljohn.** 1994. Phylogenetic analyses of virus isolates in the genus Hantavirus, family Bunyaviridae. Virology **198:**205-17.

222. **Xu, X., W. Severson, N. Villegas, C. S. Schmaljohn, and C. B. Jonsson.** 2002. The RNA binding domain of the hantaan virus N protein maps to a central, conserved region. J Virol **76:**3301-8.

223. **Yoshimatsu, K., B. H. Lee, K. Araki, M. Morimatsu, M. Ogino, H. Ebihara, and J. Arikawa.** 2003. The multimerization of hantavirus nucleocapsid protein depends on type-specific epitopes. J Virol **77:**943-52.

224. **Zou, H., Y. Li, X. Liu, and X. Wang.** 1999. An APAF-1.cytochrome c multimeric complex is a functional apoptosome that activates procaspase-9. J Biol Chem **274:**11549-56.